Activation of Cytokine and Chemokine Gene Expression in Human Bronchial Epithelium by Avian Influenza Virus H5N1

Nawiya Huipao

A Thesis Submitted in Partial Fulfillment of the Requirements for the Degree of
Doctor of Philosophy in Physiology
Prince of Songkla University
2014

Thesis Title	Activation of Cytokine and Chemokine Gene Expression in Human Bronchial Epithelium by Avian Influenza Virus H5N1
Author	Miss Nawiya Huipao
Major Program	Physiology

Major advisor

……
(Assoc. Prof. Dr. Siriphun Hiranyachattada)

Co-advisors

……
(Prof. Dr. Chumpol Pholpramool)

……
(Assoc. Prof. Dr. Anuwat Dinudom)

Examining Committee:

……Chairperson
(Asst. Prof. Dr. Arunee Thitithanyanont)

……
(Assoc. Prof. Dr. Siriphun Hiranyachattada)

……
(Prof. Dr. Chumpol Pholpramool)

……
(Dr. Pilaiwanwadee Hutamekalin)

……
(Dr. Suparerk Borwornpinyo)

The Graduate School, Prince of Songkla University, has approved this thesis as partial fulfillment of the requirements for the Doctor of Philosophy Degree in Physiology

……
(Assoc. Prof. Dr. Teerapol Srichana)
Dean of Graduate School

This is to certify that the work here submitted is the result of the candidate's own investigations. Due acknowledgement has been made of any assistance received.

……Signature
(Assoc. Prof. Dr. Siriphun Hiranyachattada)
Major Advisor

……Signature
(Nawiya Huipao)
Candidate

I hereby certify that this work has not been accepted in substance for any degree, and is not being currently submitted in candidature for any degree.

……Signature

(Nawiya Huipao)

Candidate

ชื่อวิทยานิพนธ์ การกระตุ้นการแสดงออกของยีนไซโตไคน์และคีโมไคน์ในเซลล์เยื่อบุผิวหลอดลมย่อยทางเดินหายใจของคนโดยไวรัสไข้หวัดนกสายพันธุ์ H5N1

ผู้เขียน นางสาวนวิยา ฮุยเป้า

สาขาวิชา สรีรวิทยา

ปีการศึกษา 2557

บทคัดย่อ

จากการศึกษาเมื่อไม่นานมานี้แสดงให้เห็นว่าไวรัส H5N1 สามารถทำให้เกิดการหลั่งไซโตไคน์จาก host cell ได้โดยไม่จำเป็นต้องเกิดการติดเชื้อ การศึกษาในครั้งนี้มีวัตถุประสงค์เพื่อศึกษากลไกการออกฤทธิ์ของ H5N1 ที่ถูกทำลายฤทธิ์โดย β-propiolactone (inact-H5N1) ต่อการเพิ่มการแสดงออกของยีนไซโตไคน์และคีโมไคน์ในเซลล์เยื่อบุผิวทางเดินหายใจมนุษย์ (เซลล์ 16HBE14o-) ในหลอดทดลอง ผลการศึกษาพบว่า inact-H5N1 มีผลเพิ่มการแสดงออกของยีน IL-6 และ IL-8 แต่ไม่มีผลต่อการแสดงออกของยีน TNF-α, CCL-5 และ IP-10 ซึ่งผลของ inact-H5N1 ต่อการแสดงออกของยีน IL-6 และ IL-8 จะถูกยับยั้งโดย α,2-3-specific sialidase, MRS2578, U73122, BIM, GÖ6976 และ BAPTA-AM อย่างมีนัยสำคัญทางสถิติ นอกจากนี้ยังพบว่าสารยับยั้งการส่งสัญญาณในกลุ่ม MAPK ได้แก่ PD98059, SB20358 และ SP600125 ลดการแสดงออกของยีน IL-8 อย่างมีนัยสำคัญทางสถิติ ขณะที่การแสดงออกของยีน IL-6 ถูกยับยั้งโดย SB20358 เท่านั้น และ SN-50 ซึ่งเป็นสารยับยั้ง NF-ΚB สามารถป้องกันฤทธิ์ของไวรัสต่อการแสดงออกของยีนทั้ง IL-6 และ IL-8 ได้เช่นเดียวกัน เป็นที่น่าสนใจว่าผลของ inact-H5N1 ถูกยับยั้งได้ในเซลล์ที่ได้รับสารยับยั้ง TMEM16A และ CFTR chloride channel อีกด้วย การศึกษานี้เป็นครั้งแรกที่แสดงให้เห็นว่า แม้ว่าจะไม่มีการติดเชื้อเกิดขึ้น ไวรัสไข้หวัดนกสายพันธุ์ H5N1 ยังสามารถกระตุ้นการแสดงออกของยีน IL-6 และ IL-8 ได้ ซึ่งฤทธิ์ดังกล่าวเกิดจากปฏิกิริยาระหว่าง hemagglutinin บนผิวของไวรัสกับตัวรับ α-2,3 sialic acid บนผิวเซลล์เยื่อบุทางเดินหายใจ โดยไวรัสออกฤทธิ์เพิ่มการคัดหลั่ง nucleotide ซึ่งทำให้เกิดการกระตุ้นตัวรับ purinergic ชนิด $P2Y_6R$ สำหรับกลไกที่เกิดขึ้นตามลำดับถัดมาที่ทำให้เกิดการเพิ่มการแสดงออกของยีน IL-6 และ IL-8 ประกอบไปด้วย กลไกการส่งสัญญาณผ่านทาง PLC, PKC, การเพิ่มขึ้นของแคลเซี่ยมอิออนภายในเซลล์และ MAPK นอกจากนี้ไวรัสยังมีผลเพิ่มการหลั่งคลอไรด์อิออนผ่านทาง chloride channel ชนิด TMEM16A และ CFTR ในเยื่อบุผิวทางเดินหายใจ ซึ่งการกระตุ้น chloride channel นี้พบว่ามีส่วนเกี่ยวข้องต่อการควบคุมการแสดงออกของยีน IL-6 และ IL-8 ที่เป็นผลมาจากการออกฤทธิ์ของ H5N1

Thesis Title Activation of Cytokine and Chemokine Gene Expression in Human Bronchial Epithelium by Avian Influenza Virus H5N1

Author Miss Nawiya Huipao

Major Program Physiology

Academic Year 2014

ABSTRACT

Recent studies suggested that H5N1 could induce cytokine release from host cells via an infection-independent mechanism. The present study aims to determine the mechanism by which H5N1 inactivated with β-propiolactone (inact-H5N1) increases cytokine and chemokine mRNA expression in human respiratory epithelium (16HBE14o- cells) *in vitro*. Results herein suggest that inact-H5N1 increased mRNA expressions of IL-6 and IL-8 but not those of TNF-α, CCL-5 and IP-10. Upregulations of mRNA expression of IL-6 and IL-8 were significantly inhibited by α-2,3 specific sialidase, MRS2578, U73122, BIM, GÖ6976 and BAPTA-AM. Moreover, inhibitors for MAPK signaling, including PD98059, SB20358 and SP600125 significantly suppressed mRNA expression of IL-8. On the other hand, mRNA expression of IL-6 was inhibited by SB20358 but not by PD98059 or SP600125. SN-50, an inhibitor of NF-κB, also inhibited the effect of the virus on mRNA expression of both IL-6 and IL-8. Interestingly, the effect of the inact-H5N1 was inhibited in cells treated with inhibitors of TMEM16A and CFTR Cl^- channels. This is the first study to demonstrate that, without infection, H5N1 induces mRNA expression of IL-6 and IL-8. Such effect requires an interaction between viral hemagglutinin and the α-2,3 sialic acid receptors at the cell membrane. H5N1 increases nucleotide release which, in turn, activates $P2Y_6R$ purinergic signaling. The downstream cellular mechanisms leading to increases in mRNA expression of IL-6 and IL-8 involve PLC, PKC, intracellular Ca^{2+}, and MAPKs. H5N1 also increases Cl^- secretion via the Cl^- channels, TMEM16A and CFTR, in the respiratory epithelium which is associated with H5N1-induced mRNA expression of IL-6 and IL-8.

CONTENTS

LIST OF TABLES

LIST OF FIGURES

LIST OF FIGURES (continued)

LIST OF FIGURES (continued)

LIST OF FIGURES (continued)

CHAPTER 1

INTRODUCTION

General introduction

The airway epithelial cell is the first line of defense against airborne pathogens (Vareille et al., 2011). It is well established that airway epithelial cells produce and secrete bioactive molecules including cytokines and chemokines participating in innate immunity. During influenza A virus infection, secretions from the respiratory epithelium contain cytokines and chemokines at levels higher than those found in the plasma or serum (Fritz et al., 1999; Hayden et al., 1998; Skoner et al., 1999). Moreover, under inflammatory conditions, respiratory epithelial cells also release nucleotides such as UTP (Homolya et al., 2000) and ATP (Button et al., 2007; Tarran et al., 2006). These nucleotides, in turn, activate purinergic receptors at the plasma membrane of the epithelium triggering the release of intracellular Ca^{2+} ($[Ca^{2+}]_i$) from cytosolic stores (Lazarowski et al., 2009). Consequently, the rise in $[Ca^{2+}]_i$ induces an onset of an array of physiological events including inflammatory responses (Chang, 2006; Gewirtz et al., 2000).

Avian influenza virus H5N1 is a highly pathogenic avian influenza virus (HPAI) that initially propagates among poultry and migrating birds. Currently, H5N1 infection with a high mortality rate has been detected in human population (Korteweg et al., 2008). In human, clinical pathogenesis of H5N1 infection is more potent than seasonal human influenza virus, H1N1. Similar to other respiratory pathogens, the primary target of H5N1 is epithelial cells lining the airway. Patients with H5N1 infection showed dysregulation of cytokines and chemokines in the respiratory epithelial cells (Damjanovic et al., 2012) which is likely to be the key mechanisms in the initial pathogenesis of H5N1 infection. So far, the mechanisms that underlie H5N1-mediated cytokine response in the respiratory epithelium are poorly understood. A recent study has reported that replication-deficient H5N1 strongly induces expression of cytokines in human respiratory epithelial cells (Cheng et al., 2010). Consistent with this finding, the effect of H5N1 on cytokine mRNA

production in human macrophages does not require viral replication (Sakabe et al., 2011). Furthermore, it has been reported that a recombinant H5N1 hemagglutinin induced expression of cytokines in cultured human peripheral blood mononuclear cells (Almansa et al., 2011). Together, these findings suggest that a protein or proteins present on the surface of H5N1 virus may be involved in an early initiation of the innate immune responses of H5N1 infection. It has not yet been shown, however, that which signaling pathway is responsible for, nor has it been shown if and how the viral structural proteins initiate the cytokine responses. The present study reveals that the mechanism underlying the production of cytokine and chemokine mRNA expression by inact-H5N1 involves activation of purinergic receptor(s) in the respiratory cells which upregulates cytokine production by the mitogen-activated protein kinase (MAPK) signaling pathway, and that this H5N1-induced cytokine production requires activity of Cl^- channel(s).

Literature review

1. Influenza viruses

1.1 Classification of influenza viruses

Influenza viruses are single strand, enveloped RNA viruses belonging to the family *Orthomyxoviridae* (Beigel, 2008). There are five genera of influenza viruses, influenza A, influenza B and influenza C, which are distinguished by antigenic differences in their nucleoprotein (NP) and matrix protein-1 (M1). Together with the Isavirus (infectious salmon anemia virus) and Thogotovirus genera they are from the family of *Orthomyxoviridae* (Horimoto et al., 2005). Recently, the sixth genus, which includes Quaranfil, Johnston Atoll and Lake Chad viruses, has been reported (Presti et al., 2009). Although all types of influenza can infect human, only influenza A and B can cause wide spectrum of various severe diseases. Influenza C viruses generally cause only mild upper respiratory tract symptoms in human. Normally, influenza virus types B and C have a limited antigenic variation, hence, their infections are limited when compare with the influenza virus type A (Chen et al.,

2009). Influenza A viruses are the most pathogenic and clinically relevant, and are divided into subtypes by antigenic characteristics of their two main surface glycoproteins, hemagglutinin (HA) and neuraminidase (NA) (Bouvier et al., 2008). To date, 16 different HA (H1-H16) and 9 different NA (N1-N9) of influenza A viruses have been identified (de Jong et al., 2006), hence, the standard nomenclature system for this class of virus follows the pattern H(x)N(y). Influenza A virus can be further classified as either (i) highly pathogenic avian influenza (HPAI), associated so far only with subtype H5 and H7 viruses, or (ii) low pathogenic avian influenza (LPAI), by the level of morbidity and mortality rate caused by intravenous inoculation in chickens (Adams et al., 2010). In recent years, zoonotic influenza A virus subtype H5N1 (A/H5N1) has been particularly the main focus of research amongst all other virulent strains of influenza A viruses. This is due to the high mutation rates of A/H5N1 make it capable of cross-species infection inducing severe disease and high mortality rates in hosts with no previous immunity. Thus, fear of its emergence in causing the next calamitous global pandemic has stirred intense public interest unto this topic and as a result, A/H5N1 will be the main topic of discussion in this study.

1.2 Structure of influenza virus

Under electron microscopy, influenza viruses (Fig. 1.1) have spherical or filamentous shape, ranging from 80-120 nm in diameter and 300 nm in length (Bouvier et al., 2008). Eight single strand negative sense of influenza A encode two main surface glycoproteins, HA and NA, in a ratio of approximately 4:1 (Nayak et al., 2009). A small proportion of matrix protein-2 (M2) also spans across the lipid envelope, M2 protein, punctuated by HA and NA, is a proton channel responsible for the pH-dependent endocytosis that promotes viral un-coating during viral entry phase (Adams et al., 2010; Guo et al., 2009). A matrix of M1 protein is found under the envelope membrane which encloses the virion core consisting of nuclear export protein (NEP, also known as non-structural protein NS) and ribonucleoprotein (RNP) complexes. RNP complex consists of viral RNA (vRNA) gene segments coated with nucleoprotein (NP) and the hetero-trimeric RNA-dependent RNA polymerases (RDRP). RDRP is responsible for genome transcription and replication. It is made up of three subunits: “polymerase basic” (PB1 and PB2) and “polymerase acidic”

(PA) subunits. NP has the main function of encapsidating the virus genome, leading to RNA transcription, replication and packaging (Portela et al., 2002).

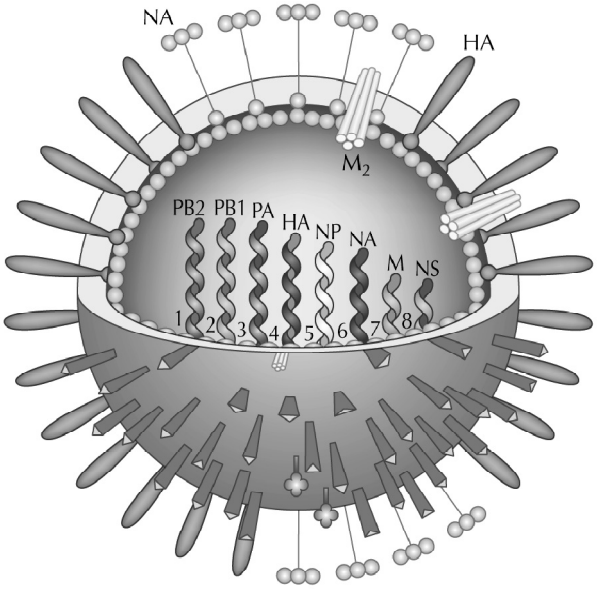

Fig. 1.1: A schematic diagram depicts the structure of influenza A virus. HA = hemagglutinin; M, M2 = matrix protein; NA = neuraminidase; NP = nucleoprotein; NS = non-structural protein; PB1, PB2, PA = polymerase proteins (Zeitlin et al., 2005).

The eight negative sensed-/single stranded-RNA gene segments of influenza A virus encode for up to 11 proteins (Table 1.1). Each gene segment is encapsulated by nucleoproteins forming a RNP and is numbered in the order of decreasing length. Gene segments 1 to 8 of A/H5N1 encodes for the subsequent PB2, PB1, PA, HA, NP, NA, M1 and NS1 proteins, respectively. In certain strains of influenza A virus, segments 2, 7 and 8, also code for additional proteins, i.e., segment 2 codes for an accessory protein, PB1-F2, a small 87 amino acid protein with pro-apoptotic activities capable of inducing cell death (Chen et al., 2001); segment 7 encodes the M2 ion channel by RNA splicing; and segment 8 codes the NEP/NS2 proteins involved in RNP export from host cell nucleus by messenger RNA (mRNA) splicing (Bouvier et al., 2008).

Table 1.1: The genomic segments of influenza A/Puerto Rico/8/1934 virus and their encoded proteins (Bouvier et al., 2008)

Segment	Segment length in nucleotides	Encoded protein (s)	Protein length in amino acids	Protein function
1	2341	PB2	759	Polymerase subunit; mRNA cap recognition
2	2341	PB1	757	Polymerase subunit; RNA elongation, endonuclease activity
		PB1-F2	87	Pro-apoptotic activity
3	2233	PA	716	Polymerase subunit; protease activity
4	1778	HA	550	Surface glycoprotein; major antigen, receptor binding and fusion activities
5	1565	NP	498	RNA binding protein; nuclear import regulation
6	1413	NA	454	Surface glycoprotein; sialidase activity, virus release
7	1027	M1	252	Matrix protein; vRNP interaction, RNA nuclear export regulation, viral budding
		M2	97	Ion channel; virus uncoating and assembly
8	890	NS1	230	Interferon antagonist protein; regulation of host gene expression
		NEP/NS2	121	Nuclear export of RNA

1.3 Avian influenza virus

As mentioned above, A/H5N1 virus pandemic was initially confined to poultry but has now emerged as a highly fatal infectious disease in the human population (Wang et al., 2009). In Asia, A/H5N1 virus first appeared in 1996 in southern China and spread to several countries such as Thailand, Vietnam, Laos, Cambodia, Indonesia, Malaysia, China, Japan and South Korea. A/H5N1 human infections was first reported in Hong Kong in 1997 causing 18 human cases and 6 deaths, approximately 33% mortality rate (Claas et al., 1998). Like all influenza A

viruses, A/H5N1 behaves in a seasonal disease pattern, in a single pandemic year, up to 50% of a population can be infected (Taubenberger et al., 2008). To date, the World Health Organization (WHO) has reported 650 laboratory-confirmed cases of H5N1 infection, 386 of which were fatal or a fatality rate of ~59% (WHO: http://www.who.int/influenza/human_animal_interface/H5N1_cumulative_table_archives/en/; accessed September 2014) (Table 1.2). The prevalence of infection is highest in the infants, elderly, pregnant women and immune incompetent individuals living in industrialized countries of temperate populations during their respective autumn and winter; however, a study has recently shown the prevalence can be all-year-round in tropical countries during their respective rainy seasons (Tamerius et al., 2011). Whilst the strict regulation of existing prevention and control programs demands seasonal vaccinations (comprised of either inactivated or attenuated viruses), and first-line antiviral drugs such as adamantane and NA-inhibitors have significantly controlled for recent pandemics; the high mutation rates of A/H5N1 have now developed resistance to virtually all treatments, posing global concern and threat for imminent pandemics (Aoki et al., 2007; Tang et al., 2010; Tosh et al., 2011). Thus, much critical researches are needed to devise new preventative and therapeutic strategies to counter new resistant strains of highly pathogenic A/H5N1. Such task demands a deeper understanding of the virulent mechanisms underlying the pathogenesis of A/H5N1 in its host.

Table 1.2: Cumulative number of confirmed human cases for avian influenza A (H5N1) reported to WHO, 2003-2014 (WHO: http://www.who.int/influenza/ human _animal_interface/H5N1_cumulative_table_archives/en/; accessed September 2014)

Country	2003-2009*		2010		2011		2012		2013		2014		Total	
	cases	deaths	cases	deaths	cases	deaths	cases	deaths	cases	deaths	cases	deaths	cases	deaths
Azerbaijan	8	5	0	0	0	0	0	0	0	0	0	0	8	5
Bangladesh	1	0	0	0	2	0	3	0	1	1	0	0	7	1
Cambodia	9	7	1	1	8	8	3	3	26	14	0	0	47	33
Canada	0	0	0	0	0	0	0	0	1	1	0	0	1	1
China	38	25	2	1	1	1	2	1	2	2	0	0	45	30
Djibouti	1	0	0	0	0	0	0	0	0	0	0	0	1	0
Egypt	90	27	29	13	39	15	11	5	4	3	0	0	173	63
Indonesia	162	134	9	7	12	10	9	9	3	3	0	0	195	163
Iraq	3	2	0	0	0	0	0	0	0	0	0	0	3	2
Laos	2	2	0	0	0	0	0	0	0	0	0	0	2	2
Myanmar	1	0	0	0	0	0	0	0	0	0	0	0	1	0
Nigeria	1	1	0	0	0	0	0	0	0	0	0	0	1	1
Pakistan	3	1	0	0	0	0	0	0	0	0	0	0	3	1
Thailand	25	17	0	0	0	0	0	0	0	0	0	0	25	17
Turkey	12	4	0	0	0	0	0	0	0	0	0	0	12	4
Viet Nam	112	57	7	2	0	0	4	2	2	1	1	1	125	62
Total	468	282	48	24	62	34	32	20	39	25	1	1	650	386

*2003-2009 total figures. Breakdowns by year available on next table

Total number of cases includes number of deaths

WHO reports only laboratory cases

All dates refer to onset of illness

In 2004, a case report from Thailand indicated a possible case of person-to-person transmission of A/H5N1 through close contact leading to death (Wang et al., 2009). A/H5N1 can be transmitted by airborne droplets expelled from infected individuals during coughing, sneezing or through contact with infected animals. First symptoms commonly emerge within the range of 2 to 9 days (Abdel-Ghafar et al., 2008). It most frequently infects the epithelial cells of the upper and lower respiratory tract. The common symptoms include high fever, chill, rhinorrhea, sore throat, dry cough, diffuse myalgia, fatigue and severe headache. In more severe cases, however, influenza may lead to life-threatening respiratory complications such as acute respiratory distress syndrome (ARDS), croup, bronchitis, bronchiolitis and pneumonia. Gastrointestinal distress such as vomiting, abdominal pain and diarrhea may also be apparent. Furthermore, manifestation of the central nervous system pathology, which leads to general encephalopathy, myelitis, Guillain-Barré syndrome and acute necrotizing encephalitis, has also been previously observed (Chen et al., 2009; Hsieh et al., 2006).

Specific affinity between the hemagglutinin on viral coat and the glycoproteins or glycolipids containing sialyl-galactosyl residues binding site of the virus on the respiratory epithelial cell surface may explain differential infection between avian and human influenza viruses. For instance, human influenza viruses bind to sialic acid receptors containing terminal 2-6-linked sialyl-galactosyl moieties [Neu5Ac(α-2,6)Gal] on the respiratory epithelial cells, whereas avian influenza viruses bind to sialic acid receptors that contain 2-3-linked sialyl-galactosyl moieties [Neu5Ac(α-2,3)Gal] (Shinya et al., 2006). Although human respiratory epithelium contains both the α-2,6 and α-2,3 sialic acid receptors (Thomas et al., 2007), the α-2,3 sialic acid receptors are expressed predominantly in the distal part of the lung (Shinya et al., 2006), which is less accessible for respiratory pathogens, making it difficult for A/H5N1 infection to occur (Fig. 1.2).

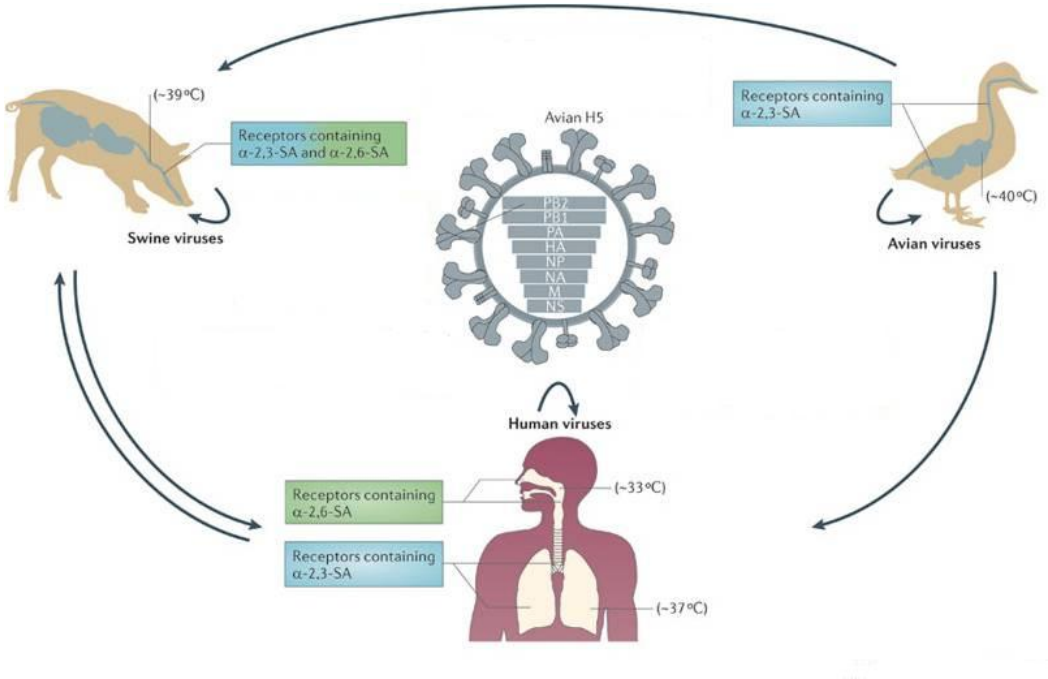

Fig. 1.2: Species-specific expressions of sialic acid receptors (Medina et al., 2011).

2. Pathophysiology of influenza virus infection

2.1 Pathogenesis of influenza virus on ion transport in the respiratory epithelium

Respiratory virus infections are associated with the accumulation of ions and fluid in the respiratory tract. A study of Kunzelmann and coworkers (Kunzelmann et al., 2000) showed that influenza virus A/PR/8/34 (PR8; H1N1) inhibits the amiloride-sensitive Na^+ current across mouse tracheal epithelium. This effect of the virus requires binding of viral hemagglutinin to a sialic-acid receptor at the plasma membrane of the epithelial cells. In mouse trachea, binding of H1 hemagglutinin to the sialic-acid receptor activates phospholipase C (PLC) and protein kinase C (PKC). In agreement with this study, a study of Chen and coworkers (Chen et al., 2004) reported a similar finding that influenza virus A/PR/8/34 (PR8; H1N1) rapidly inhibits ENaC in rat alveolar type II (ATII) cells via a PLC-and Src-mediated activation of PKC. Moreover, it has been reported that respiratory pathogen such as the respiratory syncytial virus (RSV) also inhibits the amiloride-sensitive Na^+ transport in mouse tracheal epithelium by a mechanism that involves PKC

(Kunzelmann et al., 2007). Further investigation revealed that the parainfluenza virus activates Cl^- secretion by triggering the release of ATP and activation of the apical P2Y receptors (Kunzelmann et al., 2004).

A recent study (Huipao, 2011) investigating the effect of inactivated-H5N1 (inact-H5N1) on electrolyte transport in human respiratory epithelium, H441 cells, suggested that inact-H5N1 (20 μg/ml hemagglutinin) added to a solution bating the apical cell surface induced an increase in transepithelial potential difference (V_{te}) and the equivalent short-circuit current (I_{sc}) across H441 cell monolayers. Unlike what was reported for H1N1 (Kunzelmann et al., 2000), the inact-H5N1 had no effect on the amiloride-sensitive current. On the other hand, suppressing Cl^- transport by either removing Cl^- from the extracellular bathing solution or exposing the apical membrane of H441 cells to niflumic acid, a non-specific Cl^- channel blocker (1 mM), attenuated the effect of the inact-H5N1 on I_{sc}. This effect of the inact-H5N1 was not sensitive to DIDS or $CFTR_{inh-172}$ chloride channel blocker. Taken together, this finding suggests that the inact-H5N1 increases Cl^- secretion but has no effect on Na^+ absorption via ENaC in the respiratory epithelium.

2.2 Immunopathogenesis of influenza virus infection

The primary target of virus is the epithelial cells lining the respiratory tract. As a defensive mechanism, cytokines produced by the respiratory epithelial and immune cells increases vascular permeability, allowing passage of immune cells through the endothelial barrier into the infected area. Hence, virus replication leads to increased production of cytokines at the site of infection and a continual influx of immune cells (Vogel et al., 2014). This positive feedback results in hypercytokinemia (cytokine storm), which eventually leads to the acute respiratory distress syndrome (ARDS), i.e., multiorgan failure associated with cytokine imbalance (Fig. 1.3). Infected airway epithelial cells with influenza virus produce the earliest cytokines that trigger this event.

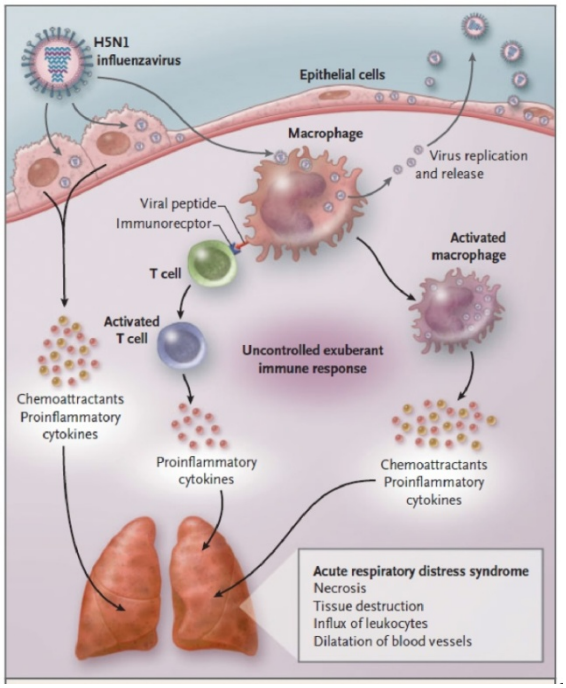

Fig. 1.3: Schematic diagram showing the mechanism of cytokine storm induced by H5N1 influenza virus. After infected with H5N1 viruses, alveolar cells and macrophages releases inflammatory cytokines and chemoattractants, which will recruit leukocytes into the lung, resulting in inflammation and tissue necrosis (Osterholm, 2005).

2.3 Cytokines in the pathogenesis of avian influenza virus infection

Invasion of pathogens are protected by the innate and adaptive immune systems. Upon A/H5N1 infection, host cells respond in many different ways in an attempt to limit the replication and spread of the virus. A/H5N1 replicates highly efficiently in respiratory epithelial cells producing enormous amount of progeny viruses; which further infects surrounding cells and alveolar macrophages (Schmolke et al., 2010). Infected cells may then go through either apoptosis or necrosis, activating both the innate and adaptive immune mechanisms and production of numerous cytokines and chemokines, including interferon-α/β/γ (IFN-α/β/γ), interleukin-1/6 (IL-1/6), tumor necrosis factor-α (TNF-α), chemokine C-C motif 2/3/4/5 (CCL2/3/4/5) and C-X-C motif chemokine 2/8/10 (CXCL2/8/10) (Julkunen et al., 2000; McGill et al., 2009; Peiris et al., 2009). Subsequently, leukocytes such as monocytes/macrophages, neutrophils, and T-lymphocytes were recruited to the site of

infection. Comparing with other strains of influenza virus, A/H5N1 is by far a stronger activator of cytokine production in the respiratory epithelium.

Several studies reported that the A/H5N1 is a better inducer of the production of cytokines than other stains of influenza viruses. Chan et al (2005) reported that A/H5N1/97 and A/H5N1/04 had a greater impact on the production of IFN-β, IL-6, interferon γ-induced protein-10 (IP-10), and that of the Regulated on Activation, Normal T Cell Expressed and Secreted (RANTES) in the bronchial epithelial cells (NHBE) and the human primary alveolar cells (type II alveolar epithelial cells) when compared with the H1N1 virus (Chan et al., 2005). Moreover, the H5N1/VN04 strain induced significantly higher levels of cytokines (RANTES, IL-6 and IP-10) than H1N1 in normal human bronchial epithelial (NHBE) cells (Chan et al., 2010). Furthermore, A/H5N1 was a more potent inducer of the production of IP-10, TNF-α and RANTES than LPAI H1N1, in human pulmonary epithelial cells, than H9N2 (Lam et al., 2010). In addition, A/H5N1 induced production of the chemokines growth-related oncogene-α (GRO-α), IP-10 and IL-8 in human bronchial/tracheal epithelial cells (Song et al., 2011).

Interestingly, in human macrophages, the effect of A/H5N1 on cytokine production did not relate to viral replication (Sakabe et al., 2011). In agreement with this finding, Imai and coworkers (Imai et al., 2008) reported that intratracheal instillation of inactivated-H5N1 triggered production of IL-6. Furthermore, a recombinant H5 hemagglutinin was found to induce the levels of IL-6, monocyte chemoattractant protein-1 (MCP-1) and macrophage inflammatory protein-1β (MIP-1β) in peripheral blood mononuclear cells (PBMCs) cells (Almansa et al., 2011). Together, these studies suggest that H5N1 may be able to induce cytokine production by respiratory epithelial cells by an infection-independent mechanism(s). It should be noted that cytokine production in respiratory epithelial cells can be activated by protein components of non-viral pathogens (Tseng et al., 2006).

2.3.1 Interleukin-6 (IL-6): IL-6, previously known as interferon-β_2, 26K factor, B-cell stimulatory factor 2, plasmacytoma growth factor, hepatocyte stimulatory factor, a hematopoietic factor, and cytotoxic T-cell differentiation factor, is a glycoprotein ranging from 21-28 kDa encoded by gene on chromosome 7 in

humans (Simpson et al., 1997). The variety of its name reflects its different biological activities. IL-6 is produced by variety of cells, including cells of the innate immune system such as macrophages, mast cells, T cells, B cells, neutrophils, and other cell sources such as fibroblast, endothelial cells epithelial cells, and astrocytes (Feghali et al., 1997). Over-production of IL-6 has been associated with pathophysiology of many diseases such as rheumatoid arthritis, type 1 diabetes, Alzheimer's disease, multiple myeloma, and systemic lupus erythematosus (Simpson et al., 1997). IL-6 is pleiotropic that played role in acute inflammation and acts as both a pro-inflammatory and an anti-inflammatory cytokine. When IL-6 binds to IL-6 receptor (IL-6R), homodimerization of gp 130 occurs, triggers the activation of the Janus kinases (JAK), followed by the phosphorylation and activation of signal transducers and activators of transcriptions-3 (STAT-3) (Akira, 1997). Another signaling that activated by IL-6 is gp 130 activates mitogen-activated protein kinase (MAPK), especially extracellular signal-regulated kinases 1/2 (ERK 1/2) signaling pathway (Fig. 1.4). These two signals induce an essential gene expression of anti-apoptotic genes and cytokine/cytokine receptor genes (Rincon, 2012).

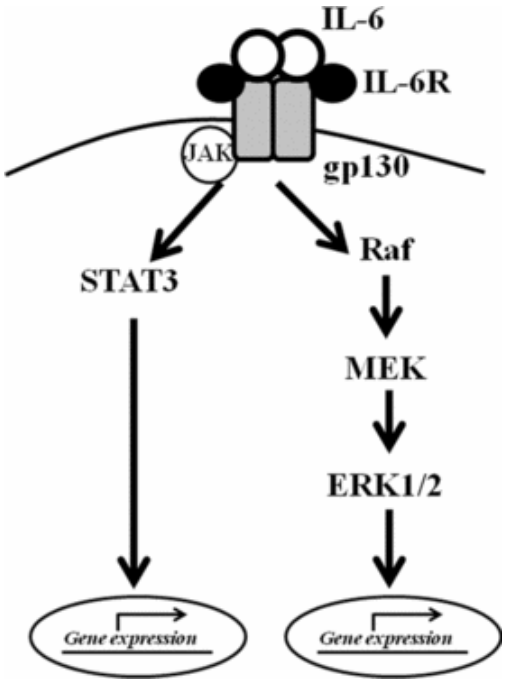

Fig. 1.4: Schematic diagram of the IL-6 signaling pathway, activating the JAK/STAT pathway and the MAPK cascade (Mihara et al., 2012).

2.3.2 Interleukin-8 (IL-8): IL-8, aka neutrophil chemotatic factor (NCF) or neutrophil activating protein (NAP-1), is a pro-inflammatory chemokine encoded polypeptide composed of 99 amino acid precursor protein, which is cleaved to 77 or 72 residue mature functional protein by gene on chromosome 4 (Hebert et al., 1993; Matsushima et al., 1988). IL-8 was produced by macrophages, epithelial cells, and other somatic cells. IL-8 functions as a chemoattractant cytokine and plays a pivotal role in acute inflammation by recruitment and activation of neutrophils in inflamed tissue (Baggiolini et al., 1992). IL-8 is also a potent angiogenic factor. Elevated IL-8 levels have been associated with pathology in a many diseases such as rheumatoid arthritis, dermatitis, respiratory distress syndrome, cystic fibrosis and chronic bronchitis (Baggiolini, 1993). These diseases are all inflammation characterized by neutrophil infiltration and tissue damages (Hoffmann et al., 2002). IL-8 binds to two separate receptors, CXCR1 and CXCR2, a seven-transmembrane G proteins couple receptor (Holmes et al., 1991). After binding, CXCR receptors translocate to the cytoplasmic granule, and then, activate G proteins dissociate into G_{α} and $G_{\beta\gamma}$ subunit (Mukaida, 2003). $G_{\beta\gamma}$ subunit activates phosphatidylinositol 3-kinase (PI3K), which in turn generates phosphatidylinositol 3,4,5-trisphosphate (PIP_3) (Servant et al., 2000). PIP_3 is involved in various cellular processes such as cell survival, cytoskeleton regulation and cell polarization. $G_{\beta\gamma}$ subunit also activates PLC that, in turn, activates PKC/p38 signaling pathway, and also, increases the intracellular Ca^{2+} level (Fig. 1.5).

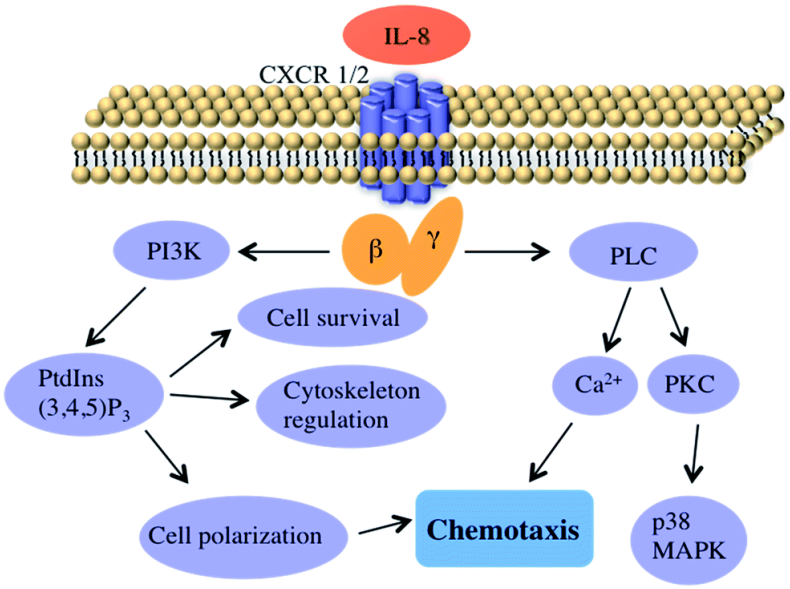

Fig. 1.5: Schematic diagram of the IL-8 signaling pathway in neutrophil chemotaxis (Wu et al., 2014).

2.4 Molecular pathways by which influenza viruses induce cytokine production

It has been reported that expression levels of IL-6 and IL-8 in human lung fibroblast were significantly suppressed by ERK 1/2 and p38 MAPK inhibitors (Hayashi et al., 2000). In the human bronchial epithelial cells, lysophosphatidic acid-induced IL-8 secretion was inhibited by p38 MAPK and c-Jun N-terminal kinases (JNK) inhibitors (Saatian et al., 2006). These findings suggest that the production of IL-6 and IL-8 involve the MAPK signaling mechanism. Consistent with this notion, RSV infection increased the activity of ERK 1/2 and IL-8 production in A549 cells and that pretreatment with ERK 1/2 inhibitor inhibited the production of IL-8 (Chen et al., 2000). Furthermore, in HeLa 229 cells, *Chlamydia trachomatis* infection induced IL-8 mRNA production which is dependent on ERK1/2 but independent of p38 and JNK MAPK (Buchholz et al., 2007). Intracellular Ca^{2+} signaling may also be involved in the mechanism. In the intestinal epithelium, induction of IL-8 secretion by *Salmonella typhimurium* infection required an increase in intracellular [Ca^{2+}] and involved the nuclear factor-κB (NF-κB) signaling pathway (Gewirtz et al., 2000).

The cellular signaling mechanisms induced by influenza virus infection involve activation of the MAPK and the downstream transcription factors NF-κB

(nuclear factor kappa-light-chain-enhancer of activated B cells) (Flory et al., 2000; Kujime et al., 2000; Ludwig et al., 2001; Ludwig et al., 2006; Pahl et al., 1995; Pleschka et al., 2001). It has been reported that, in human bronchial epithelial cells, H3N2 increased p38 MAPK, ERK and JNK and activated production of RANTES (Kujime et al., 2000). The mechanism by which H9N2 regulates IL-1β, IL-6, and IL-8 production in chicken macrophages requires ERK1/2 (Xing et al., 2010). A previous study suggested that both p38 MAPK and ERK1/2 were activated in H5N1-infected human macrophages and that a p38 MAPK inhibitor reduced viral-induced TNF-α expression in this cell type (Lee et al., 2005). Moreover, in human monocyte-derived macrophages, H5N1 activated phosphorylation of p38, ERK 1/2 and JNK and the induction of pro-inflammatory cytokine (Geiler et al., 2011). Taken together, these studies suggest that MAPK signaling is critically important for the mechanism by which H5N1 promotes cytokine production in the respiratory epithelial cells (Fig. 1.6).

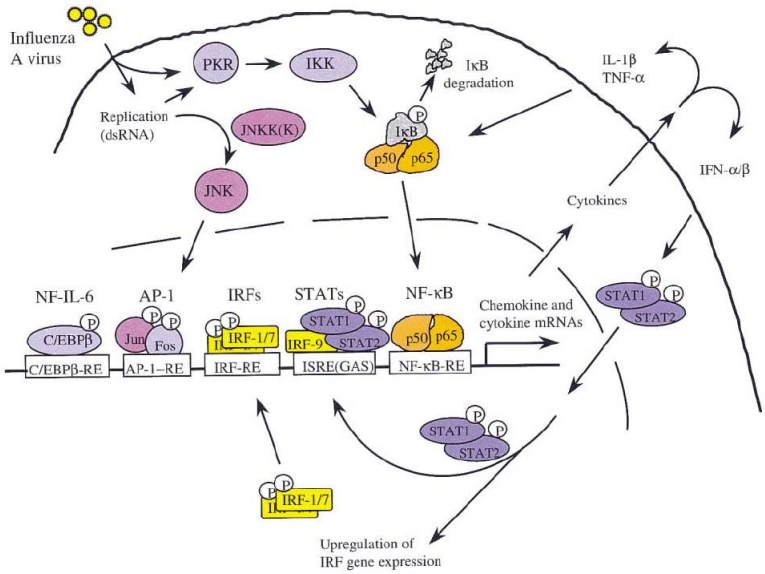

Fig. 1.6: Schematic diagram showing the cellular signalings that induce cytokine production by influenza A virus. Influenza A virus activates transcription factors including NF-κB and activator protein-1 (AP-1). After virus infection, viral replication by dsRNA activates protein kinase R (PKR, dsRNA-activated protein kinase), IκB kinase (IKK) and NF-κB, as well as an activation of MAPK, JNK and AP-1, resulting in the cytokine and chemokine mRNA expression (Julkunen et al., 2001).

3. Purinergic receptors

3.1 Overview of purinergic receptors

Nucleotides (ATP, ADP, UTP and UDP) are important signaling molecules that intermediate various biological effects via plasma membrane receptors named purinergic receptors. Two types of purinergic receptors described as adenosine or P1 receptors, and P2 receptors that activated by extracellular nucleotides, such as ATP, ADP, UTP, and UDP (Burnstock, 2007). P1 receptor is further subdivided into four subtypes A_1, A_{2A}, A_{2B}, and A_3, all of which couple to G proteins. According to the differences in molecular structure and transduction mechanisms, P2 receptor is divided into ionotropic (ligand-gated ion channel) P2X receptors ($P2X_{1-7}$) and metabotropic (G protein-coupled) P2Y receptors (Y_1, Y_2, Y_4, Y_6, Y_{11}, Y_{12}, Y_{13} and Y_{14}) (Burnstock et al., 2004; Erb et al., 2006). The agonist selectivity and signaling properties of purinergic receptors are summarized in Table 1.3.

Table 1.3: Purinergic receptors, their agonists and signaling pathways (Lazarowski et al., 2009)

	Agonist	Signaling
P2X receptors		
$P2X_1$-$P2X_7$	ATP	ATP-gated cation channel
P2Y receptors		
$P2Y_1$	ADP	G_q/PLCβ→Ca^{2+}/PKC
$P2Y_2$	ATP = UTP	G_q/PLCβ→Ca^{2+}/PKC
$P2Y_4$	UTP	G_q/PLCβ→Ca^{2+}/PKC
$P2Y_6$	UDP	G_q/PLCβ→Ca^{2+}/PKC
$P2Y_{11}$	ATP	G_q/PLCβ→Ca^{2+}/PKC and G_s→AC/cAMP
$P2Y_{12}$	ADP	G_i→↓AC/↓cAMP
$P2Y_{13}$	ADP	G_i→↓AC/↓cAMP
$P2Y_{14}$	UDP-glucose	G_i→↓AC/↓cAMP
Adenosine receptors		
A_1, A_3		G_i→↓AC/↓cAMP
A_{2a}, A_{2b}		G_s→AC/cAMP

Gq, Gs, Gi = G protein-coupled receptors; PLC = phospholipase C; PKC = protein kinase C; cAMP = cyclic adenosine monophosphate; AC = adenylyl cyclase; ↓ = inhibition.

The occurrence of ecto-enzymes in many different "extracellular ATP-metabolizing tissues" have indicated possible existence of endogenous ATP regulatory systems via an autocrine or paracrine signaling pathway (Zimmermann, 2000). Whilst nucleotides were traditionally thought to be intracellular metabolites, recent studies suggested extracellular functions of nucleotides as mediators for downstream cellular signaling pathways (Jeter et al., 2004). It is well established that airway epithelial cells are inadequately innervated and receive minimal regulations from the endocrine system. It is, therefore, reasonable to deduce that ATP may serve as a signal transducer within the respiratory system via an autocrine or paracrine pathway. In supporting this notion, the airway epithelial cells release physiological levels of both ATP and UTP in response to mechanical stress (Button et al., 2007; Grygorczyk et al., 1997; Homolya et al., 1999; Okada et al., 2006).

The discovery of several P2Y receptor subtypes, which recognise and respond to uridine nucleotides such as UDP and UTP (Burnstock et al., 2000) has contributed unyielding evidence that UTP may also contribute to autocrine and paracrine signaling. Recent research has revealed that human purinoceptors subtype $P2Y_2$ were responsive to UTP and ATP activation upon receptor binding, whilst $P2Y_4$ and $P2Y_6$ receptors were discriminately responsive to UTP and UDP respectively (Abbracchio et al., 2006). P2Y subtype receptors belong to a superfamily of G protein-coupled receptors. Upon receptor activation, the G_{α}-subunit is dissociated from the $G_{\beta\gamma}$-subunit within the G-protein complex. The dissociated G_{α}-subunit will then stimulate a downstream enzyme: either adenylate cyclase (AC) or PLC (Abbracchio et al., 2006; Chang, 2006). In human respiratory airways, ATP and UTP most typically activate $G_{\alpha q}$-coupled $P2Y_2$ receptors, which then stimulate a PLC-β isoform (PLCβ) (Brown et al., 1991; Cressman et al., 1999; Homolya et al., 1999).

PLC belongs to a class of membrane enzymes that cleaves phospholipids embedded within eukaryotic cell membranes. It plays a vital physiological role in mediating downstream signal transductions which in turns facilitate intracellular molecules, hence producing a physiological response. There are 13 isoforms of mammalian PLC, which can be categorized into six subfamilies (β, γ, δ, ε, ζ, η) based on their structural formation. There are four types of PLCβ protein (PLCβ1-4), which cleaves the phosphatidyl-inositol 4,5-biphosphate (PIP_2) embedded

within the lipid membrane, forming diacyglycerol (DAG) and inositol 1,4,5-triphosphate (IP_3) (Ashby et al., 2002). Subsequent elevation in IP_3 levels then enters into the cytoplasm and stimulates IP_3-sensitive Ca^{2+} channels located on the smooth endoplasmic reticulum, which mobilizes intracellular stores of calcium and increases cytosolic Ca^{2+} concentration (Ashby et al., 2002; Chang, 2006; Clapham, 2007). Induced release of intracellular free Ca^{2+} have multitude subsequent effects, including stimulation of calmodulin (CaM) and its kinases (CaMK), PKC, JNKs and p38 MAPK (Clapham, 2007). Despite being activated by the IP_3 pathway, PKC can also be stimulated directly by the membrane bound DAG, which have a net stimulation on downstream effectors such as phospholipase A2 (PLA_2), an enzyme producing arachidonic acid (Chakraborti, 2003).

3.2 Purinergic receptor and immunoinflammation

It is well established that P2Y receptors are involved in diverse inflammatory disorders. During inflammation of the respiratory tract, extracellular nucleotide concentrations are increased, and the following activation of P2Y receptors mediates the release of IL-6 (Douillet et al., 2006) and IL-8 (Muller et al., 2005) from bronchial epithelial. In human THP-1 monocytic cells, UDP induced IL-8 production and this effect of UDP was attenuated by antagonists or antisense oligonucleotides directed against $P2Y_6$. Moreover, in 1321N1 astrocytoma cells, activation of $P2Y_6R$ is essential for UDP-mediated IL-8 release (Warny et al., 2001). Moreover, $P2Y_6$ receptor activation is involved in the mechanism by which UDP induced the productions of IL-8, TNF-α, MCP-1 and IP-10 (Cox et al., 2005). Furthermore, the effect of lipopolysaccharide (LPS) on the production of IL-8 was inhibited by apyrase, an enzyme that hydrolyzes nucleotide triphosphates and diphosphates, suggesting the effect of LPS on IL-8 production is mediated by purinergic signaling in an autocrine fashion (Warny et al., 2001). These findings emphasize the physiological significant of the purinergic signaling in the inflammatory responses.

Objectives and Hypotheses

Objective 1: To investigate the infection-independent effect of avian influenza virus H5N1 on cytokine/chemokine gene expression in human respiratory epithelium.

Hypothesis 1: Avian influenza virus H5N1 can rapidly increase production of cytokines and chemokines in human respiratory epithelial prior to the onset of infection and viral propagation.

Objective 2: To determine the mechanism by which structural protein (or proteins) of H5N1 activate(s) cytokine and chemokine gene expression in human respiratory epithelium.

Hypothesis 2.1: The effect of the inact-H5N1 on cytokine and chemokine productions is mediated by the viral hemagglutinin and that an interaction between the hemagglutinin and the α-2,3 sialic acid receptors at the host cell membrane is essential to mediate this effect of the virus.

Hypothesis 2.2: The signaling mechanism by which the inact-H5N1 induces cytokine and chemokine production in the respiratory epithelium involves purinergic receptor signaling.

Hypothesis 2.3: The effect of inact-H5N1 on cytokine and chemokine productions in the respiratory epithelium is mediated via MAPK signaling pathway.

CHAPTER 2

MATERIALS AND METHODS

1. Materials and equipments

1.1 Cell culture

The human bronchial epithelial cell line, 16HBE14o- cells, was kindly provided by Assoc. Prof. Dr. Anuwat Dinudom (University of Sydney, New South Well, Australia). HBE were grown in Minimum Essential Medium (MEM) supplemented with 10% heat-inactivated fetal bovine serum (FBS), 2 mM L-glutamine and 100 U/ml penicillin-streptomycin (pen/strep). Cells were maintained in a 25-cm^2 T-flask (Corning, New York, U.S.A.) under humidified atmosphere containing 5% CO_2 at 37°C and subcultured before they reach 80% confluence. For cytokine mRNA expression experiments, cells were seeded on a 24-well culture plate at a density of 2×10^5 cells/well and grown in culture medium. One day after seeding, cells were washed twice with PBS and then replaced with serum free medium for 18-24 hr before the experiment. For Ussing chamber studies, cells were seeded on a Snapwell (Corning) at a density of 3×10^5 cells/well and grown in culture medium. Twenty four hours after seeding, cells were washed with spent media, removed and then replaced with 100 µl of fresh media on the apical side of the Snapwell and 1.5 ml of the media in bottom compartment. This was then repeated every 48 hr. Monolayers were incubated for 4-5 days until tight junctions are developed.

1.2 Preparations of inactivated-H5N1 (inact-H5N1) avian influenza virus

H5N1 virus used in this study was prepared by Asst. Prof. Dr. Arunee Thitithanyanont with an assistance of Ms. Suwimon Wiboon-ut in a Bio-safety level 3 (BSL-3) facilities of the Department of Microbiology, Mahidol University. The avian influenza virus (A/open-billed stork/Nakhonsawan/BBD010 4F/04; H5N1) was produced in embryonated chicken eggs (ECEs) obtained from the Bureau of Veterinary Biologics, Department of Livestock Development, Nakhonratchasima,

Thailand. The virus was grown and replicated in ECEs (5 pfu/egg) incubated at 37°C for 37-38 hr. The allantoic and amniotic fluids were subsequently harvested from the ECEs, pooled then spun at 4,000 rpm for 5 min at 4°C. All pellets obtained were pooled and treated with 1.5 M NaCl for 1 hr at 4°C. The virus in the pellet were then recovered by centrifugation at 4,000 rpm for 5 min at 4°C, the supernatant collected to measure HA and PFU titers and subsequently filtered through a 0.8 μM-filter membrane. The virus was concentrated by filtering with a Labscale Tangential Flow Filtration System (Millipore, Darmstadt, Germany) with a 1,000 KDa MWCO membrane cassette (PelliconXL, Millipore, Darmstadt, Germany). The virus was then inactivated with 0.1% β-propiolactone (BPL) at 37°C for 2 hr and purified by ultrafiltering with 50 KDa MWCO membrane (Amicon Ultra-15, Millipore, Darmstadt, Germany). Infectivity test was performed by adding the purified BPL-inactivated H5N1 to MDCK cell culture and the cytopathic effect determined. The quantity of HA was determined by hemagglutination ELISA kit (Sino Biological, Beijing, China).

1.3 Chemicals

1. 2′(3′)-O-(4-Benzoylbenzoyl) adenosine 5′-triphosphate (BzATP), B6396, Sigma, St. Louis, Missouri, U.S.A.
2. 4',6-diamidino-2-phenylindole (DAPI), 268298, Calbiochem, Darmstadt, Germany.
3. α 2,3-sialidase, 4455, Takara Bio, Inc., Shiga, Japan.
4. A/Vietnam/1203/2004 (H5), 3006, Protein Sciences Corp., Meriden, Connecticut, U.S.A.
5. Absolute ethanol AR grade, A-3581, Labscan Asia, Bangkok, Thailand.
6. Acrylamide, A8887, Sigma, St. Louis, Missouri, U.S.A.
7. Adenosine, A9251, Sigma, St. Louis, Missouri, U.S.A.
8. Adenosine 5'-diphosphate (ADP), A4386, Sigma, St. Louis, Missouri, U.S.A.

9. Adenosine 5'-triphosphate (ATP), A7699, Sigma, St. Louis, Missouri, U.S.A.
10. AllStars negative control siRNA (scramble siRNA), 1027280, Qiagen, Venlo, Limburg, Netherlands.
11. Ammonium persulfate, 2300, Calbiochem, Darmstadt, Germany.
12. Apyrase, A6410, Sigma, St. Louis, Missouri, U.S.A.
13. BAPTA-AM, B6769, Molecular Probes Inc, Leiden, Netherlands.
14. Bisindolymaleimide II (BIM), 4128, Tocris Bioscience, Bristol, U.K.
15. Bovine serum albumin (BSA), 126579, Calbiochem, Darmstadt, Germany.
16. Bradford protein assay, 500-0006, Bio-Rad, Hercules, California, U.S.A.
17. Calcium chloride ($CaCl_2$), C3881, Sigma, St. Louis, Missouri, U.S.A.
18. CFTR(inh)-172, C2992, Sigma, St. Louis, Missouri, U.S.A.
19. CFTR antibody, M3A7, Thermo Scientific, Massachusetts, U.S.A.
20. CFTR siRNA, 1027416, Qiagen, Venlo, Limburg, Netherlands.
21. Chroloform AR grade, A-3505, Labscan Asia, Bangkok, Thailand.
22. Cytochalasin D, C8273, Sigma, St. Louis, Missouri, U.S.A.
23. Deoxyribonuclease I (DNase I), EN0521, Thermo Scientific, Massachusetts, U.S.A.
24. D-glucose, G8270, Sigma, St. Louis, U.S.A.
25. Diethyl pyrocarbonate (DEPC), DB0154, Bio Basic Inc, Markham, Ontario, Canada.
26. Dimethyl sulfoxide (DMSO), D2650, Sigma, St. Louis, Missouri, U.S.A.
27. DOG1/TMEM16A antibody, NBP1-19037, Novus Biologicals, Littleton, Colorado, U.S.A.
28. ECL anti-rabbit IgG, NA9340, GE Healthcare, Buckinghamshire, U.K.
29. EmbryoMax® ultrapure water with 0.1% gelatin, ES-006-B, Millipore, Darmstadt, Germany.
30. Fetal bovine serum (FBS), 43640, J R Scientific Inc, Woodland, California, U.S.A.

31. Fluorescein *maackia amurensis* lectin (MAL I), FL-1311, Vector Laboratories, Burlingame, California, U.S.A.
32. Fluorescein *sambucus nigra* (Elderberry) bark lectin, FL-1301, Vector Laboratories, Burlingame, California, U.S.A.
33. GÖ6976, 2253, Tocris Bioscience, Bristol, U.K.
34. Glycine, 161-0724, Bio-Rad, Hercules, California, U.S.A.
35. H5 (H5N1) (A/Vietnam/1203/2004), IT-003-0051p, Immune Technology Corp., New York, U.S.A.
36. HEPES, H3375, Sigma, St. Louis, U.S.A.
37. HEPES sodium salt, H3784, Sigma, St. Louis, U.S.A.
38. Hexokinase, H4502, Sigma, St. Louis, Missouri, U.S.A.
39. iScript™ select cDNA synthesis Kit, 170-8897, Bio-Rad, Hercules, California, U.S.A.
40. Isopropanol AR grade, A-3515, Labscan Asia, Bangkok, Thailand.
41. JAK 3 inhibitor VI, 856436-16-3, Calbiochem, Darmstadt, Germany.
42. L-Glutamine solution, 82700, J R Scientific Inc, Woodland, California, U.S.A.
43. Lipofectamine™ 2000 reagent, 11668-019, Invitrogen, Carlsbad, California, U.S.A.
44. Luminata™ crescendo western HRP substrate (ECL), WBLUR0100, Merck Millipore, Darmstadt, Germany.
45. Magnesium chloride ($MgCl_2$), M2670, Sigma, St. Louis, Missouri, U.S.A.
46. Methanol, 1060092500, Merck Millipore, Darmstadt, Germany.
47. Minimum essential medium (MEM), 41500-034, GIBCO, Carlsbad, California, U.S.A.
48. MRS2179, 0900, Tocris Bioscience, Bristol, U.K.
49. MRS2578, M0319, Sigma, St. Louis, Missouri, U.S.A.
50. *N,N*-Methylenebisacrylamide, M7256, Sigma, St. Louis, Missouri, U.S.A.
51. OmniPur® WFI quality water, 7732-18-5, Calbiochem, Darmstadt, Germany.

52. $P2Y_6R$ siRNA, 1027416, Qiagen, Venlo, Limburg, Netherlands.
53. p38 MAPK antibody, 8690, Cell Signaling Tech, Danvers, Massachusetts, U.S.A.
54. p44/42 MAPK (Erk1/2) antibody, Cell Signaling Tech, Danvers, Massachusetts, U.S.A.
55. Paraformaldehyde, 818715, Merck Millipore, Darmstadt, Germany.
56. PD98059, 1213, Tocris Bioscience, Bristol, U.K.
57. Penicillin/streptomycin solution (pen/strep), 20001, J R Scientific Inc, Woodland, California, U.S.A.
58. Phosphatase inhibitor cocktail set II, 524625, Calbiochem, Darmstadt, Germany.
59. Phospho-p38 MAPK antibody, 4511, Cell Signaling Tech, Danvers, Massachusetts, U.S.A.
60. Phospho-p44/42 MAPK (Erk1/2) antibody, 4370, Cell Signaling Tech, Danvers, Massachusetts, U.S.A.
61. Potassium chloride (KCl), P3911, Sigma, St. Louis, Missouri, U.S.A.
62. Precision plus protein standards (Kaleidoscope), 161-0375, Bio-Rad, Hercules, California, U.S.A.
63. Protease inhibitor cocktail tablets, 04693159001, Roche Applied Science, Mannheim, Germany.
64. SB203580, 1202, Tocris Bioscience, Bristol, U.K.
65. SN-50, 481480, Calbiochem, Darmstadt, Germany.
66. Sodium bicarbonate ($NaHCO_3$), S5761, Sigma, St. Louis, Missouri, U.S.A.
67. Sodium chloride (NaCl), 106404, Merck Millipore, Darmstadt, Germany.
68. Sodium dodecyl sulfate (SDS), L5750, Sigma, St. Louis, Missouri, U.S.A.
69. SP600125, 1496, Tocris Bioscience, Bristol, U.K.
70. Suramin, S2671, Sigma, St. Louis, Missouri, U.S.A.
71. SYBR® select master mix, 4472908, Applied, Biosystems, Carlsbad, California, U.S.A.

72. T16Ainh-A01, 4538, Tocris Bioscience, Bristol, U.K.
73. Tetramethylethylenediamine (TMED), 8920, Calbiochem, Darmstadt, Germany.
74. TMEM16A siRNA, 1027416, Qiagen, Venlo, Limburg, Netherlands.
75. Trizama® base, T1503, Sigma, St. Louis, Missouri, U.S.A.
76. Trizol reagent, 15596-029, Invitrogen, Carlsbad, California, U.S.A.
77. Trypsin 0.25% solution, 82702, J R Scientific Inc, Woodland, California, U.S.A.
78. U73122, 1268, Tocris Bioscience, Bristol, U.K.
79. Uridine 5'-diphosphate (UDP), U4625, Sigma, St. Louis, Missouri, U.S.A.
80. Uridine 5'-triphosphate (UTP), U6750, Sigma, St. Louis, Missouri, U.S.A.

1.4 Equipments

1. Balance, Model 1000C-3000D, Precisa, Dietikon, Switzerland.
2. Balance, Model Mettler AE 240, American Instrument Exchange, Illinois, U.S.A.
3. Centrifuge, Model 5424R, Eppendorf, Hamburg, Germany.
4. CO_2 incubator, Model 2323-2, Shel lab, Cornelius, Oregon, U.S.A.
5. Electrophoresis system, Model mini-protein® tetra cell, Bio-Rad, Hercules, California, U.S.A.
6. Inverted microscope, Model Eclipse TS100-F, Nikon Instruments, Tokyo, Japan.
7. Laminar flow, Clean model: V6, Lab Service, Bangkok, Thailand.
8. Mac Lab, Model MacLab/4s, ADInstruments, New South Wales, Australia.
9. Magnetic stirrer, Model Cole-Palmer 9×9 aluminum, American Instrument Exchange, Illinois, U.S.A.
10. Micro-Ussing chamber, Model P2300, Physiologic Instruments, San Diego, U.S.A.

11. NanoDrop®, Model ND-1000, Thermo Scientific, Massachusetts, U.S.A.
12. pH meter, Model pH900, Precisa, Dietikon, Switzerland.
13. Pipette filler, Model Powerpette® pro, Jencons Scientific, Franklin, Tennessee, U.S.A.
14. Pipetman, Model P10, P20, P100 and P1000, Gilson, Villiers-le-Bel, France.
15. Power supply, Model powerpac basic, Bio-Rad, Hercules, California, U.S.A.
16. Thermal cycler, Model PTC-100TM, MJ Research, Inc. , Waltham, Massachusetts, U.S.A.
17. Touch™ Real-Time PCR Detection System, Model CFX96, Bio-Rad, Hercules, California, U.S.A.
18. Ultra-microbalance, Model MC5, Sartorius, Goettingen, Germany.
19. Vortex mixer, Model VX-100, Labnet, New Jersey, U.S.A.

2. Methods

2.1 Reverse transcriptase-PCR (for detail see Appendix C)

Total RNA was extracted from cells using TRIzol Reagent according to the manufacturer's instruction. After treatment with DNase I (Thermo), 1 µg of the treated-RNA was reverse transcribed to cDNA using iScript™ select cDNA synthesis kit (Bio-Rad) by a thermal cycler (model PTC-100TM, MJ Research, Inc. , Waltham, Massachusetts, U.S.A.), which were further amplified by real-time PCR. The sense and antisense primers for real-time PCR were presented in Table 2.1. The real-time PCR reactions were performed in duplicate using SYBR select master mix (Applied, Biosystems) on a CFX96 Touch™ Real-Time PCR Detection System (Bio-Rad, Hercules, California, U.S.A.). The PCR conditions were 50°C for 2 min and then 95°C for 2 min, followed by 40 cycles of 95°C for 15 sec and 60°C for 1 min. The GAPDH gene was used as an endogenous control for normalization. The comparative delta-delta C_T method was used to analyze the results with the expression level of the respective gene.

Table 2.1 Primers used for real-time PCR experiments

Gene	Accession No.	Forward and Reverse Primers	Product length (bp)	Cycles
IL-6	NM_000600	5'-GAACTCCTTCTCCACAAGCG-3'	120	40
		5'-GCGGCTACATCTTTGGAATC-3'		
IL-8	NM_000584	5'-CCAACACAGAAATTATTGTAAAGC-3'	113	40
		5'-TGAATTCTCAGCCCTCTTCAA-3'		
TNF-α	NM_000594	5'-AGCCCATGTTGTAGCAAACC-3'	134	40
		5'-TGAGGTACAGGCCCTCTGAT-3'		
CCL-5/RANTES	NM_002985	5'-TACCATGAAGGTCTCCGC-3'	199	40
		5'-GACAAAGACGACTGCTGG-3'		
CXCL-10/IP-10	NM_001565	5'-TTCAAGGAGTACCTCTCTCTAG-3'	177	40
		5'-CTGGATTCAGACATCTCTTCTC-3'		
P2Y6R	NM_001277208	5'-CCACAGGCATCCAGCGTAAC-3'	106	40
		5'-AGGAAGCCGATGACAGTGAGAG-3'		
TMEM16A	NM_018043	5'-GCAAACATGGAGGACCACTT-3'	148	40
		5'-GCCGTATTACCAGCCATCAT-3'		
CFTR	NM_000492	5'-CACTCCTCATGGGGCTAATCT-3'	142	40
		5'-CTGATCTTCCCAGCTCTCTGA-3'		
GAPDH	NM_001289746	5'-ATGACATCAAGAAGGTGGTG-3'	177	40
		5'-CATACCAGGAAATGAGCTTG-3'		

2.2 Transfection of siRNA (for detail see Appendix D)

On the day of transfection, after trypsinized, HBE cells were transfected with 100 pmol $P2Y_6R$ siRNA (Qiagen) or TMEM16A siRNA (Qiagen) or CFTR siRNA (Qiagen) using Lipofectamine^{TM} 2000 (Invitrogen) according to the manufacturer's instructions, and then, seeded on a 24-well culture plate at a density of 2.5×10^5 cells/well and grown in MEM medium without antibiotics. AllStars negative control siRNA (Qiagen) was used as a negative control and was introduced into the cells using the same protocol. One day after transfection and seeding, cells were washed with PBS and then replaced with serum free medium for 18-24 hr. before the experiment.

2.3 Protein extraction and Western blot analysis (for detail see Appendix E)

16HBE14o- cells were seeded on a 12-well culture plate at a density of 5×10^5 cells/well. One day after seeding, cells were washed twice with PBS and incubated in serum free medium for 18-24 hr before the experiment. Total proteins from cells were extracted with RIPA buffer (Merck) containing protease inhibitor (Roche) and phosphatase inhibitor (Calbiochem). The protein concentration in all samples was determined by Bradford protein assay (Bio-Rad) at wavelength 595 nm, using bovine serum albumin (BSA) as the standard. Equal amounts of protein samples (30 μg) were mixed with 2X sample-loading buffer and denatured by boiling for 5 min. The samples were separated by SDS-PAGE (12% polyacrylamide). Following electrophoretic separation, proteins were transferred to PVDF membranes. The membranes were then incubated for 1 hr at room temperature in TBST containing 5% fat-free milk. After the blocking step, membranes were incubated overnight at 4°C with primary antibody against phospho-ERK1/2 (cell signaling) at 1:2000 dilution, total-ERK1/2 (cell signaling) at 1:2000 dilution, phospho-p38 MAPK (cell signaling) at 1:1000 dilution or total-p38 MAPK (cell signaling) at 1:2000 dilution. After four washes with TBST (5 min each), membranes were incubated with horseradish peroxidase-conjugated goat anti-rabbit IgG (GE Health Science) at 1:5000 dilution. The membranes were washed several times with TBST and developed using ECL reagent, and then, exposed to green X-ray film (Kodak).

2.4 Confocal immunofluorescent staining

16HBE14o- cells were seeded on a slide chamber at a density of 1 × 10^4 cells/well. Two days after seeding, the culture medium was removed, and cells were washed twice with PBS and fixed in 4% paraformaldehyde for 10 min and then incubated in blocking solution (1% BSA) for 1 hr. After blocking the nonspecific binding, cells were incubated overnight at 4°C with 1:100 rabbit anti-human TMEM16A antibody (Novus Biologicals) or 1:50 mouse anti-human CFTR antibody. After labeling, cells were washed three times with PBS and then incubated with 1:1000 Alexa Fluo 488-conjugated mouse anti-rabbit secondary antibody (green signal) or Alexa Fluo 568- conjugated goat anti-mouse secondary antibody (red signal) for 1 hr at room temperature. Negative control was obtained by incubating cells with secondary antibody in the absence of primary antibody. Cells were washed 2 times with PBS and then incubated with DAPI for 5 min to stain the cell nuclei (blue) at a concentration of 1μg/ml. For sialic acid staining, cells were chilled to 4ºC, and then 10 μg/ml lectin (MAA for α-2,3 or SNA for α-2,6 sialic acid receptor) in MEM was added to cells. Cells were incubated at 4ºC for 20 min, rinsed 3 times with PBS, and then fixed with 4% paraformaldehyde. Cells were washed 2 times with PBS and then incubated with DAPI for 5 min to stain the cell nuclei (blue) at a concentration of 1 μg/ml. Fluorescent imaging was performed by confocal laser-scanning microscope (model FV1000; Olympus, Tokyo, Japan).

2.5 Short-circuit current experiments

A conventional Ussing chamber technique was used to determine the equivalent short-circuit current (I_{sc}), representing ion transport property, of 16HBE14o- cell monolayer in open-circuit conditions. Ussing chamber was separated into two compartments, apical and basolateral, divided by a monolayer of epithelial sheet. The temperature inside the tissue chamber was maintained at 37°C and each compartment was continuously bubbled with air to provide a constant O_2 pressure and to circulate the bathing solution. Voltage and current electrodes were inserted into the chamber to measure transepithelial potential difference (V_{te}) and to apply short current pulses, respectively. Transepithelial resistance (R_{te}) was

determined by applying short current pulses of 3 μA and both R_{te} and the equivalent short-circuit current (I_{sc}) was calculated according to Ohm's law (V = IR).

2.5.1 Bathing solutions

HEPES buffer solution contained (in mM): NaCl (130), KCl (4), H-HEPES (5), Na^+-HEPES (5), $MgCl_2$ (1), $CaCl_2$ (1) and glucose (5). The solution was adjusted to pH 7.4.

2.5.2 Ussing chamber setup

A pair of $Ag/AgCl_2$ electrodes connected to 3 M KCl agar bridge (4% agar) was inserted into the tissue chamber to measure transepithelial potential difference (V_{te}). The chamber was connected to a MacLab/4s data acquisition system (ADInstruments, Dunedin, New Zealand) and a high impedance device (University of Sydney) to prevent current drawn from equipment in the circuit. V_{te} was monitored continuously, with reference to the basolateral side of the epithelium by a Chart V 5.4 program. Transepithelial resistance (R_{te}) was determined by applying short (200 ms) current pulses (3 μA, every 6 s) to obtain voltage deflections using for calculating R_{te}. V_{te} was allowed to stabilize for at least 10 min before treatments.

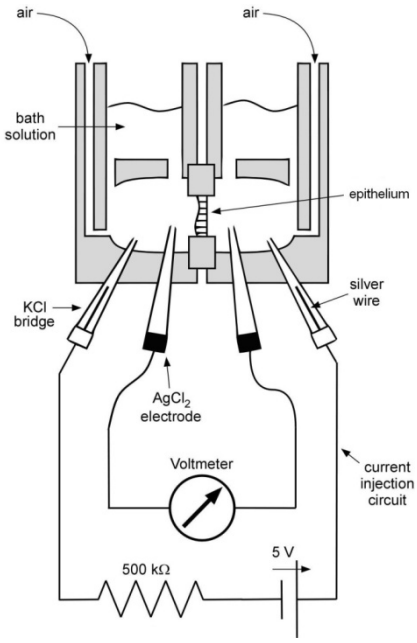

Fig. 2.1: Diagram of electrical measurements in Ussing chamber system in this study (courtesy from Cook's laboratory, University of Sydney, New South Well, Australia).

2.5.3 Measurements of short-circuit currents

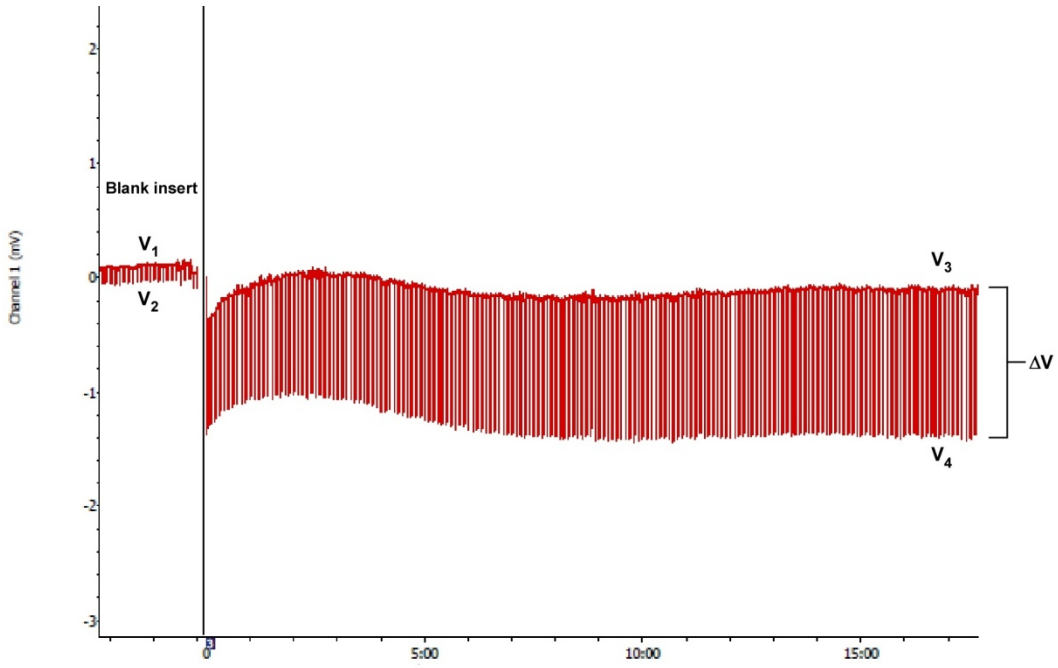

Fig. 2.2: Original recording from Ussing chamber showing the transepithelial potential difference of 16HBE14o- monolayer.

2.5.3.1 Calculation of the resistance of blank insert (R_b)

R_b ($\Omega.cm^2$) = $[V_1 - V_2] / I$

when R_b = resistance of blank insert

V_1 = offset voltage obtained with a blank insert

V_2 = offset voltage during applying current pulses (I)

I = injected current (3µA)

2.5.3.2 Calculation of the total transepithelial resistance (R_{te})

$R_{te}(\Omega.cm^2)$ = $R_i - R_b$

$R_i(\Omega.cm^2)$ = $[V_3 - V_4] / I$

$R_{te}(\Omega.cm^2)$ = $\{[V_3-V_4]/I\} - \{[V_1-V_2]/I\}$

when R_i = resistance of insert containing cell monolayer

V_3 = transepithelial potential (V_{te})

V_4 = V_{te} during applying the current pulses (I)

2.5.3.3 Calculation of the equivalent short-circuit current (I_{sc})

$$I_{sc}\ (\mu A/cm^2) = V / R$$
$$= [V_1 - V_3] / R_{te}$$

3. Experimental protocols

3.1 The effect of inact-H5N1 on cytokine/chemokine mRNA expression in 16HBE14o- cells

To determine the cytokine/chemokine mRNA expressions in response to inact-H5N1, 16HBE14o- cells were exposed to inact-H5N1, at a concentration equivalent to 20 μg/ml H5 hemagglutinin for 3, 6, and 12 hr. At the end of exposure period, cells were harvested and assay for analysis of TNF-α, IL-6, IL-8, CCL-5 and IP-10 mRNA expressions. The data were compared with the negative control, allantoic fluid. The expression level of mRNA was determined by qPCR as described in 2.1.

3.2 Determination of the cellular signaling pathway responsible for the effect of inact-H5N1 in 16HBE14o- cells

To identify the cellular signaling effectors involved with pharmacological blockers, 16HBE14o- cells were incubated for 1 hr in serum free medium with appropriate pharmacological inhibitors. Thereafter, cells were exposed to virus and/or allantoic fluid for 3 hr. The mRNA expression levels of the interested cytokines and chemokines in these cells were determined as described in 2.1. The pharmacological inhibitors used included: 1 U/ml α,2-3 specific sialidase, 100 μM suramin, 20 μM MRS2179, 10 μM MRS2578, 2U/ml apyrase, 10 μM U73122, 50 μM BAPTA-AM, 1μM BIM, 10 μM GÖ6976, 10 μM SB203580, 50 μM PD98059, 10 μM SP600125, 10 μM SN-50, 760 nM JAK3 inhibitor, 30 μM T16Ainh-A01, and 20 μM CFTR(inh)-172.

To confirm the role of $P2Y_6R$ and TMEM16A in H5N1-mediated cytokine production, expression of the $P2Y_6R$ or TMEM16A in 16HBE14o- cells were knockdown with appropriate siRNAs two days before the experiment.

Thereafter, cells were exposed with the virus and/or allantoic fluid for 3 hr. The mRNA expression level in virus-treated cells was then determined.

4. Statistical analysis

All data are expressed as mean ± standard error (S.E.M.). Statistical difference was obtained using the unpaired Student's *t*-test and $p < 0.05$ are considered to be statistically significant.

CHAPTER 3

RESULTS

1. Inactivated-H5N1 induces cytokine/chemokine mRNA expression in human respiratory epithelium

1.1 The effect of inact-H5N1 on cytokine/chemokine mRNA expression in 16HBE14o- cells

To investigate the effect of inact-H5N1 on cytokine/chemokine mRNA expression in human respiratory epithelium, 16HBE14o- cells were exposed to the inact-H5N1 (20 μg/ml hemagglutinin) for 3, 6, or 12 hr and mRNA expressions of the cytokines and chemokines of interest were analysed by qRT-PCR. Data depicted in Fig. 3.1 suggest that the inact-H5N1 has no effect on mRNA expression of CCL-5 (Fig. 3.1B) or IP-10 (Fig. 3.1C). The level of mRNA expression of TNF-α at 3 hr after exposure to the virus, however, decreased significantly ($p < 0.01$), when compared with that of the cells treated with allantoic fluid, but was not significantly different from that of the control untreated cells (Fig. 3.1A). Of note, at this time point, mRNA expression level of TNF-α in cells treated with allantoic fluid or inact-H1N1 was significantly higher than that of the untreated cells. No significant effects of the virus, allantoic fluid or inact-H1N1 were observed at 6 or 12 hr. Interestingly, inact-H5N1 increased mRNA expression level of IL-6 (Fig. 3.2) and IL-8 (Fig. 3.3). An increased mRNA expression of IL-6 to 16.76 ± 1.99 fold (n = 3, $p < 0.001$) was detected at 3 hr after exposure to the virus followed by a decline to 8.61 ± 2.37 fold (n = 3, $p < 0.05$) at 6 hr and returned to a level not significantly different from the baseline level (1.64 ± 0.47 fold, n = 3) at 12 hr after exposure (Fig. 3.2). Three hours after the cells were treated with the inact-H5N1, mRNA expression of IL-8 was increased to 22.17 ± 4.10 fold (n = 3, $p < 0.01$). This effect of the inact-H5N1 reached a maximum level (50.22 ± 10.8 fold, n = 3, $p < 0.01$) 6 hr after the cells were exposed to the virus before declining to 20.11 ± 5.26 fold (n = 3, $p < 0.01$) at 12 hr (Fig. 3.3). No effect of the inact-H1N1 on mRNA expression of any cytokines or chemokines of interest was observed except its effect on mRNA expression of TNF-α

at 3 hr after exposure (Figs. 3.1, 3.2 & 3.3).

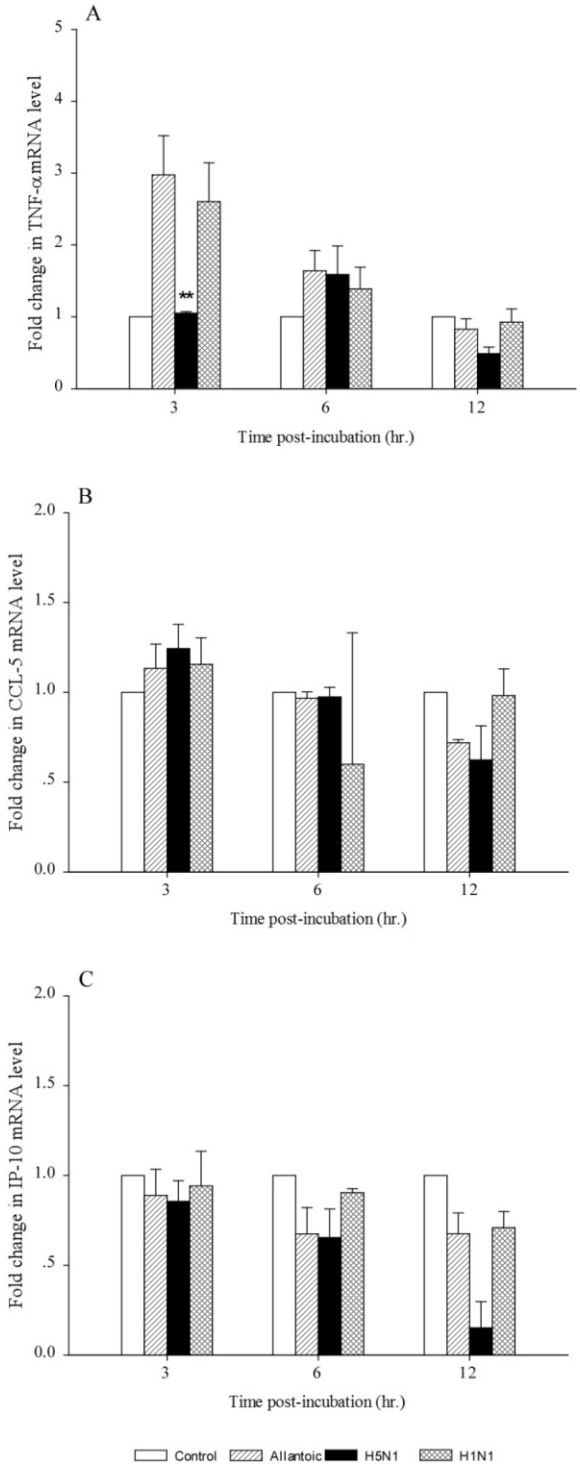

Fig. 3.1: mRNA expression level of TNF-α (A), CCL-5 (B) and IP-10 (C) in 16HBE14o- cells at 3 hr, 6 hr or 12 hr after-exposure to allantoic fluid, inact-H5N1, inact-H1N1 or untreated control. Values are means ± SEM (n = 3). ** indicates $p < 0.01$ compared with that of the cells treated with allantoic fluid (unpaired Student's *t*-test).

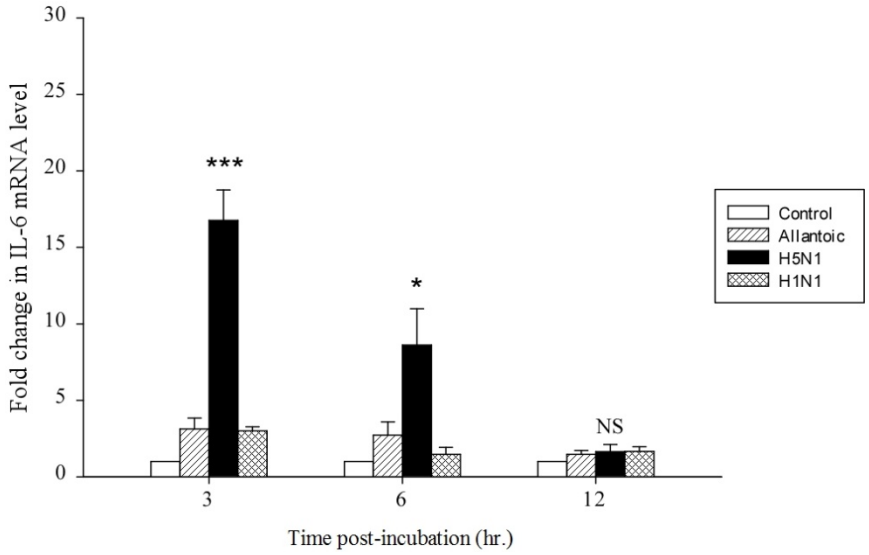

Fig. 3.2: mRNA expression level of IL-6 in 16HBE14o-. Cells were incubated with allantoic fluid, inact-H5N1, inact-H1N1 or untreated (control). Values are means ± SEM (n = 3).
*, *** and NS indicates $p < 0.05$, $p < 0.001$ and no statistical difference compared with data from the group treated with allantoic fluid (unpaired Student's *t*-test).

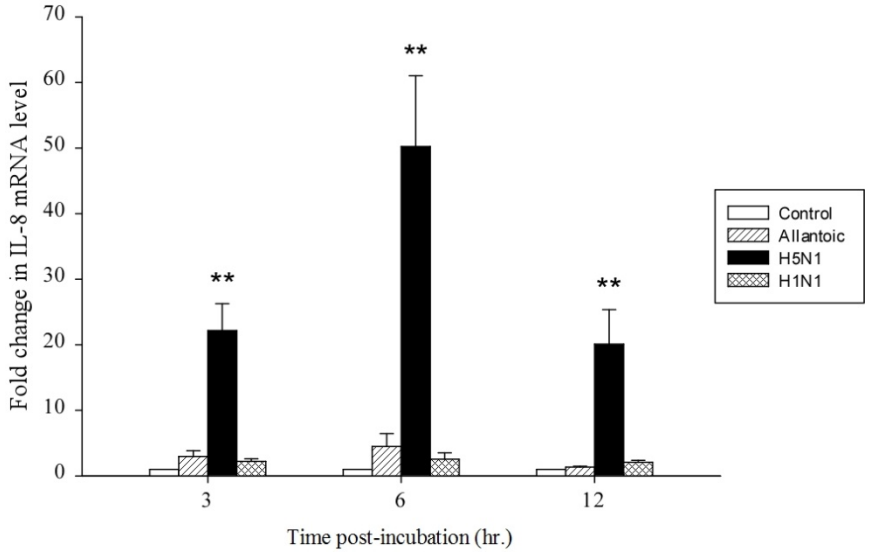

Fig. 3.3: mRNA expression level of IL-8 in 16HBE14o-. Cells were treated with allantoic fluid, inact-H5N1, inact-H1N1 or untreated (control). Values are means ± SEM (n = 3).
** indicates $p < 0.01$ compared with data from the group treated with allantoic fluid (unpaired Student's *t*-test).

1.2 α-2,3 sialic acid receptor is required for inact-H5N1-induced IL-6 and IL-8 mRNA expression

It is well established that the interaction between hemagglutinin (HA) of H5N1 and α-2,3 sialic acid receptor at the host cell membrane is critical for pathogenesis of H5N1 infection. Interestingly, it has been reported that H5-HA is directly responsible for increasing transcription of IP-10 and IRF-1 (Xu et al., 2012) and translation of IL-8 and CCL-5 (Cheng et al., 2010) in A549 human pulmonary epithelial cells. To investigate whether the effect of inact-H5N1 on IL-6 and IL-8 mRNA expression observed in this study requires H5HA/sialic acid receptor interact, 16HBE14o- cells were treated with 1 U/ml sialidase for 1 hr, to inactivate the α-2,3 sialic acid receptor, before being exposed to inact-H5N1. Expression of IL-6 and IL-8 mRNA were analysed 3 hr after the cells were treated with the inact-virus. In cells treated with sialidase, the effects of the inact-H5N1 on mRNA expression of IL-6 (Fig. 3.4A) and IL-8 (Fig. 3.4B) were reduced by 60% ($n = 4$, $p < 0.001$) and 40% ($n = 4$, $p < 0.01$), respectively. To confirm the presence of α-2,3 receptor, 16HBE14o- cells were stain with MAL I, a leucoagglutinin that binds to α-2,3sialic acid receptor, or SNA, a leucoagglutinin that binds to α-2,6 sialic acid receptor, both of which were tagged with fluorescein (FITC). Fluorescent lectin labeled cells were then analysed by confocal microscopy. As depicted in Fig 3.5, the cells were stained with both MAL I (Fig. 3.5B) and SNA (Fig. 3.5E) indicating the presence of both α-2,3 and α-2,6 sialic acid receptors in this cell type. To determine whether the effect of the inact-H5N1 on mRNA expression of IL-6 and IL-8 was mediated by H5-HA, the cells were treated with two commercial hemagglutinin, H5HA-1 (Immune Technology Corp.) or H5HA-2 (Protein Sciences Corp.). These H5HAs, however, failed to alter mRNA expression of IL-6 (Fig 3.6A) or IL-8 (Fig. 3.6 B).

To explore a role of actin cytoskeleton on the mechanism by which inact-H5N1 induces IL-6 and IL-8 mRNA expression, 16HBE14o- cells were treated with 2 μM cytochalasin D, an actin depolymerizer. Under these conditions the effect of the inact-H5N1 virus on mRNA expression of IL-6 and IL-8 was reduced by 60% ($n = 3$, $p < 0.001$) and 75% ($n = 3$, $p < 0.001$), respectively (Fig. 3.4).

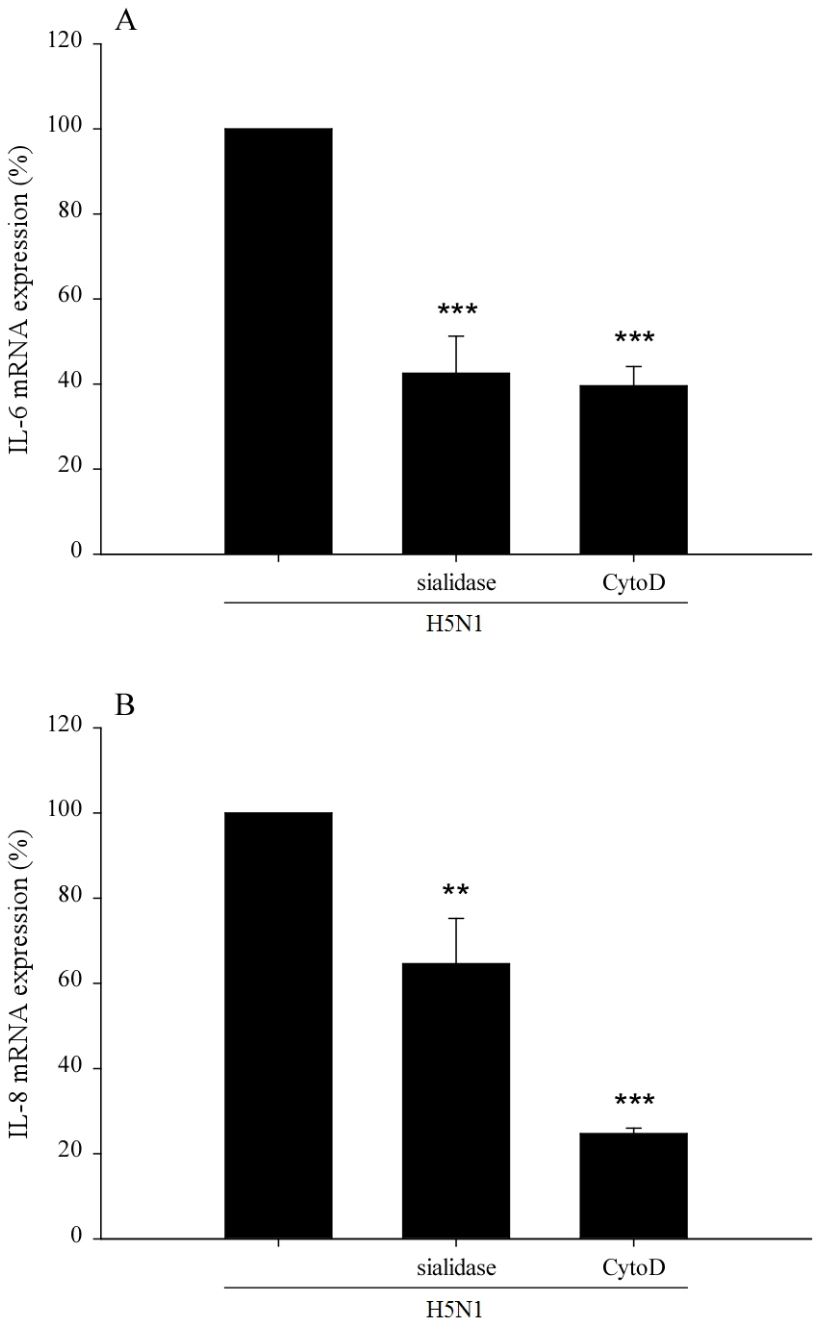

Fig. 3.4: Role of α-2,3 sialic acid receptor and actin cytoskeleton in the mechanism by which inact-H5N1 increases mRNA expression of IL-6 and IL-8 mRNA. 16HBE14o- cells were incubated for 1 hr with 1 U/ml sialidase or 2 µM cytochalasin D (CytoD) before exposing to inact-H5N1 (20 µg/ml hemagglutinin). Three hour after, cells were harvested for qRT-PCR analysis for mRNA expression of IL-6 (A) and IL-8 (B). All data were normalized with that obtained from cells treated with allantoic fluid and reported as percentage of the normalized control H5N1 treated group. Values are means ± SEM (n = 3-4). ** $p < 0.01$, *** $p < 0.001$ compared to the control, unpaired Student's *t*-test.

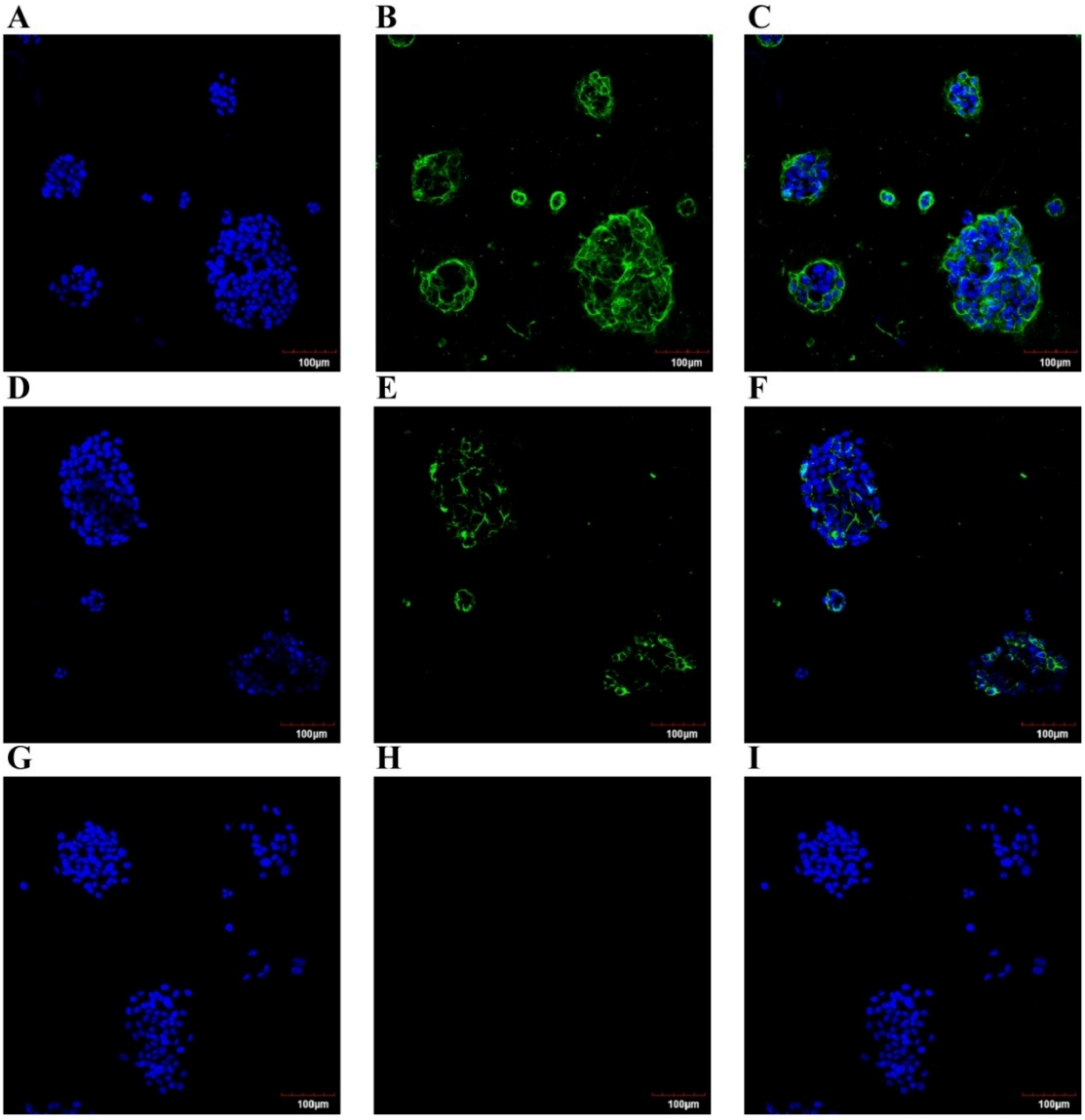

Fig. 3.5: α-2,3 and α-2,6 sialic acid receptors are expressed in 16HBE14o- cells. A, D and G; nuclei stained blue with DAPI. B; cells were stained with MAL I to detected α-2,3 sialic acid receptor (green). E; cells were stained with SNA for detected α-2,6 sialic acid receptor (green). H; negative control. C, F and I; images were merged to show nuclear/sialic acid receptors localization. Confocal images were taken at×200 magnification.

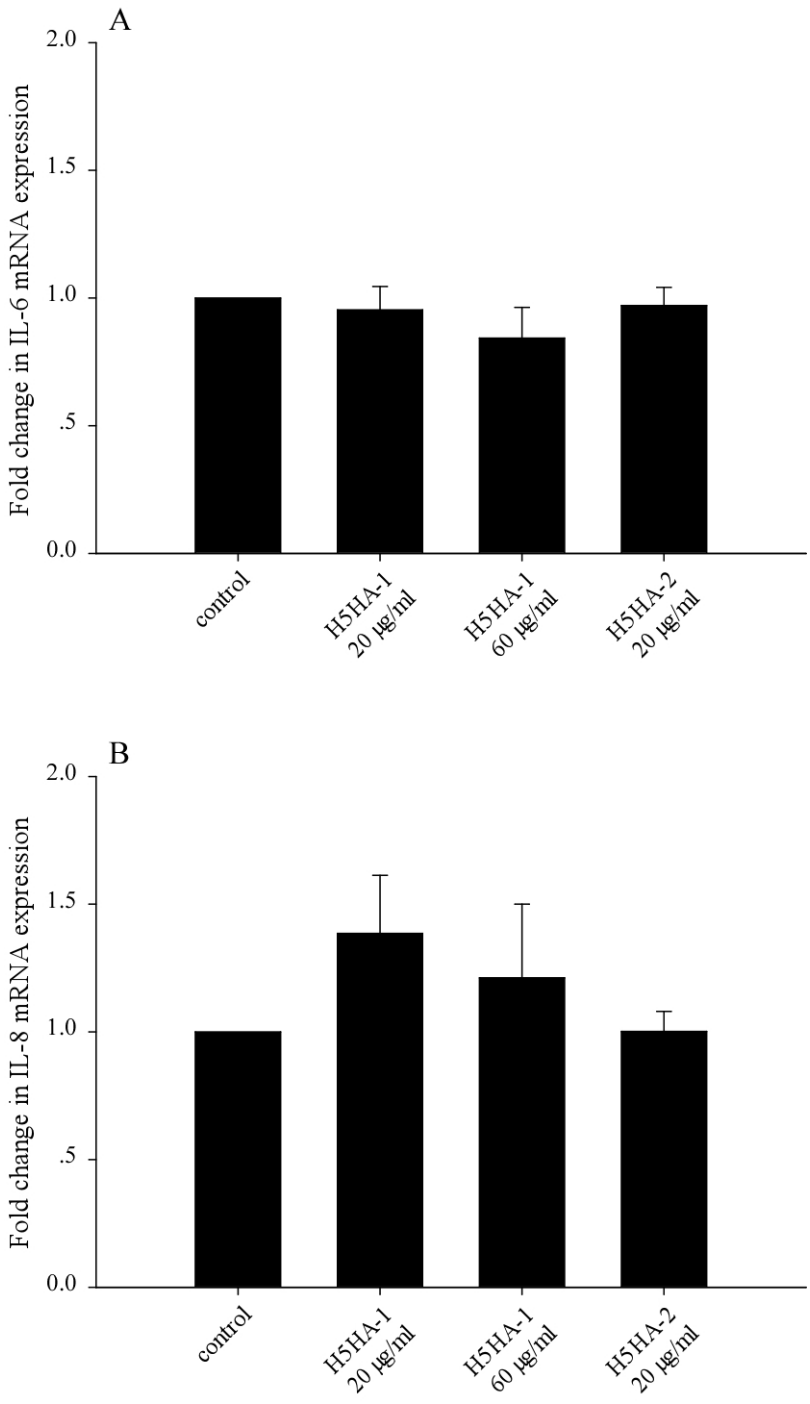

Fig. 3.6: mRNA expression level of IL-6 (A) and IL-8 (B) in 16HBE14o- cells treated for 3 hr with commercial H5 hemagglutinin. H5HA-1 was purchased from Immune Technology Corp. and H5HA-2 was purchased from Protein Sciences Corp. Data are average from 3 experiments.

2. Cellular mechanism by which inact-H5N1 induces mRNA expression of IL-6 and IL-8 mRNA expression

2.1 Role of purinergic receptors

Nucleotides, such as ATP and UTP released in response to physical and pathological stimuli are known to be involved in host-defense mechanisms of the respiratory epithelium. Previous studies suggest that, during infection, purinergic signaling is involved in mediating cytokine production in the respiratory cells (Boots et al., 2009; Shi et al., 2012). To investigate a role of purinergic signaling in the mechanisms by which inact-H5N1 stimulates mRNA expression of IL-6 and IL-8, before exposing to the virus 16HBE14o- cells were treated with apyrase (2U/ml), an enzyme that hydrolyzes nucleotide triphosphates and nucleotide diphosphates. Under these conditions, the effect of H5N1 on mRNA expression level of IL-6 and IL-8 was significantly reduced by 25% ($n = 4$, $p < 0.05$) and 55% ($n = 3$, $p < 0.001$), respectively (Fig. 3.7). Blocking the purinergic receptor with 100 μM suramin also reduced the effect of inact-H5N1 on the IL-6 and IL-8 mRNA expression by 40% ($n = 3$, $p < 0.001$) and 30% ($n = 3$, $p < 0.01$), respectively (Fig. 3.7).

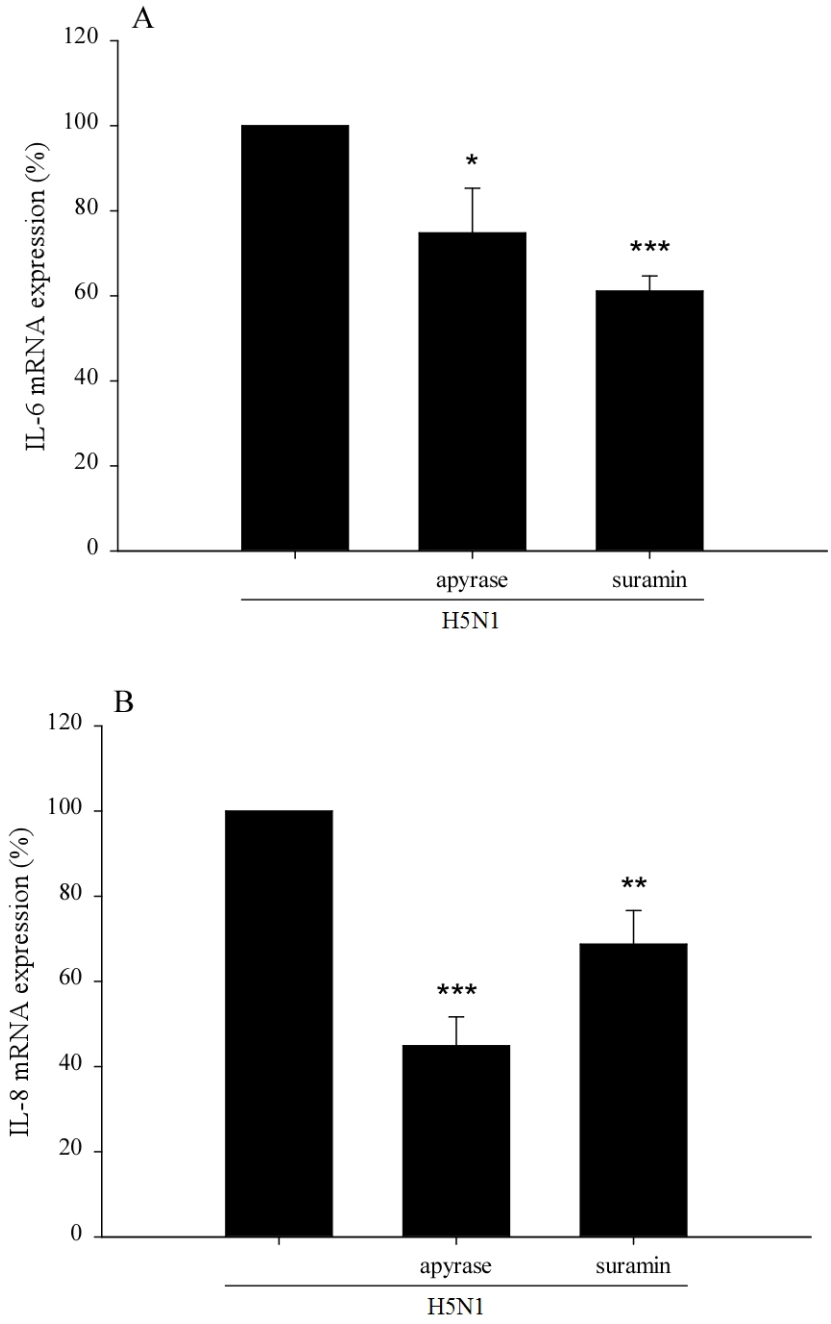

Fig. 3.7: Apyrase and suramin inhibit the effect of inact-H5N1 on mRNA expression of IL-6 and IL-8. 16HBE14o- cells were treated for 1 hr with apyrase (2 U/ml) or suramin (100 µM) before being exposed to inact-H5N1 (20 µg/ml hemagglutinin). Three hour after, cells were harvested for qRT-PCR analysis for mRNA expression of IL-6 (A) and IL-8 (B). Values are means ± SEM (n = 3-4). * $p < 0.05$, ** $p < 0.01$, *** $p < 0.001$ compared to the control, unpaired Student's *t*-test.

2.2 Nucleotides increase mRNA expression of IL-6 and IL-8

To determine purinoceptor(s) that may involve in the infection-independent effect of H5N1 on mRNA expression of IL-6 and IL-8, cells were treated with pharmacological agonists (100 μM) of purinoceptor, including ATP (non-specific P2Rs), ADP ($P2Y_1R$), UTP ($P2Y_2R$), UDP ($P2Y_6R$), BzATP ($P2X_7R$) or adenosine ($A_{2B}R$) and mRNA expression was determined three hours after. Expression of IL-6 was increased 1.96 ± 0.32 fold by ATP (n = 3, $p < 0.05$), 2.35 ± 0.24 fold by ADP (n = 3, $p < 0.01$) and 1.23 ± 0.10 fold by UDP (n = 3, $p < 0.05$) but partially inhibited by adenosine (Fig. 3.8A). UTP, BzATP were without effect. On the other hand, mRNA expression level of IL-8 was increased 6.18 ± 2.05 fold by ATP (n = 3, $p < 0.05$), 5.71 ± 0.72 fold by ADP (n = 3, $p < 0.001$), 2.17 ± 0.06 fold by UTP (n = 3, $p < 0.001$), 4.44 ± 0.28 fold by UDP (n = 3, $p < 0.001$) and 1.60 ± 0.14 fold by BzATP (n = 3, $p < 0.01$) (Fig. 3.8).

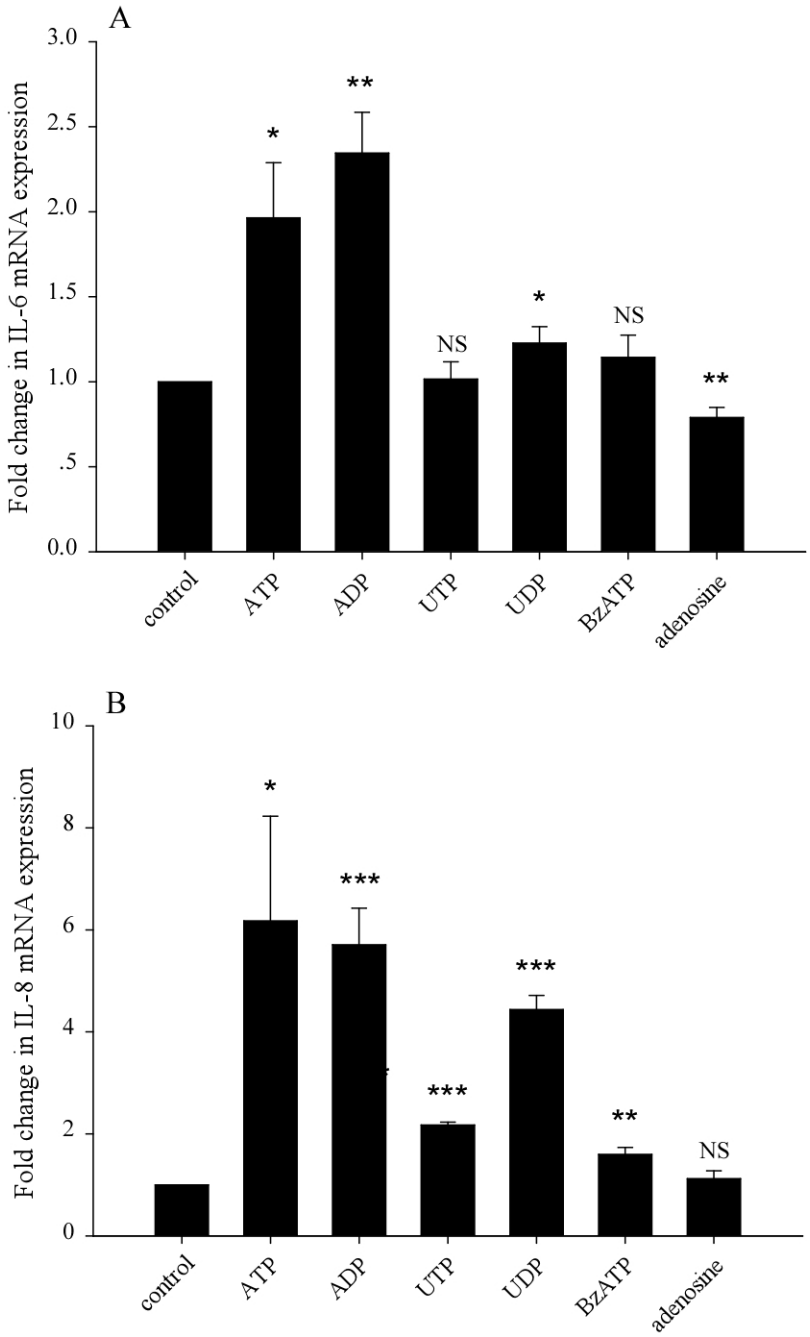

Fig. 3.8: Agonist potency profile for IL-6 (A) and IL-8 (B) mRNA expression suggests involvement of P2Y receptor, especially, $P2Y_1R$ and $P2Y_6R$. 16HBE14o- cells were incubated with 100 μM ATP, ADP, UTP, UDP, BzATP or adenosine for 3 hr. Values are means ± SEM (n = 3). *, **, *** and NS indicate $p < 0.05$, $p < 0.01$, $p < 0.001$ and no statistical difference compared to control non treated cells, respectively, unpaired Student's *t*-test.

2.3 Inact-H5N1 increases IL-6 and IL-8 mRNA via activation of $P2Y_6R$

To determine the purinoceptors involved in the signaling pathway by which inact-H5N1 increases IL-6 and IL-8 mRNA expression, 16HBE14o- cells were treated for 1 hr with MRS2179, a $P2Y_1R$ antagonist or MRS2578, a $P2Y_6R$ antagonist, before the inact-H5N1 was introduced. qRT-PCR analysis 3 hr later revealed H5N1-induced IL-6 and IL-8 mRNA expression in cells treated with MRS2578 was reduced by 45% (n = 3, $p < 0.01$, Fig 3.9A) and 70% (n = 3, $p < 0.01$, Fig. 3.9B), respectively, whereas, the expression in cells treated with MRS2179, a blocker of $P2Y_1R$ (20 μM), was not altered.

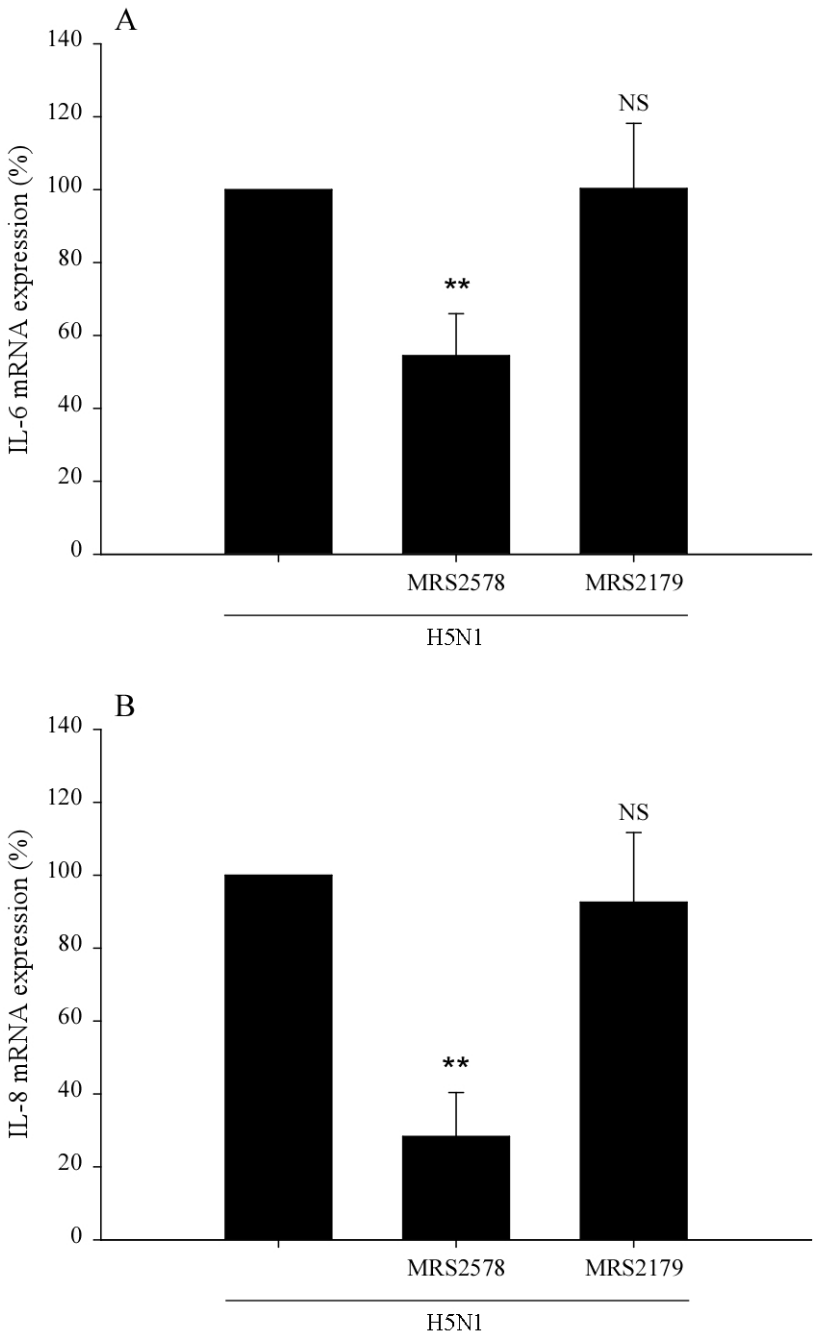

Fig. 3.9: The effect of inact-H5N1 on cytokine mRNA expression is mediated via $P2Y_6R$. 16HBE14o- cells were treated with MRS2578 (10 μM) or MRS2179 (20 μM) 1 hr before being inact-H5N1 (20 μg/ml hemagglutinin) was introduced. Cells were harvested 3 hr later for qRT-PCR analysis of IL-6 (A) and IL-8 (B). Values are means ± SEM (n = 3).

** and NS indicate $p < 0.01$ and no statistical difference compared to the control, unpaired Student's *t*-test.

To confirm the role of $P2Y_6R$, the expression of the receptor in 16HBE14o- cells was knocked down by a specific siRNA. qRT-PCR analysis revealed that mRNA expression of the $P2Y_6R$ in cells transfected with the siRNA directed against $P2Y_6R$ was decreased by 70% ($n = 3$, $p < 0.001$; Fig. 3.10A). Consistent with the above results showing that $P2Y_6R$ is an important element of the signaling pathway by which inact-H5N1 regulates mRNA expression of IL-6 and IL-8, the siRNA directed against $P2Y_6R$ blocked inact-H5N1-induced mRNA expression of IL-6 and IL-8 by 30% ($n = 3$, $p < 0.01$) and 50% ($n = 3$, $p < 0.001$), respectively, when compared with that of the cells transfected with a scramble siRNA (Fig. 3.10B).

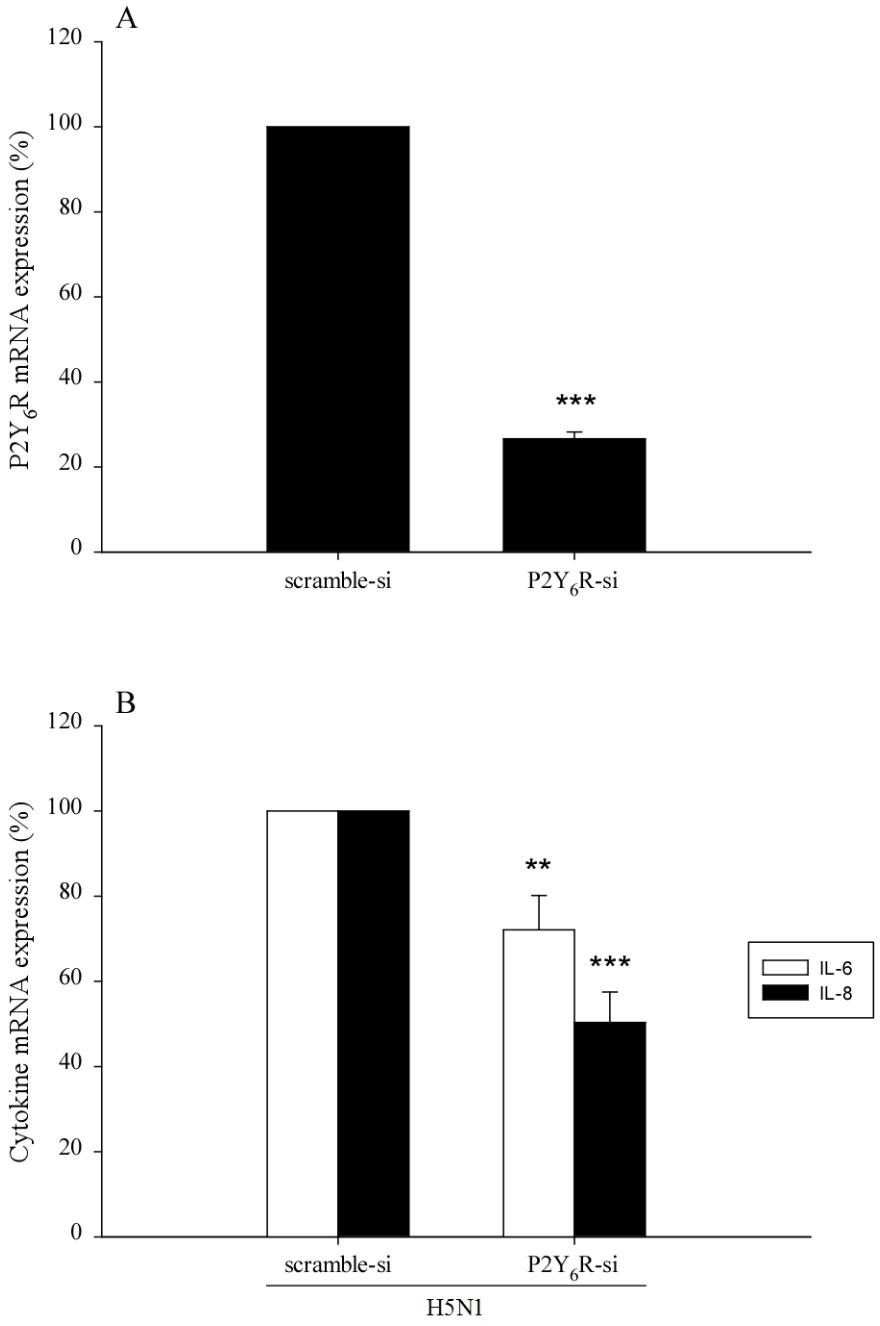

Fig. 3.10: A; an siRNA directed against $P2Y_6R$ decreased mRNA expression of $P2Y_6R$. 16HBE14o- cells were transfected with an siRNA directed against $P2Y_6R$ or a scrambled-siRNA (100 pmol) and mRNA expression of $P2Y_6R$ was measured 48 hr later. B; H5N1-induced mRNA expression of IL-6 and IL-8 transfected with siRNA directed against $P2Y_6R$ or scrambled-siRNA. Values are means ± SEM (n = 3). ** $p < 0.01$, *** $p < 0.001$ compared to the control, unpaired Student's *t*-test.

2.4 Role of PLC, PKC and Ca^{2+} signaling

$P2Y_6R$ belongs to the G-protein-coupled receptor with cellular signaling pathways that may involve PLC, PKC and intracellular Ca^{2+} signaling (Lazarowski et al., 2009). 16HBE14o- cells were treated with a PKC inhibitor, BIM (1 μM) before UDP was introduced to activate $P2Y_6R$. BIM attenuated UDP-induced IL-8 mRNA expression by 50% (Fig. 3.11), suggesting that PKC is involved in the $P2Y_6R$-mediated signaling pathway that regulates mRNA expression of IL-8.

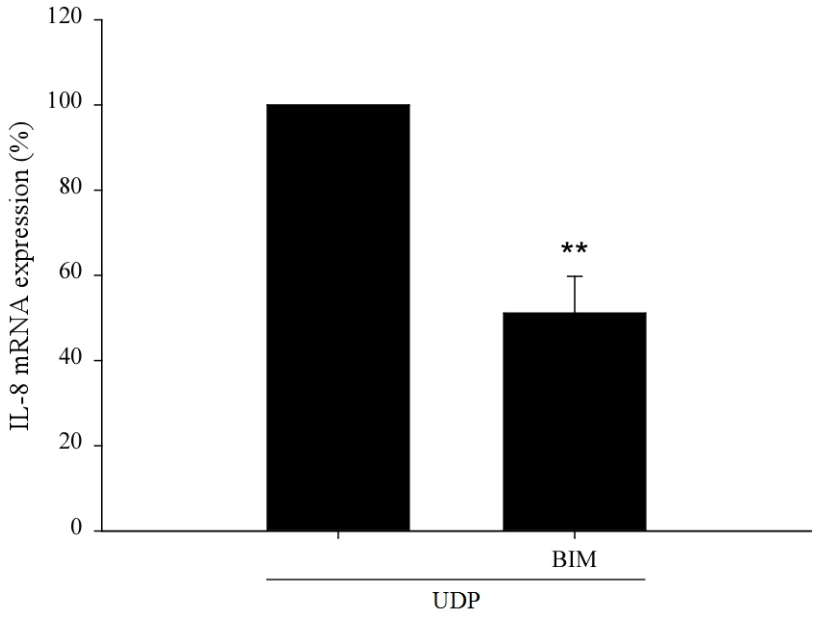

Fig. 3.11: Effect of UDP on IL-8mRNA expression in 16HBE14o- cells is inhibited by BIM. Cells were treated with BIM (1 μM) for 1 hr before UDP (100 μM) was introduced. Cells were harvested 3 hr later for qRT-PCR analysis of IL-8 mRNA expression. Values are means ± SEM (n = 3). ** $p < 0.01$ compared to the control, unpaired Student's *t*-test.

Next, the cells were treated for 1 hr with a pharmacological inhibitor of PLC (U73122, 10 μM), inhibitors of PKC (BIM, 1 μM or GÖ6976, 10 μM) or a membrane permeable Ca^{2+} chelator (BAPTA-AM, 10 μM) before the inact-H5N1 was introduced. In the presence of U73122, the effect of virus on IL-6 and IL-8 mRNA expression was reduced by 35% (n = 3, $p < 0.05$) and 75% (n = 3, $p < 0.001$), respectively (Fig. 3.12). In cells treated with BIM, the effect of virus on mRNA expression of IL-6 and IL-8 was reduced by 40% (n = 3, $p < 0.001$) and 65% (n = 3, $p < 0.001$), respectively. In cells treated with GÖ6976, the effect of virus on mRNA expression of IL-6 and IL-8 was reduced by 60% (n = 3, $p < 0.01$) and 75% (n = 3, $p < 0.001$) (Fig. 3.12). On the other hand, BAPTA-AM reduced the positive effect of the inact-H5N1 on mRNA expression of IL-6 by 60% and that of IL-8 by 80%. Taken together, these findings suggest that PLC, PKC and intracellular Ca^{2+} signaling are part of the signaling pathway(s).

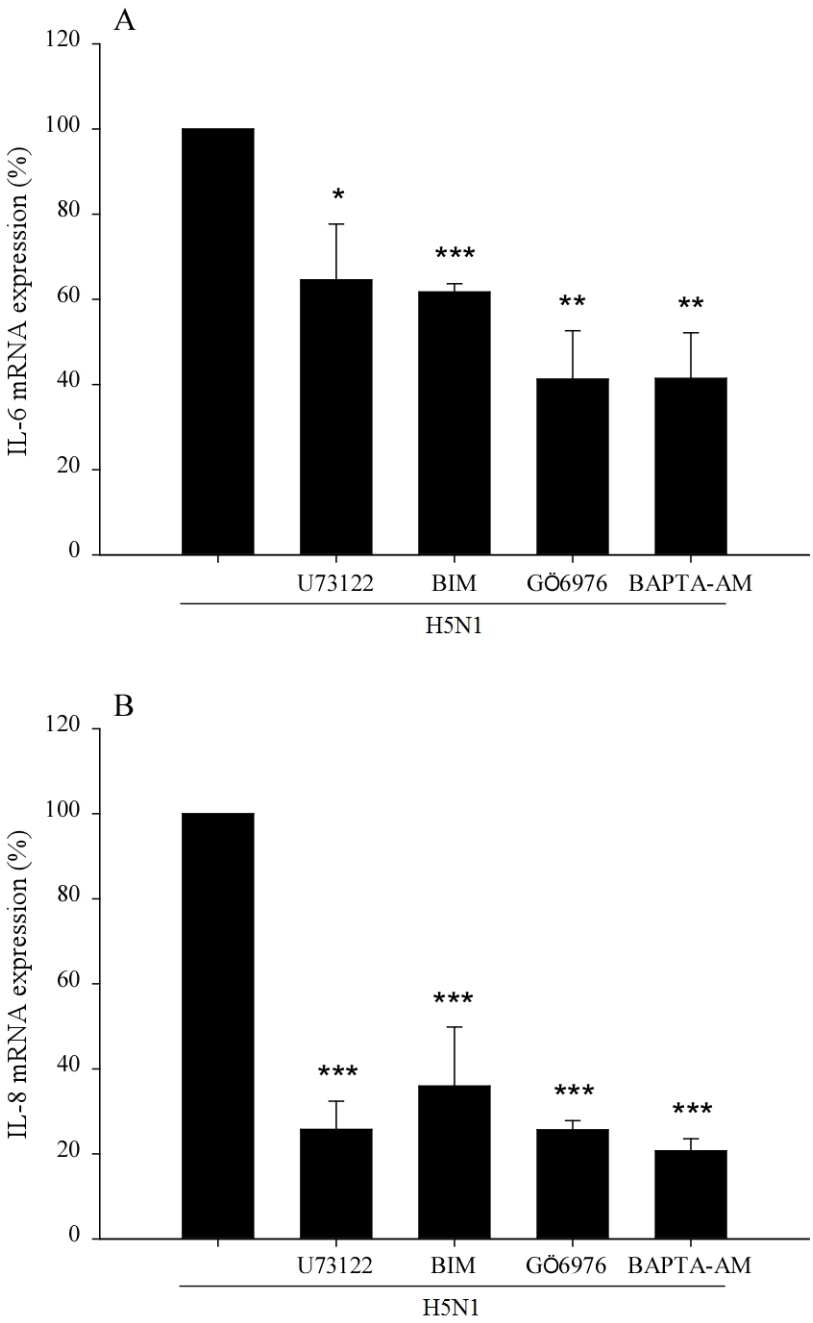

Fig. 3.12: The effect of inact-H5N1 on cytokine mRNA expression in 16HBE14o- is inhibited by U73122, BIM, GÖ6976 and BAPTA-AM. Cells were incubated for 1 hr with U73122 (10 μM), BIM (1 μM), GÖ6976 (10 μM) or BAPTA-AM (50 μM) before being exposed to inact-H5N1 (20 μg/ml hemagglutinin). Cells were harvested 3 hr later for qRT-PCR analysis of mRNA expression of IL-6 (A) and IL-8 (B). Values are means ± SEM (n = 3). * $p < 0.05$, ** $p < 0.01$, *** $p < 0.001$ compared to the control, unpaired Student's *t*-test.

2.5 Role of MAP kinases and NF-κB

Previous reports suggested that influenza virus infection increased production of pro-inflammatory cytokines by a mechanism that involves activating mitogen-activated protein kinase (MAPK) (Kujime et al., 2000; Lee et al., 2005), including the extracellular signal-regulated protein kinases (ERKs), p38 MAPK, the c-Jun NH2-terminal kinase (JNK), or a downstream transcription factor, NF-κB (Hedges et al., 2000; Mogensen et al., 2001). To investigate whether these signaling molecules are involved in the signaling pathway(s) by which inact-H5N1 regulates mRNA expression of IL-6 and IL-8, activity of ERK1/2, p38, and JNK kinases in 16HBE14o- cells were inhibited by specific pharmacological blockers, PD98059, SB203580 or SP600125, respectively. The effect of the inact-H5N1 on mRNA expression of IL-6 was significantly reduced by SB203580 (40%, n = 3, $p < 0.01$) but not by PD98059 or SP600125 (Fig. 3.13). On the other hand, the effect of inact-H5N1 on mRNA expression of IL-8 was attenuated by all three MAPK inhibitors, i.e., 60% reduction ($p < 0.001$) by PD98059, 80% reduction ($p < 0.001$) by SB203580 and 35% reduction ($p < 0.001$) by SP600125 (Fig. 3.13).

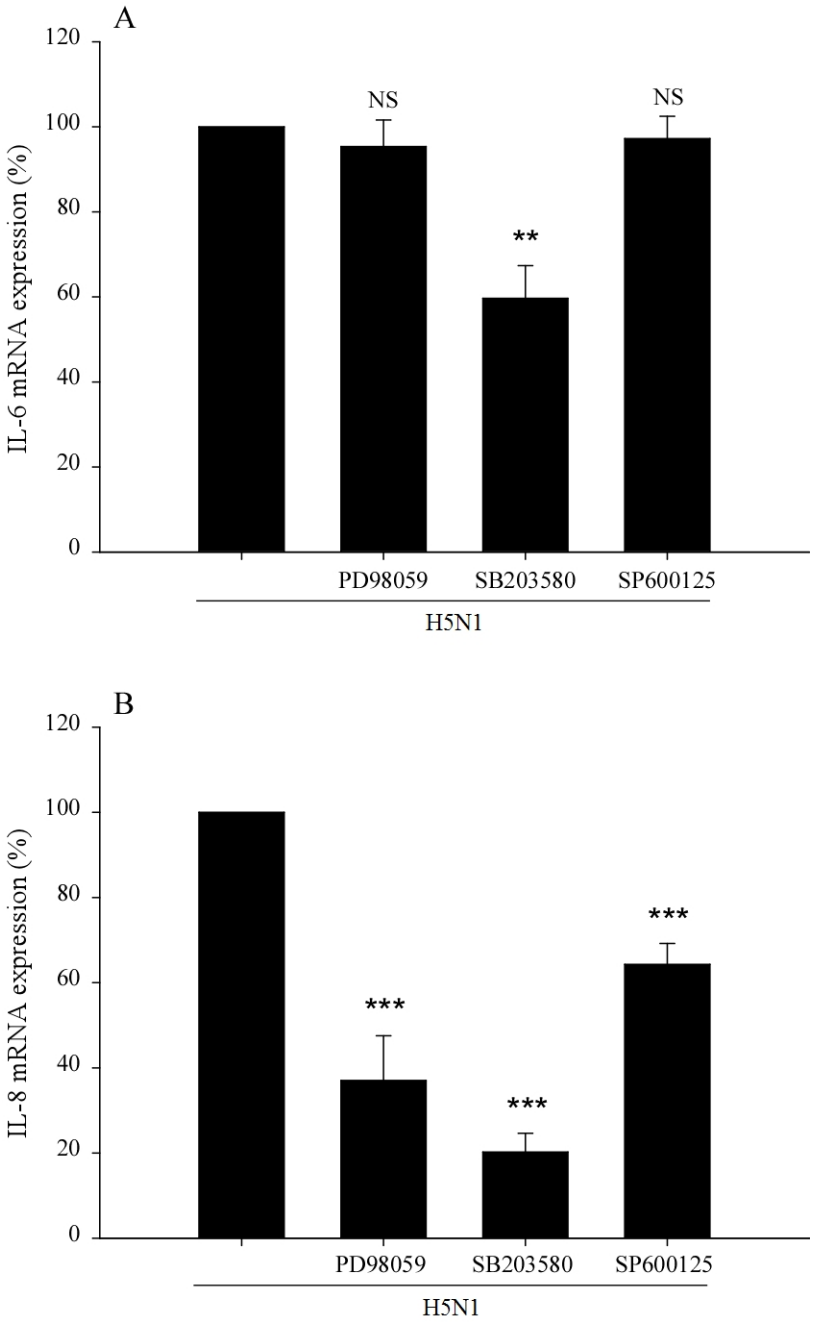

Fig. 3.13: Contribution of MAPK signaling in the mechanism by which inact-H5N1 regulates mRNA expression of IL-6 and IL-8. 16HBE14o- cells were treated for 1 hr with PD98059 (50 µM), SB203580 (10 µM) or SP600125 (10 µM), before inact-H5N1 (20 µg/ml hemagglutinin) was introduced. Three hour after, cells were harvested for qRT-PCR analysis of IL-6 (A) and IL-8 (B) mRNA expression. Values are means ± SEM (n = 3). **, *** and NS indicate $p < 0.01$, $p < 0.001$ and no statistical difference compared to the control, unpaired Student's *t*-test.

Next, the effect of H5N1 on activity of p38 and ERK1/2 in HBE cells was investigated by determining phosphorylation of the kinases. Phosphorylation level of ERK1/2 in 16HBE14o- was determined by immunoblot analysis at 0.5, 1, 2, and 3 hr after exposure to the virus. As depicted in Fig. 3.14, 30 min after treatment, phospho-ERK1/2 increased to a 3.24 fold in the inact-H5N1 treated group (n = 1) when compared with that of allantoic fluid treated group. ERK1/2 phosphorylation remained at this level (2.27 fold, n = 1) 3 hr after treatment.

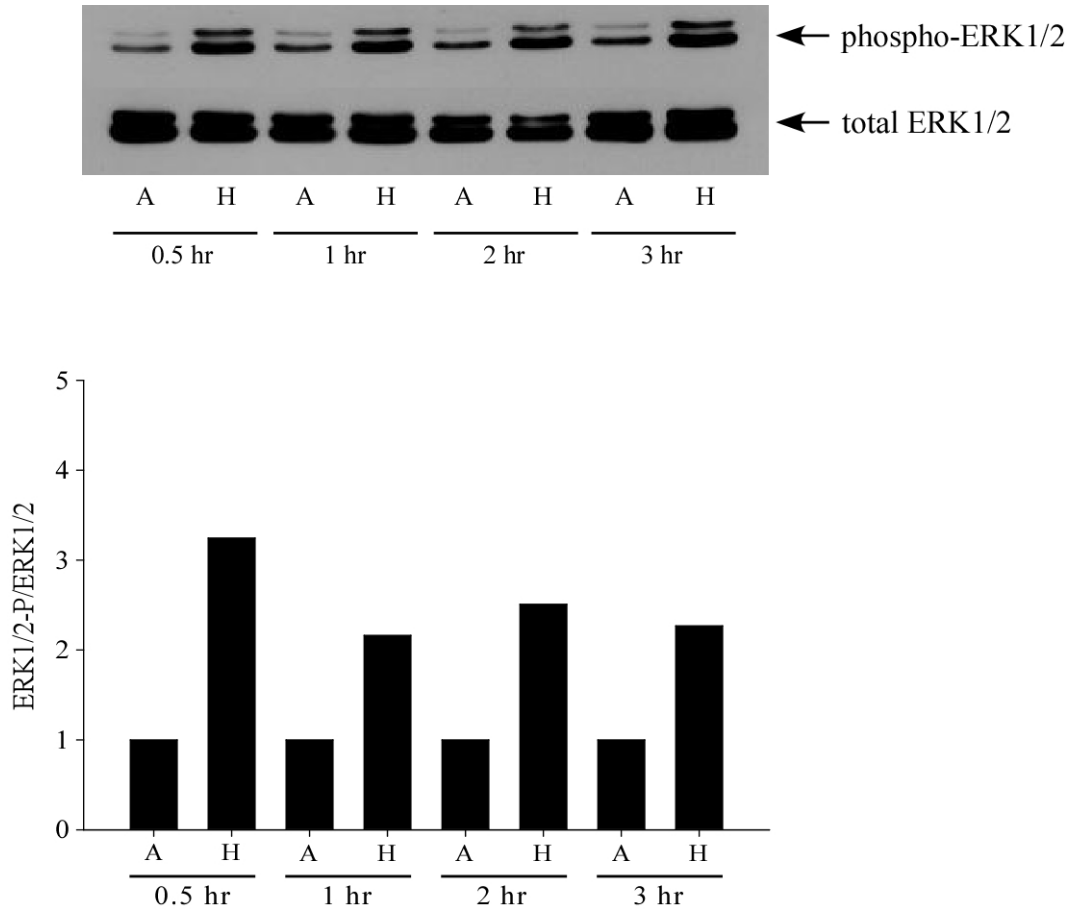

Fig. 3.14: Representative immunoblot analysis of phospho- and total ERK1/2 protein expression in 16HBE14o- cells treated with inact-H5N1 (20 μg/ml hemagglutinin). Cells were treated with allantoic fluid (A) or inact-H5N1 (20 μg/ml hemagglutinin, H). Protein samples were harvested at 0.5, 1, 2, and 3 hr after incubation with the virus as indicated. The level of total ERK1/2 in each lane was used as a control for an amount of protein loaded. Quantitative analysis was performed by ImageJ software and the amount of phospho-ERK1/2 was determined as a function of total ERK1/2 detected in the same band (n = 1).

As depicted in Fig. 3.15, 0.5 hr after exposure to the inact-H5N1, phospho-p38 in the inact-H5N1 treated group increased to a 2.98 fold (n = 1) when compared with that of allantoic fluid treated but decreased to 1.67 fold (n = 1) 3 hr after treatment.

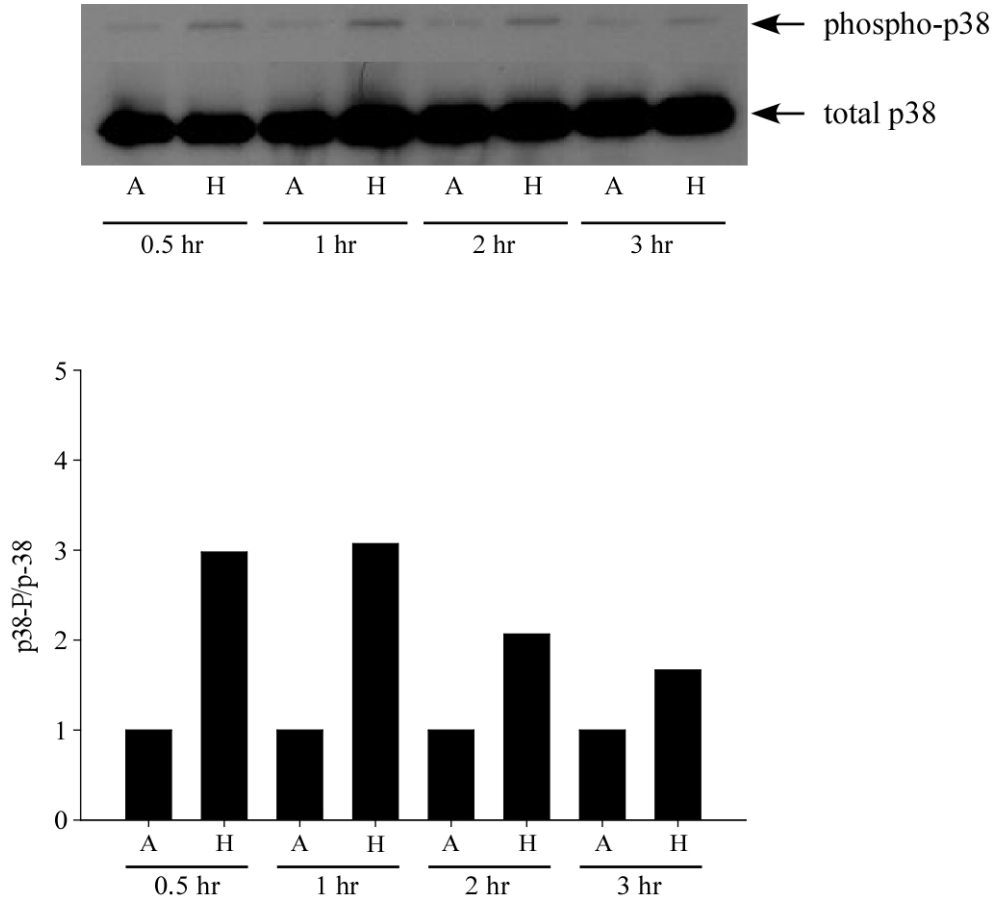

Fig. 3.15: Activation of p38 MAP kinase in 16HBE14o- cells exposed to inact-H5N1. Cells were exposed to allantoic fluid (A) or inact-H5N1 (20 µg/ml hemagglutinin, H). Protein samples were harvested at 0.5, 1, 2, and 3 hr after incubation. The phosphorylation level of p38 MAP kinase was assayed by Western analysis using specific antibodies (n = 1).

Moreover, to investigate the upstream signaling pathway by which phosphorylation of ERK1/2 or p38 MAPK are activated by inact-H5N1, 16HBE14o- cells were treated for 1 hr with pharmacological inhibitors of ERK1/2 (PD98059, 50 μM), p38 MAPK (SB203580, 10 μM), TMEM16A ($T16A_{inh\text{-}A01}$, 30 μM), CFTR ($CFTR_{inh172}$, 20 μM), or a membrane permeable Ca^{2+} chelator (BAPTA-AM, 10 μM) before the inact-H5N1 was introduced. Data in Figs. 3.16 & 3.17 suggest that, 30 min after exposure to the inact-H5N1, phosphorylation of ERK1/2 and p38 MAPK increased to a 1.79 ± 0.02 fold (n = 3, $p < 0.05$) and 2.51 ± 0.12 fold (n = 3, $p < 0.05$), respectively, when compared with that of allantoic fluid treated group. These effects of the virus was attenuated by PD98059 (100 %, n = 3, $p < 0.001$) and SB203580 (45 %, n = 3, $p < 0.05$). Interestingly, $T16A_{inh\text{-}A01}$ and BAPTA-AM significantly reduced the effect of inact-H5N1 on phosphorylation of ERK1/2 by 70 % and 100 %, respectively, but had no effect on phosphorylation of p38 MAPK.

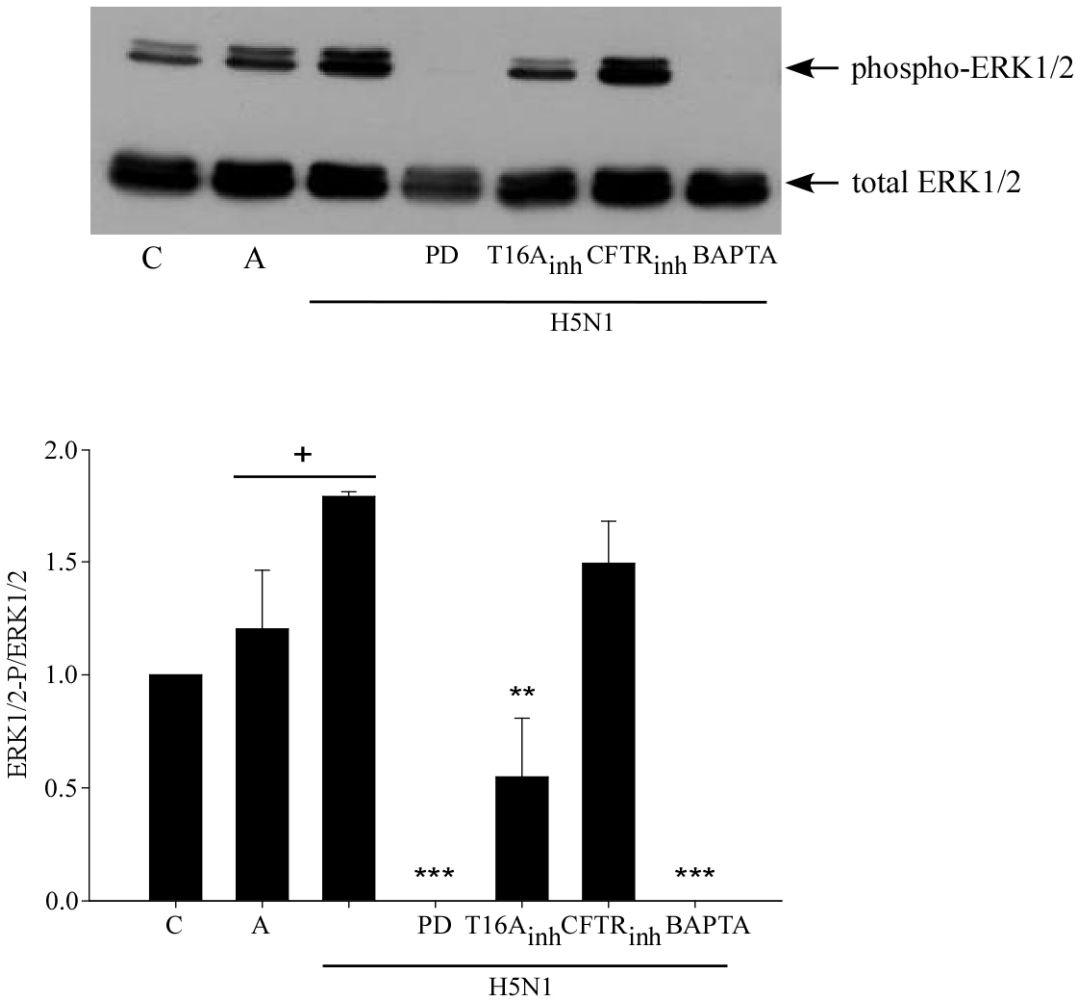

Fig. 3.16: Representative densitometric analysis of phospho- and total ERK1/2 protein expression in 16HBE14o- cells treated with inact-H5N1 (20 µg/ml hemagglutinin). Cells were treated with allantoic fluid (A), inact-H5N1 (20 µg/ml hemagglutinin, H) or untreated (C). Cell were incubated for 1 hr with PD98059 (50 µM), T16A$_{inh\text{-}A01}$ (30 µM), CFTR$_{inh172}$ (20 µM) or BAPTA-AM (10 µM) before being exposed to inact-H5N1. Thirty minutes after, protein samples were harvested and the level of total ERK1/2 and phospho-ERK were determined. Quantitative analysis was performed by ImageJ software and the amount of phospho-ERK1/2 was determined as a function of total ERK1/2 detected in the same band. Values are means ± SEM (n = 3). + indicates $p < 0.05$ compared with data from the group treated with allantoic fluid. **, *** and NS indicate $p < 0.01$, $p < 0.001$ and no statistical difference compared with data from the group treated with inact-H5N1 (unpaired Student's *t*-test).

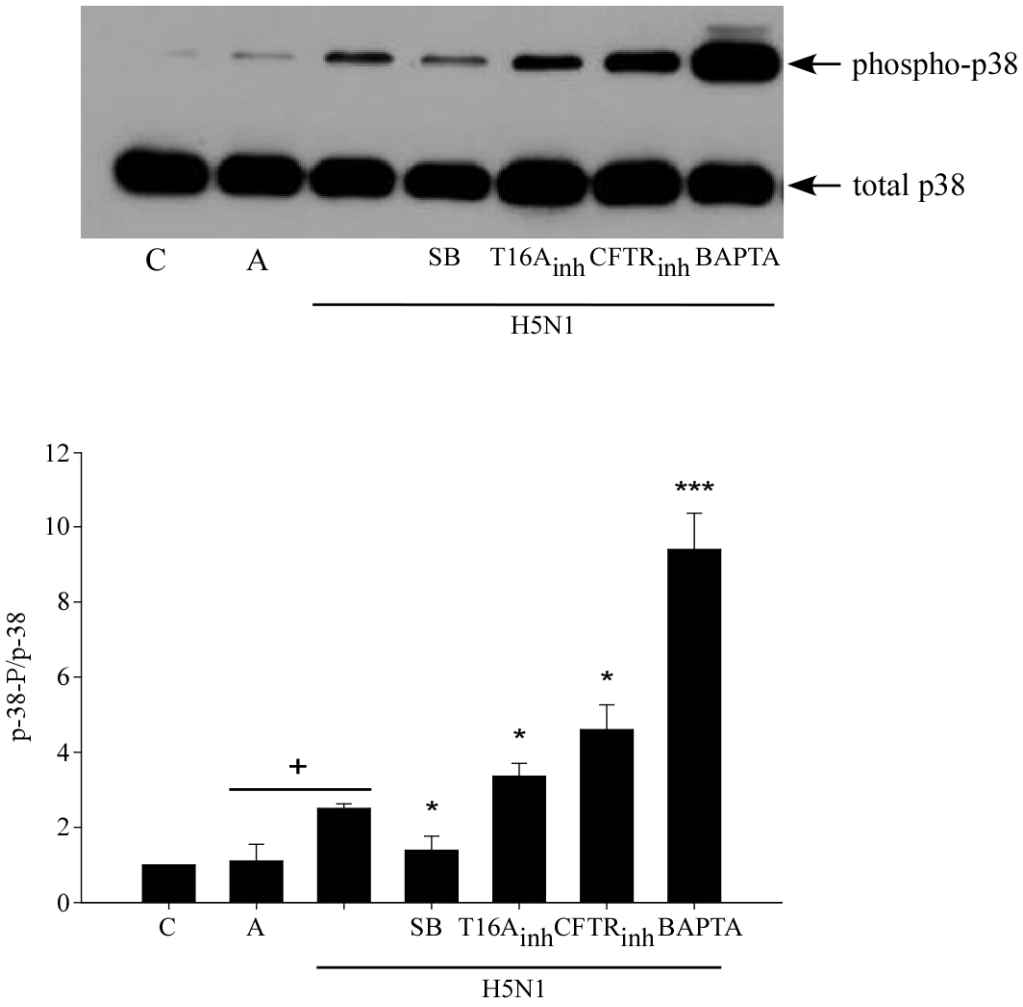

Fig. 3.17: Densitometric analysis of phospho- and total p38 MAP kinase in 16HBE14o- cells exposed to inact-H5N1. Cells were exposed to allantoic fluid (A), inact-H5N1 (20 µg/ml hemagglutinin, H) or untreated (C). Cell were incubated for 1 hr with SB203580 (10 µM), $T16A_{inh\text{-}A01}$ (30 µM), $CFTR_{inh172}$ (20 µM) or BAPTA-AM (10 µM) before being exposed to inact-H5N1. Thirty minutes after, protein samples were harvested and the level of total p38 and phospho-p38 were determined by western analysis using specific antibodies. Values are means ± SEM (n = 3). + indicates $p < 0.05$ compared with data from the group treated with allantoic fluid (n = 3). *, *** and NS indicate $p < 0.05$, $p < 0.001$ and no statistical difference compared when compared with data from the group treated with inact-H5N1 (unpaired Student's *t*-test).

NF-κB plays a principle role as a regulator of inflammatory cytokines expression (Blackwell et al., 1997). To investigate whether NF-κB is involved in the mechanism by which inact-H5N1 regulates mRNA expression of IL-6 and IL-8, 16HBE14o- cells were treated with a pharmacological NF-κB blocker, SN-50 (10 μM), for 1 hr before virus treatment. Under this condition the effects of the virus on mRNA expression of IL-6 and IL-8 were reduced by 30% and 35%, respectively (Fig. 3.18).

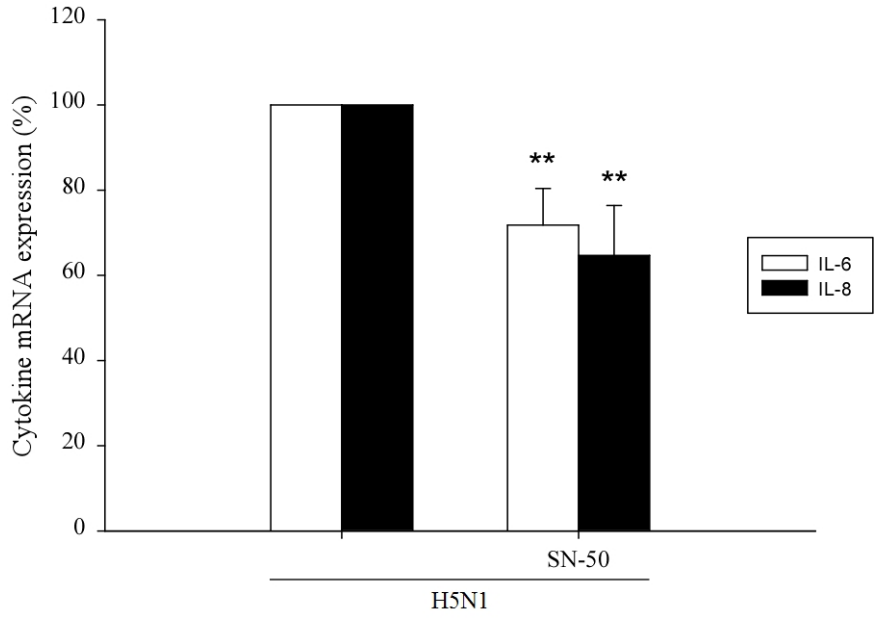

Fig. 3.18: SN-50 attenuates the effect of inact-H5N1 on mRNA expression of IL-6 and IL-8. To investigate the contribution of NF-κB on inact-H5N1-induced cytokine mRNA expression, 16HBE14o- cells were treated with SN-50 (10 μM) for 1 hr before inact-H5N1 (20 μg/ml hemagglutinin) was introduced. Three hour after, cells were harvested for qRT-PCR analysis of mRNA expression of IL-6 (open bars) and IL-8 (closed bars). Values are means ± SEM (n = 4). ** $p < 0.01$ compared to the control, unpaired Student's *t*-test.

It has been previously reported that H5-HA increases innate immune response in the respiratory epithelial cells via a cellular signaling pathway that involves Janus kinase 3 (JAK3) (Xu et al., 2012). The contribution of JAK3 in inact-H5N1 mediated cytokine response was investigated by treating the cells with JAK3 inhibitor. As depicted in Fig. 3.19, JAK3 inhibitor attenuated mRNA expression of IL-8 (n = 3, $p < 0.01$) but not that of IL-6.

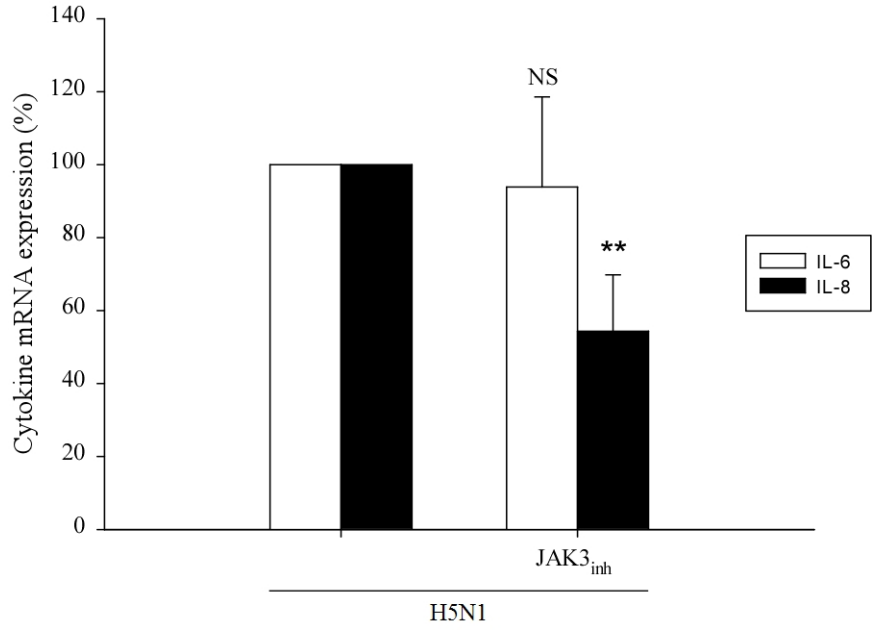

Fig. 3.19: JAK3 attenuates the effect of inact-H5N1 on mRNA expression of IL-8. 16HBE14o- cells were treated with JAK3 inhibitor ($JAK3_{inh}$, 760 nM) for 1 hr before inact-H5N1 (20 µg/ml hemagglutinin) was added to the culture media. Three hour after, cells were harvested for qRT-PCR analysis of mRNA expression of IL-6 (open bars) and IL-8 (closed bars). Values are means ± SEM (n = 3). ** and NS indicate $p < 0.01$ and no statistical difference compared to the control, unpaired Student's *t*-test.

3. Role of CFTR and TMEM16A chloride channels

3.1 Inact-H5N1 increases chloride current in 16HBE14o- cells

My recent study using Ussing chamber techniques to investigate an effect of inact-H5N1 on electrolyte transport in human respiratory epithelial, H441 cells, suggested that inact-H5N1 increases Cl^- secretion in this cell type (Huipao, 2011). To investigate the effect of inact-H5N1 on Cl^- transport in 16HBE14o- cells. The cells were grown on permeable supports and transepithelial ion transport properties were determined. 16HBE14o- monolayers have a mean transepithelial potential difference (V_{te}), transepithelial resistant (R_{te}) and equivalent short-circuit current (I_{sc}) of 0.49 ± 0.09 mV (n = 20), 1006.08± 142.03 $\Omega.cm^2$ (n = 20) and 0.5 ± 0.08 $\mu A/cm^2$ (n = 20), respectively. Inact-H5N1 caused a 2.54 ± 0.19 mV (n = 5) increasing in V_{te} (apical side becomes more negative, Fig. 3.20A) and a 45.20 ± 1.33 $\Omega.cm^2$ (n = 5) decreasing in R_{te}, corresponding to a 6.19 ± 0.55 $\mu A/cm^2$ increasing in I_{sc} (n = 5) (Fig. 3.20B). In a separate experiment, cells were treated for 10 min with TMEM16A inhibitor, $T16A_{inh\text{-}A01}$ (30 μM) before the virus was introduced. Under these conditions, V_{te} was increased by 1.91 ± 0.25 mV, corresponding to a 3.74 ± 0.43 $\mu A/cm^2$ increasing in I_{sc}, a value that is significantly lower than that of the control group (n = 5, $p < 0.01$, Fig. 3.20B). Next, 16HBE14o- monolayers were treated a CFTR inhibitor, $CFTR_{inh172}$ (20 μM). Under this condition the inact-H5N1-induced I_{sc} was 0.53 ± 0.21 $\mu A/cm^2$ (n = 5, $p < 0.001$, Fig. 3.20B).

To confirm the expressions of TMEM16A and CFTR in 16HBE14o- cells, each group of cells was treated with either a specific antibody directed against TMEM16A or that directed against CFTR and an appropriate fluorescein-tagged secondary antibodies was added to detect the corresponding proteins under confocal microscopy. Data in Fig. 3.21 suggest the presence of both TMEM16A and CFTR Cl^- channels.

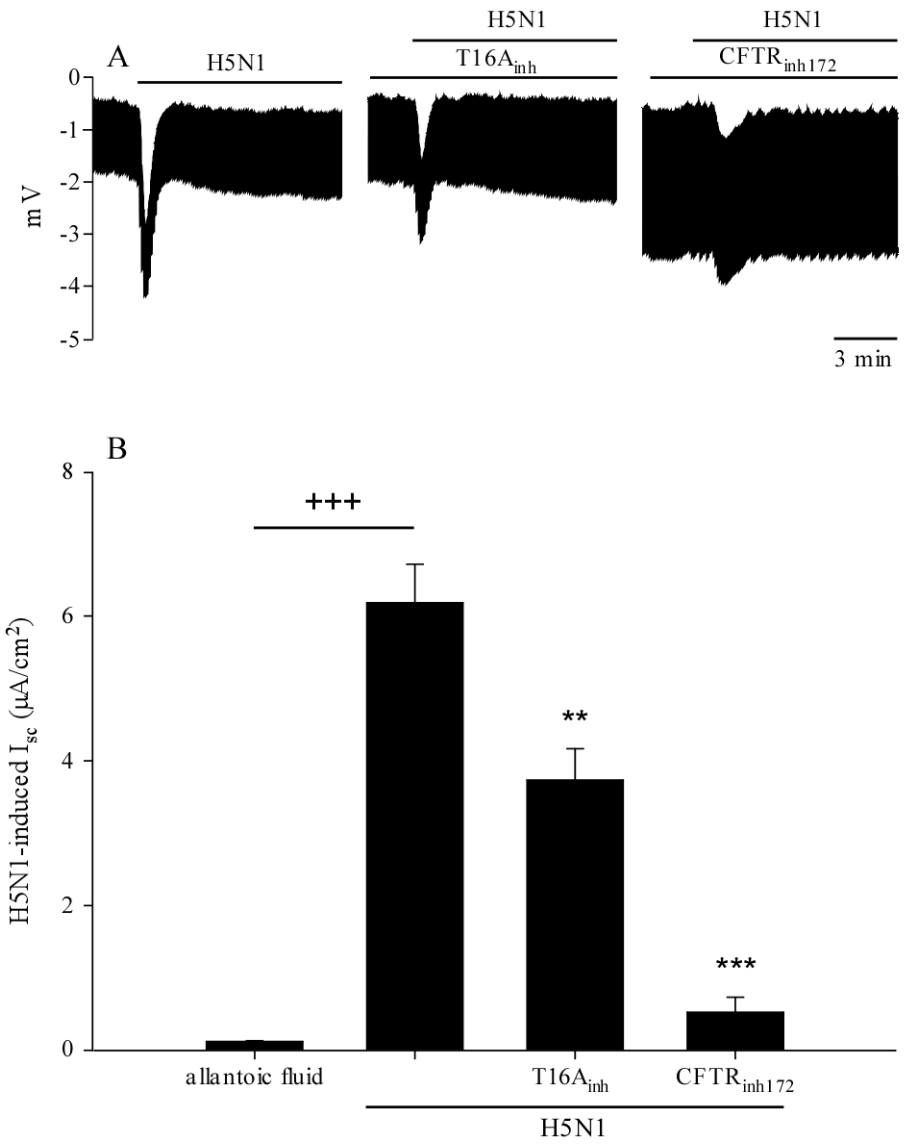

Fig. 3.20: The effect of inact-H5N1 on I_{sc} is Cl^--dependent and sensitive to TMEM16A and CFTR inhibitors. TMEM16A and CFTR Cl^- channel mediates the effect of inact-H5N1 on transepithelial potential difference (V_{te}) and short-circuit current (I_{sc}) in 16HBE14o- cells. A) Representative recordings of V_{te} in HBE cells treated with inact-H5N1 (20 µg/ml hemagglutinin) without or with the inhibitors. B) Changes in I_{sc} in inact-H5N1 treated HBE cell monolayer without or with TMEM16A or CFTR inhibitor. Values are means ± SEM (n = 5). +++ indicates $p < 0.001$ compared with data from the group treated with allantoic fluid, ** and *** indicates $p < 0.01$ and $p < 0.001$ compared to control-virus (unpaired Student's *t*-test).

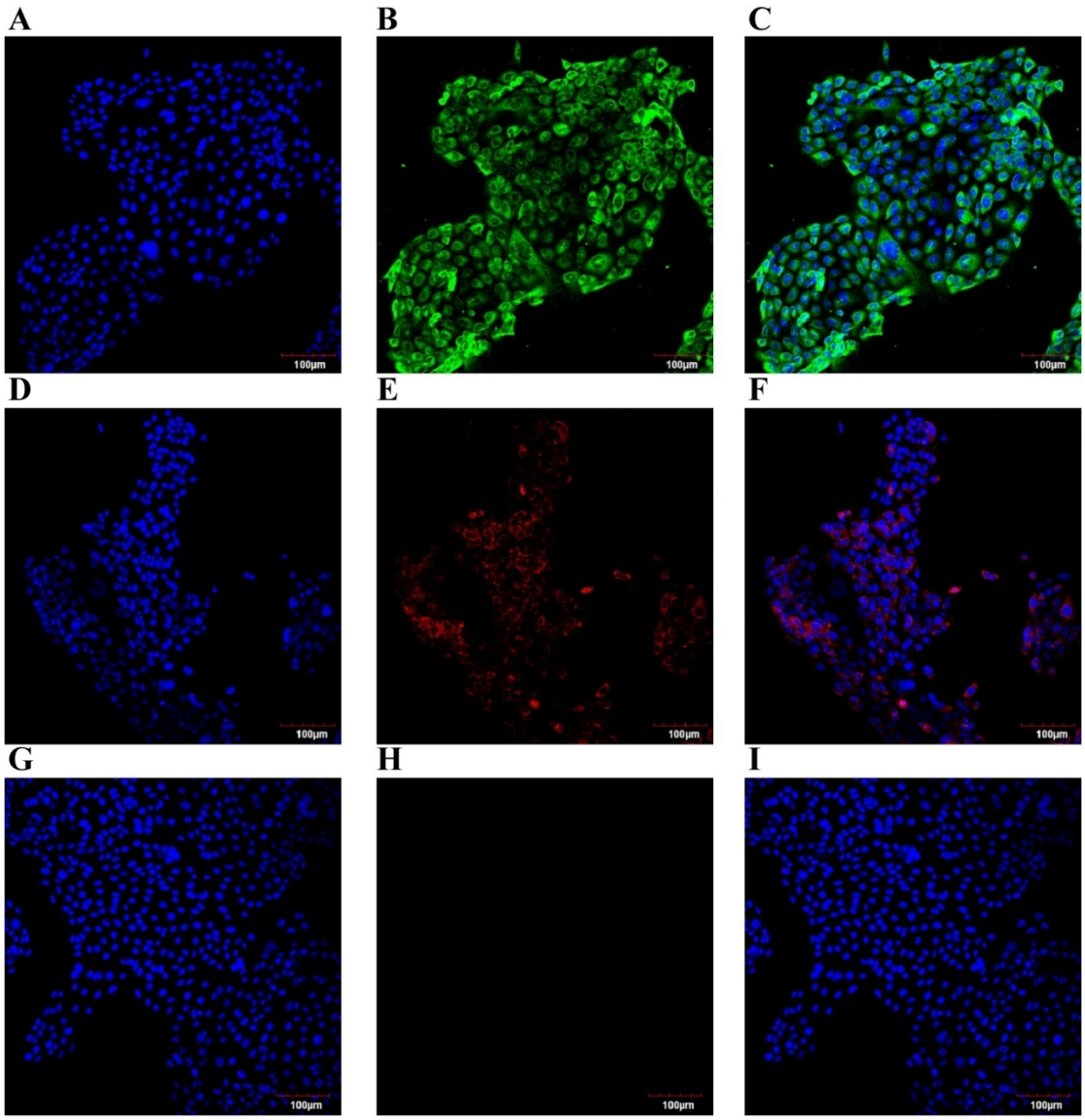

Fig. 3.21: TMEM16A and CFTR chloride channels are expressed in 16HBE14o- cells. A, D and G; nuclei stained blue with DAPI. B; cells were stained with primary specific to TMEM16A follow by Alexa Fluo 488-conjugated mouse anti-rabbit secondary antibody (green). E; cells were stained with specific to CFTR follow by Alexa Fluo 568- conjugated goat anti-mouse secondary antibody (red). H; negative control. C, F and I; images were merged to show nuclear/Cl^- channel localization. Confocal images were taken at×200 magnification.

3.2 TMEM16A$_{inh}$ and CFTRinh$_{172}$ attenuated the effects of inact-H5N1 on mRNA expressions of IL-6 and IL-8

Recent study suggested that niflumic acid, a blocker of the calcium-activated chloride channel (CLCA), attenuated histamine-induced IL-6 and IL-8 mRNA expression in human conjunctival epithelial cells (HCEC) (Lim et al., 2013). It is, therefore, conceivable that CLCA may play an important role in the regulation of IL-6 and IL-8 production. Since inact-H5N1 increases both TMEM16A and CFTR Cl^- currents, the role of these channels on the cellular mechanism that regulates mRNA expression of IL-6 and IL-8 was investigated. 16HBE14o- cells were treated with T16A$_{inh-A01}$ (30 μM) or CFTR$_{inh172}$ (20 μM). Under these conditions, inact-H5N1-induced IL-6 mRNA expression was reduced by 60% (n = 3, $p < 0.01$) in cells treated with T16A$_{inh-A01}$ and by 50% (n = 3, $p < 0.001$) in cells treated with CFTR$_{inh172}$ (Fig. 3.22A). The expression of IL-8 mRNA, on the other hand, was reduced by 85% in the cells treated with T16A$_{inh-A01}$ and by 70% in cells treated with CFTR$_{inh172}$ (Fig. 3.22B).

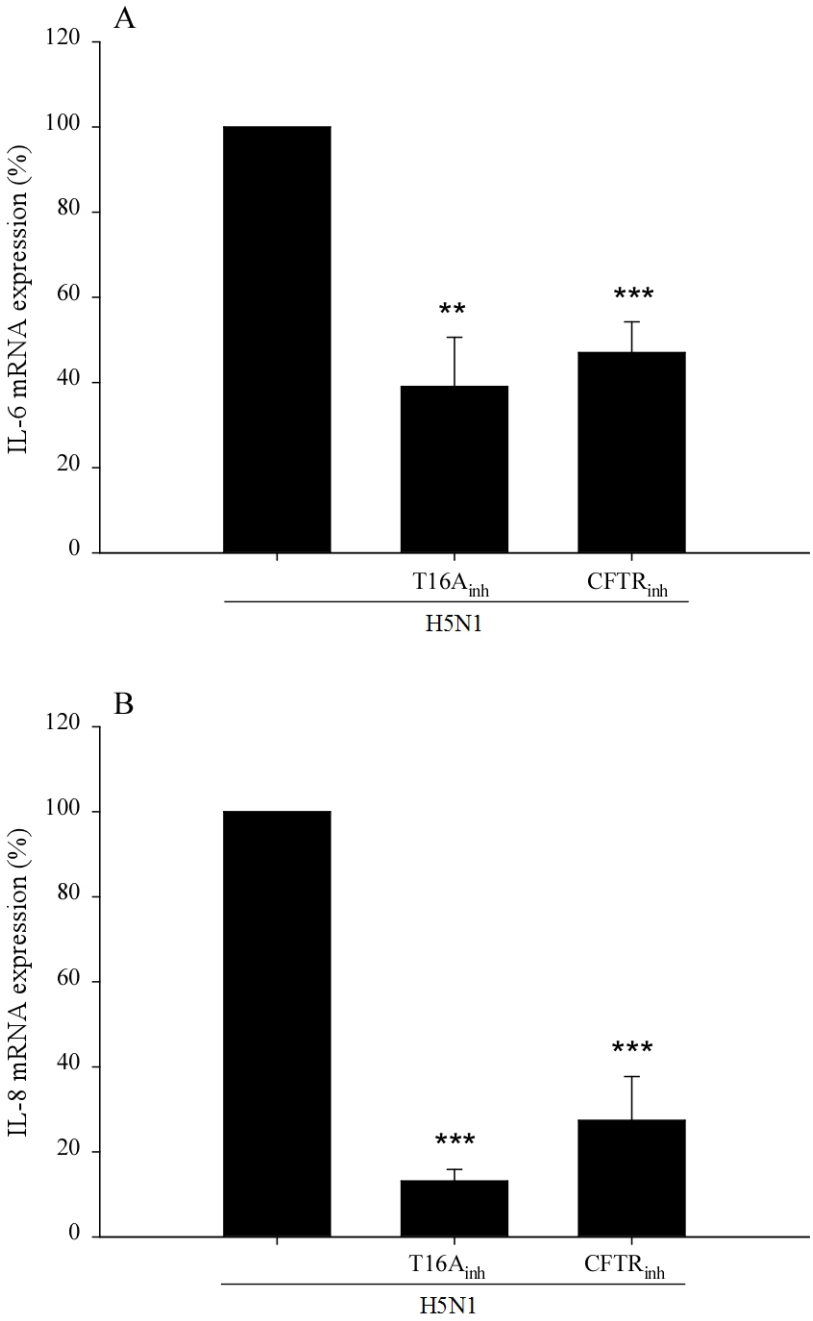

Fig. 3.22: T16A$_{inh\text{-}A01}$ and CFTR$_{inh172}$ attenuated the effect of inact-H5N1 on cytokine mRNA expression. 16HBE14o- cells were treated for 1 hr with an inhibitor of TMEM16A (T16A$_{inh\text{-}A01}$, 30 μM) or an inhibitor of CFTR (CFTR$_{inh172}$, 20 μM) before inact-H5N1 (20 μg/ml hemagglutinin) was introduced. Three hour after, cells were harvested for qRT-PCR analysis of mRNA expression of IL-6 (A) and IL-8 (B). Values are means ± SEM (n = 3).

** $p < 0.01$, *** $p < 0.001$ compared to the control, unpaired Student's *t*-test.

Next, the effectiveness of the siRNA against TMEM16A was determined. The mRNA expression of the channel in cells transfected with the specific siRNA was decreased by 70% (n = 3, $p < 0.001$) (Fig. 3.23A). In consistent with the results shown in Fig 3.22, the effect of inact-H5N1 on mRNA expression of IL-6 and IL-8 in cells transfected with the siRNA directed against TMEM16A was reduced by 40% (n = 3, $p < 0.001$) and 45% (n = 3, $p < 0.01$), respectively (Fig. 3.23B). Fig. 3.24 depicts the expression level of CFTR in 16HBE14o- cells transfected with two commercial siRNAs directed against CFTR. None of the siRNA can inhibit CFTR expression more than 40%, which is not effective enough to suppress activity of CFTR and to be used in our study.

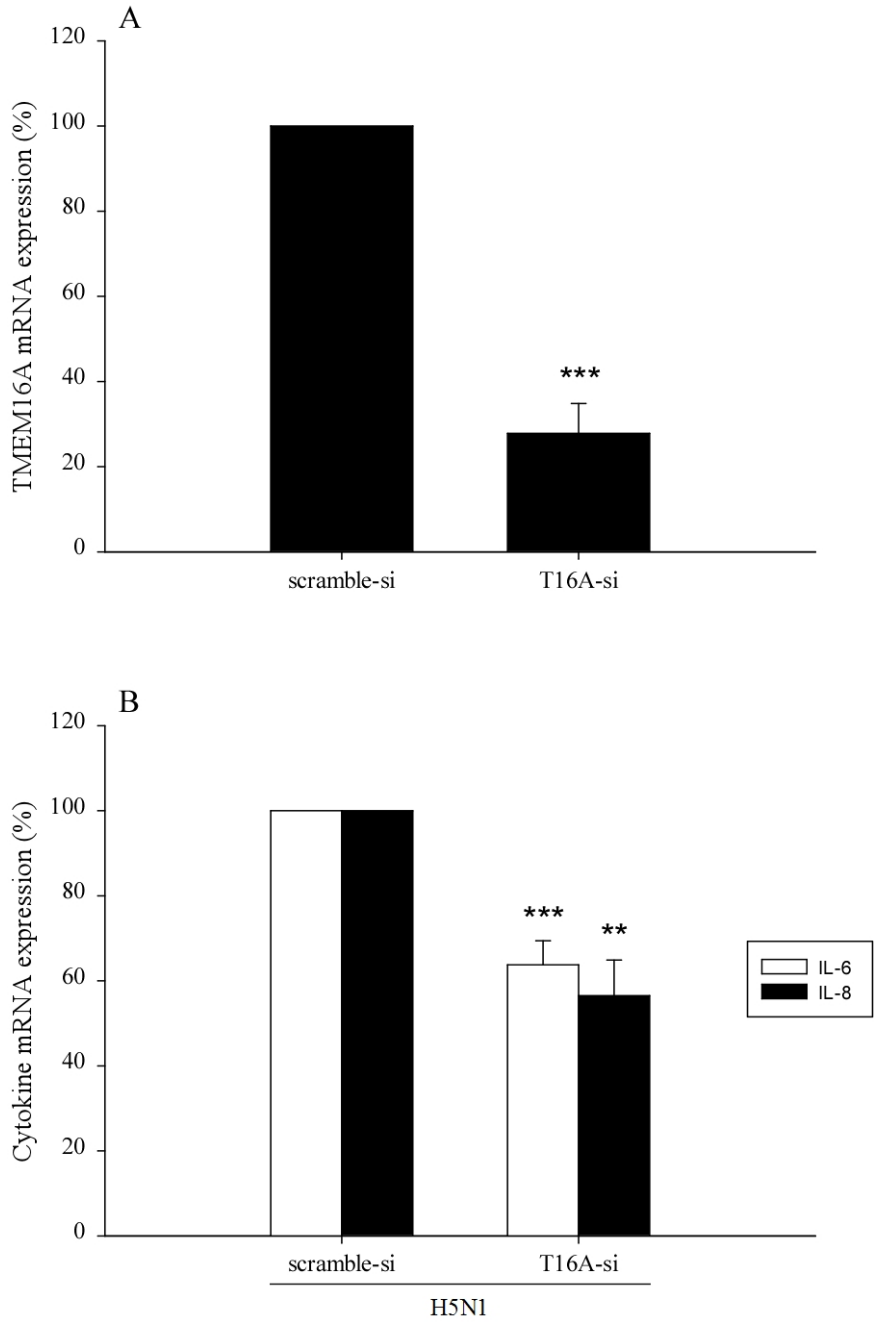

Fig. 3.23: Involvement of TMEM16A channel in inact-H5N1-induced increases in cytokine mRNA expression. HBE cells were transfected with a siRNA directed against TMEM16A chloride channel (T16A-si, 100 pmol) or a control scrambled siRNA (scrambled) for 48 hr. (A) Expression of mRNA of TMEM16A Cl^- channel was determined by qRT-PCR. (B) The siRNA transfected cells were treated with inact-H5N1 (20 µg/ml hemagglutinin) for 3 hr before being harvested and analysed for mRNA expression of IL-6 (open bars) and IL-8 (closed bars). Values are means ± SEM (n = 3). ** $p < 0.01$, *** $p < 0.001$ compared to the control, unpaired Student's *t*-test.

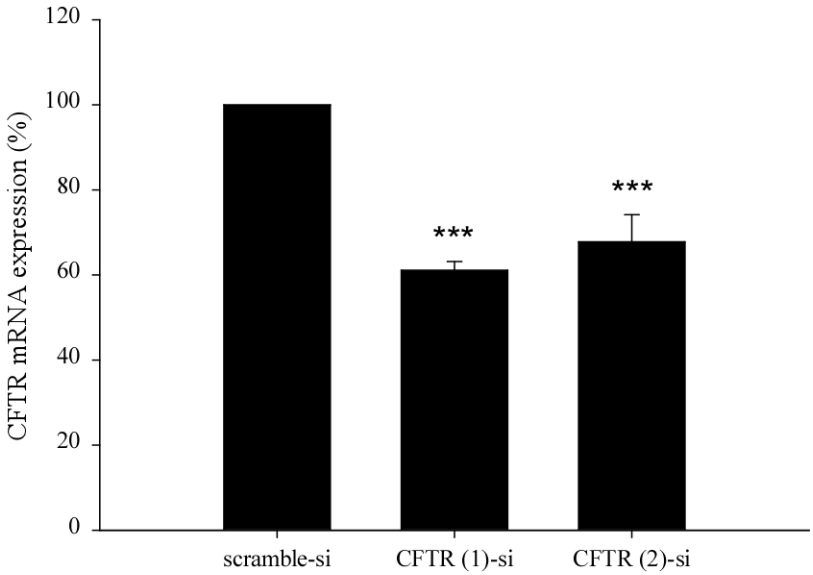

Fig. 3.24: Involvement of CFTR chloride channel in inact-H5N1-induced increases in cytokine mRNA expression. HBE cells were transfected with two different siRNA directed against CFTR chloride channel (100 pmol) or a control siRNA (scrambled) for 48 hr before the expression of mRNA of CFTR was determined by qRT-PCR. CFTR-1 was purchased from Thermo Scientific whereas CFTR-2 was purchased from Qiagen. Values are means ± SEM (n = 3). *** $p < 0.001$ compared to the scramble-siRNA, unpaired Student's *t*-test.

Finally the effect of inact-H5N1 on mRNA expression of TMEM16A and CFTR Cl^- channel was determined by qRT-PCR. 16HBE14o- cells were incubated in inact-H5N1 for 3 hr before expression of the Cl^- channels were determined. Data in Fig. 3.25 suggest that expressions of both TMEM16A and CFTR were small but significantly increased in cells treated with inact-H5N1.

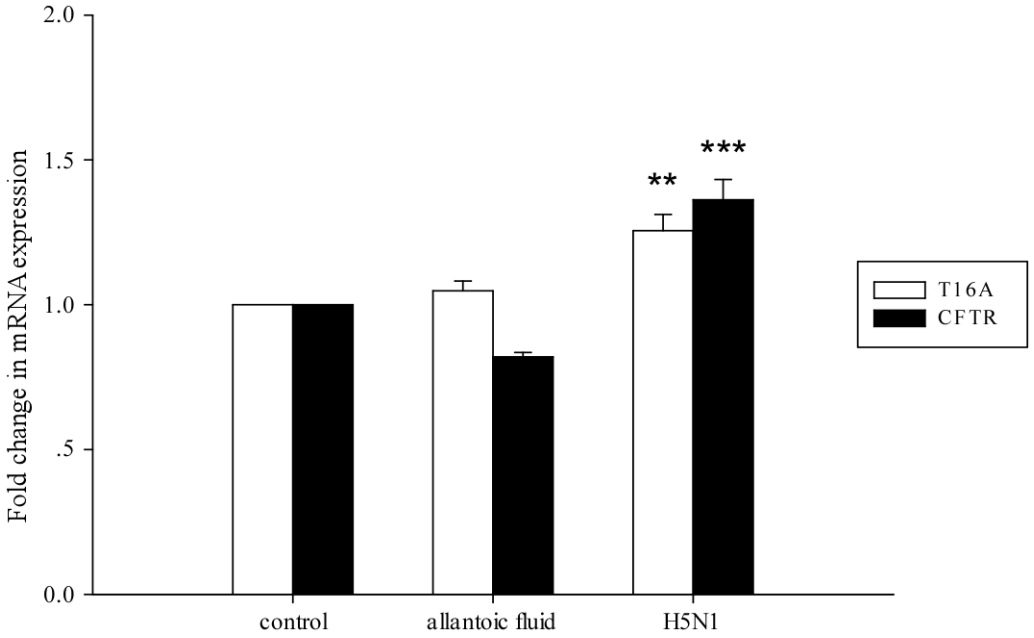

Fig. 3.25: The effect of inact-H5N1 on mRNA expression of TMEM16A (T16A) and CFTR chloride channel. 16HBE14o- cells were exposed to allantoic fluid and inact-H5N1 or untreated control for 3 hr, mRNA of TMEM16A and CFTR channels were determined by qRT-PCR. Values are means ± SEM. ** and *** indicate $p < 0.01$ and $p < 0.001$ compared with that of the cells treated with allantoic fluid (n = 3, unpaired Student's *t*-test).

CHAPTER 4

DISCUSSION

The airway epithelial cells are the first line of defense between our body and the inhaled air that contains harmful particles and infectious organisms, such as dust, air pollution, tobacco smoke, microbial and viruses etc. (Eder et al., 2006). Respiratory viral infections have been considered to be one of the major causes of common human illnesses. The most commonly found respiratory virus are RSV (*respiratory syncytial virus*), parainfluenza virus, rhinovirus, adenovirus and influenza virus (Nichols et al., 2008). Influenza A viruses that cause the infection in human are classified into two types, LPAI (low pathogenic avian influenza), such as human seasonal H1 or H3, causes a mild disease and HPAI (highly pathogenic avian influenza), such as H5 or H7, causes a severe illness. H5N1 is an avian influenza virus currently epidemic among wild birds and poultry in several Asian countries. The virus can transmit from birds to human causing a rapid and severe dysregulation of inflammatory and immune responses resulting in a high mortality rate (de Jong et al., 2006; Peiris et al., 2004). The clinical features that cause mortality in H5N1 infected patients include ARDS (acute respiratory distress syndrome) and multiple organ failure associated with the exacerbation of pro-inflammatory cytokine responses (de Jong et al., 2006; Peiris et al., 2004; To et al., 2001). This cytokine storm is characterized by the extreme production and secretion of a large numbers and levels of pro-inflammatory cytokines, including TNF-α, IL-6, MIP-1, MIG, IP-10, MCP-1 RANTES and IL-8 (Us, 2008). The pro-inflammatory cytokines are usually released by cells of the immune system, however, the respiratory epithelial cells which are the primary target of H5N1 virus are the first to produce the inflammatory response against the infection (Ebisawa et al., 1969). It has been reported that, in response to H5N1 infection, the bronchial epithelial cells increase productions of TNF-α, IL-6, IL-8, CCL-5 and IP-10 (Lam et al., 2010). This early production of cytokines and chemokines by the respiratory epithelium is most likely to play a primary and critical role in initiating the subsequent pathogenic responses including an initiation of the cytokine storm (Korteweg et al., 2008).

A major aim of this study is to determine the mechanism that underlies the infection-independent effect of H5N1 on cytokine and chemokine gene expressions in the respiratory epithelium. This study was inspired by previous reports that BPL-inact-H5N1 (VN04) can induce the production of CCL-5, IL-6 and IL-8 in A549 cells within 6 hr after exposure (Cheng et al., 2010) and that the inact-H5N1 increased the level of IL-6 found in the bronchoalveolar lavage fluid of mice (Imai et al., 2008). In the present study, the effect of inact-H5N1 on cytokine/chemokine mRNA expression in 16HBE14o-, the cell model of this study, was determined. This cell type was chosen for the present study because of the presence of α-2,3sialic acid receptor for the hemagglutinin of H5N1, a characteristic of the distal lung epithelium, and that this cell type contains both the TMEM16A and CFTR Cl^- channels, which are characteristics of a common respiratory epithelial cell. Since some of these characteristics are missing in some cultured reparatory epithelial cell types, the use of 16HBE14o- is, therefore, appropriate.

In agreement with the previous reports (Chan et al., 2005; Chan et al., 2010; Song et al., 2011), mRNA expressions of IL-6 and IL-8 in 16HBE14o- cells were elevated within 3 hr after exposure to inact-H5N1, while, exposure to the inact-H1N1 had no effect on any cytokine or chemokine mRNA expression (Figs. 3.2 & 3.3). Unlike the response to life-H5N1 infection (Lam et al., 2010), no effect of the inact-H5N1 on mRNA expressions of TNF-α, CCL-5 and IP-10 could be detected (Fig. 3.1). It has been reported that production of TNF-α could only be induced by life-virus but not by UV-inact-virus (Nain et al., 1990), which is similar to what has been observed in the present study. The difference in the profile of cytokine response between life and inact-H5N1 demonstrated in the present study suggests that a component(s) of viral envelope is capable of initiating mRNA transcription of selective cytokines and chemokines, including IL-6 and IL-8, whereas expression and production of others such as TNF-α, CCL-5 and IP-10 are initiated in an infection-dependent manner. It should be noted that the positive effect of the inact-H5N1 on IL-6 mRNA expression in 16HBE14o- cells was peaked within 3 hr after the cells were exposed to the virus but significantly declined within 6 hr. No effect of the virus on IL-6 mRNA expression was detected in hour12^{th} (Fig. 3.2). In contrary, the effect of the inact-H5N1 on IL-8 mRNA expression peaked 6 hr after the cells were exposed

to the virus and a significant 20 folds increase of the IL-8 expression was detected 12 hr after the exposure (Fig. 3.3). The difference in the profile of IL-6 and IL-8 mRNA expression responses to the inact-H5N1 suggests that the underlying infection-independent mechanisms by which H5N1 regulates IL-6 and IL-8 production are fundamentally different.

It has been hypothesized that the double-stranded RNAs (dsRNA) of the influenza viruses are attributable to the induction of cytokine production (Brydon et al., 2005). The mechanisms that underlie this dsRNA-induced cytokine response, however, have not yet been well understood. The Toll-like receptor 3 (TLR3) of the host cells is generally believed to be responsible for generating the primary cellular signaling that initiate immune responses to viral infection (Edelmann et al., 2004). Activation of TLR3 by dsRNA requires the process of viral infection (Jelinek et al., 2011). Evidence presented herein, however, suggested that binding of the viral envelope to the host cell membrane may be efficient in stimulating an onset of an immune response from the respiratory epithelial cells. In supporting this notion, it has been reported that a recombinant H1 hemagglutinin of the virus that caused the 1918 influenza pandemic induced production of cytokines and chemokines in the lung of mice (Kobasa et al., 2004). Moreover, H2 hemagglutinin or an UV-inact H2 virus can induced innate immune responses in murine B lymphocytes by a process that does not depend on sensing of the viral RNA (Marshall-Clarke et al., 2006). Furthermore, H5 hemagglutinin is directly responsible for increasing transcription of IP-10 and Interferon Regulatory transcription Factor-1 (IRF-1) gene in A549 human pulmonary epithelial cells (Xu et al., 2012).

The viral envelope of H5N1 composes of two surface glycoproteins, hemagglutinin and neuraminidase, that are associated with high induction of cytokines and chemokines (Kobasa et al., 2004; Tumpey et al., 2005). H5 and H1 hemagglutinin have preference for different glycolipid sialic acid receptors, i.e., α-2,3 and α-2,6 at the host cell membrane, respectively. These sialic acid receptors are present in the 16HBE14o- cells (Fig. 3.5). The data present herein suggest that the effect of the inact-H5N1 on IL-6 and IL-8 mRNA expression is mediated via the α-2,3 sialic acid receptor. The inhibitory effect of α-2,3-specific sialidase, an enzyme that dismantles α-2,3 linkage of membrane α-2,3 sialic acid receptor, on the effect of

the inact-H5N1 on IL-6 and IL-8 mRNA expression (Fig. 3.4) confirms this notion. An interaction between the H5-HA and the α-2,3 sialic acid receptor is certainly essential for stabilizing the viral particle to the host cells. It is, however, possible that H5-HA/α-2,3 sialic acid receptor interaction triggers the receptor to propagate a cellular signaling responsible for an activation of IL-6 and IL-8 mRNA expression. Since the two commercial recombinant H5 hemagglutinins used in the present study failed to increase mRNA expression of IL-6 and IL-8 in HBE cells (Fig. 3.6), this possibility seems unlikely. It is, therefore, conceivable that although the binding between H5 hemagglutinin and the α-2,3 sialic acid receptor of the respiratory epithelial cells is essential, other component or components of the viral envelope may subsequently trigger an onset of the cellular signaling mechanisms that upregulate the cytokine production. Interestingly, cytochalasin D, an alkaloid that is a potent inhibitor of actin polymerization, hence inhibits endocytosis of the virus particle, inhibited inact-H5N1-mediated IL-6 and IL-8 mRNA expression. This finding suggests that induction of IL-6 and IL-8 mRNA expression may also require cellular uptake of the virus particle. Considering an extensive role of actin cytoskeleton in a broad array of cellular functions, the effect of cytochalasin D may actually be due to the fact that one of the downstream effect or molecules of the inact-H5N1-mediated cellular signaling pathway(s) is regulated by actin and, thus, the signaling mechanism for activating IL-6 and IL-8 mRNA expression is disrupted when the activity of actin is inhibited by cytochalasin D.

A variety of stimuli, such as mechanical stimuli, inflammatory stimuli, often in the area of cellular damage, are capable of initiating nucleotide (i.e. ATP or UTP) release from cells (Bucheimer et al., 2004). In mouse bronchoalveolar epithelium infected with RSV, increased UTP levels caused a reduction of alveolar fluid clearance (Davis et al., 2004). In addition, influenza A virus increased ATP and UTP release from the respiratory epithelium and an activation of adenosine receptors by the released nucleotides has been known to play an important role in stimulating CFTR-mediated anion secretion in the respiratory cells (Wolk et al., 2008). It has also been reported that activation of purinergic receptors, P2X and P2Y receptors, can affect cytokine production (Gabel, 2007). The positive effect of the inact-H5N1 on mRNA expressions of IL-6 and IL-8 in 16HBE14o- cells is likely mediated via the

purinergic signaling. The inhibitory effect of suramin, a broad spectrum P2Y receptor (P2YR) antagonist, (Fig. 3.7) on the effect of the inact-H5N1 on mRNA expressions of IL-6 and IL-8 supports this conclusion. Moreover, apyrase, an enzyme that hydrolyzes nucleotide triphosphates and nucleotide diphosphates, abolished the effect of the inact-H5N1 (Fig. 3.7). Given that, under the experimental conditions, apyrase targets extracellular nucleotides, the inhibitory effect of apyrase on the inact-H5N1-mediated IL-6 and IL-8 mRNA expression suggests that the inact-H5N1 must induce a release of nucleotide triphosphates and/or nucleotide diphosphates, which in turn act in paracrine or autocrine manner to activate cellular signaling leading to increased productions of IL-6 and IL-8.

Consistent with the role of nucleotides in the activation of cytokine production, several agonists of purinegic receptors upregulated mRNA expressions of IL-6 and IL-8 (Fig. 3.8). It has been reported that ATP and 2MesADP, both are $P2Y_1R$ agonist, induced secretion of IL-6 in astrocytes (Fujita et al., 2009). Although the agonist for $P2Y_1R$, ADP, strongly increased mRNA expressions of both IL-6 and IL-8 in 16HBE14o- cells, further analysis using a specific $P2Y_1R$ antagonist, MRS2179 and $P2Y_6R$ antagonist, MRS2578, revealed that the $P2Y_6R$ but not $P2Y_1R$ involved in this process (Fig. 3.9). The role of $P2Y_6R$ is further strengthen by a finding depicted in Fig. 3.10 that knocking-down the expression of $P2Y_6R$ significantly blundered the effect of the inact-H5N1 on mRNA expressions of both IL-6 and IL-8 in 16HBE14o- cells. Notably, the $P2Y_6R$-specific siRNA does not completely abolish the effect of the inact-H5N1. This inefficiency of the siRNA may be due to a low level of $P2Y_6R$ expression in the presence of the siRNA is capable of generating a cellular signal(s) that can sufficiently upregulate production of the cytokines. $P2Y_6R$ is a $G_{q/11}$-coupled receptor. Its cellular signaling involves activation of PLC, IP_3, DAG, PKC and elevation of intracellular Ca^{2+}concentration ($[Ca^{2+}]_i$) (Boeynaems et al., 2005; Burnstock, 2007). Consistent with this notion, the effect of the inact-H5N1 on the cytokine mRNA expression was attenuated by pharmacological agents that inhibit the activity of PLC (U73122), PKC (BIM and GÖ6976) and by sequestering $[Ca^{2+}]_i$ with BAPTA-AM (Fig. 3.12).

Several lines of evidence suggested that MAPK play a key role in the regulation of cytokine production. ERK1/2 and p38 MAPK are known to regulate

production of IL-8 in cystic fibrosis lung epithelial cells (Bhattacharyya et al., 2011) and in the alveolar macrophages (Koch et al., 2004). Furthermore, the cellular signaling pathway by which *Chlamydia* induces IL-8 mRNA expression in epithelial cells (Buchholz et al., 2007) and H9N2 induces production of IL-1β, IL-6 and IL-8 in chicken macrophages, involve ERK1/2 (Xing et al., 2010). In addition, activation of $P2Y_6R$ increased IL-8 expression is ERK1/2-dependent (Warny et al., 2001). p38 MAPK has been known to be involved in the signaling pathway by which influenza A virus subtype H3N2 activates mRNA expression of a chemotactic cytokine, RANTES, in human bronchial epithelial cell (Kujime et al., 2000). Indeed, H5N1 increases production of pro-inflammatory cytokines in human macrophages in a p38 MAPK-dependent manner (Hui et al., 2009; Lee et al., 2005).

Data obtained in the present study suggest that inact-H5N1 increases phosphorylation of both ERK1/2 and p38 MAPK in 16HBE14o- cells (Figs. 3.14 & 3.15). IL-6 mRNA expression in response to the inact-H5N1, however, was attenuated by SB203580 but not by PD98059 or SP600125 (Fig. 3.13A), suggesting that p38 but not ERK1/2 or JNK are involved in the signal transduction mechanisms by which the inact-H5N1 upregulates mRNA expression level of this cytokine. Since SB203580 abolished only 40% of inact-H5N1-mediated IL-6 mRNA expression, a possibility that a cellular mechanism that is mediated by unidentified cellular signaling molecule(s) other than p38 MAPK, ERK1/2 and JNK may be involved in the induction of IL-6 mRNA expression should not be totally excluded. On the other hand, SB203580, PD98059 and SP600125 inhibited H5N1-induced IL-8 mRNA expression (Fig. 3.13B), hence the signaling mechanism that upregulates IL-8 production involves all three MAPKs. Apparently, both SB203580 and PD968059 have stronger inhibitory effects on H5N1-mediated IL-8 mRNA expression than that of SP600125. This data suggest that p38 and ERK1/2 signalings may be the major regulatory pathways that H5N1 uses to upregulate a rapid IL-8 production in the respiratory epithelium prior to infection. The sensitivity of the H5N1-mediated cellular signaling system that upregulates IL-8 to ERK1/2 and JNK, therefore, emphasizes the fundamental difference between the mechanisms by which the virus regulate mRNA expression of IL-6 and that of IL-8. The finding that the effect of inact-H5N1 on the activation of ERK1/2 is abolished in cells treated with BAPTA-

AM (Fig. 3.16) is consistent with this be a cellular mechanism that is Ca^{2+}-dependent, as it should for $P2Y_6R$-mediated signaling. The effect of BAPTA-AM on inact-H5N1-mediated p38 MAPK phosphorylation (Fig. 3.17) cannot be demonstrated, however. This is because BAPTA-AM itself increases phosphorylation of p38 MAPK in virus untreated cells (data not shown).

It has been reported in a study (Huipao, 2011) prior to this present study that inact-H5N1 increases Cl^- secretion in H441 respiratory epithelia cell via TMEM16-A, a Ca^{2+}-activated Cl^- channel (CACC). In 16HBE14o- cells, inact-H5N1 not only increases Cl^- secretion by TMEM16A but also by the CFTR Cl^- channel (Fig. 3.20). Interestingly, the effect of inact-H5N1 on phosphorylation of ERK1/2 attenuated in cells treated with $T16A_{inh}$, a specific blocker of TMEM16A but not by $CFTR_{inh}$, a specific blocker for CFTR. This finding suggests a relationship between activity of TMEM16A and ERK1/2 signaling. The blockers, however, do not have a similar effect on H5N1-mediated p38 MAPK phosphorylation (Fig. 3.17). Indeed, both $T16A_{inh}$ and $CFTR_{inh}$ increased phosphorylation of p38 MAPK in inact-H5N1 treated cells (Fig. 3.17) but not in the virus untreated cells (data not shown). The reason for this activation of the MAPK by the Cl^- channel blockers is currently unknown.

Little is known about the role of Cl^- channels on the regulation of cytokine production. It has been reported that niflumic acid, a CACC blocker, reduced histamine-induced IL-6 and IL-8 mRNA expression in human conjunctival epithelial cells (HCEC) (Lim et al., 2013) and that histamine increased CACC expression in HCEC (Leverkoehne et al., 2002; Seo et al., 2011). Together, these findings suggested that function of CACC may play a role in the regulation of IL-6 and IL-8 mRNA expression. Interestingly, inact-H5N1 increased mRNA expression of both the TMEM16A and CFTR Cl^- channels (Fig. 3.25). Furthermore, inact-H5N1-induced IL-6 and IL-8 mRNA expression was attenuated in cells treated with $T16A_{inh}$ or $CFTR_{inh}$ (Fig. 3.22). Taken together with the finding that siRNA knocking-down expression of TMEM16A attenuates the effect of inact-H5N1 on IL-6 and IL-8 mRNA expression (Fig. 3.23), these data suggest that the activity of TMEM16A is required for H5N1 to mediate its infection-independent effect on IL-6 and IL-8 mRNA expression. On this note, the effect of siRNA knocking-down CFTR

expression on the effect of inact-H5N1 on IL-6 and IL-8 mRNA expression cannot be demonstrated in the present study. This is due to the fact that none of the commercially available siRNAs directed against CFTR are effective enough to reduce expression of CFTR in 16HBE14o- cells to an adequately low level (Fig. 3.24). These siRNAs can suppress not more than 40% of the total CFTR mRNA expression. Such inhibitory effect may be too low, and hence CFTR activity remains high enough to support mRNA expression of the cytokines.

Does Cl^- conductance play role in the regulation of IL-6 and IL-8 production in the respiratory epithelium? Previous studies suggested that modification of the cellular Cl^- flux via CACC may influence expression of cytokines (Moss et al., 1996; Moss et al., 2000). Data in Fig. 3.20, suggest that inact-H5N1 increases Cl^- secretion via both TMEM16A and CFTR. Since inhibition of CFTR also had an adverse effect on the inact-H5N1-induced IL-6 and IL-8 mRNA expression (Fig. 3.22), it appears that interfering with any Cl^- conductance can alter the effect of inact-H5N1 on IL-6 and IL-8 mRNA expression. It is, therefore, tempted to speculate that Cl^- conductance and perhaps the intracellular Cl^- concentration that changes when the chloride channels were activated may have a role to play in the mechanisms that upregulate IL-6 and IL-8 mRNA expression.

It is well established that NF-κB is involved in innate immune response. The hemagglutinin of the influenza virus H7N1 activates transcription of NF-κB (Pahl et al., 1995) whereas *Salmonella typhimurium* induced IL-8 secretion via Ca^{2+}-mediated activation of NF-κB (Gewirtz et al., 2000). Moreover, NF-κB p50 transgenic mice did not produce a cytokine response to H5N1 infection (Droebner et al., 2008). Data herein suggest that SN-50, a NF-κB inhibitor, inhibits approximately 30% of the inact-H5N1-mediated IL-6 and IL-8 mRNA response (Fig. 3.18). On this note, a MAPK-dependent but NF-κB-independent pathway has been reported to mediate the upregulation of pro-inflammatory cytokines response to viral infections (Meusel et al., 2003).

One other regulatory molecule that may be involved in inact-H5N1-mediated IL-6 and IL-8 mRNA expression is Janus kinase 3 (JAK3). The Janus kinase (JAK) belong to the family non-receptor tyrosine kinases, in mammals including JAK1, JAK2, JAK3 and Tyk2, that play an important role in activation of

Signal Transducer and Activator of Transcription (STAT) protein that transduces cytokine-mediated signals through JAK-STAT pathway (Rane et al., 2000). It has been reported that H5 hemagglutinin induced cytokine production in pulmonary epithelial cells involved activation of JAK3 (Xu et al., 2012). In the present study, a specific JAK3 inhibitor, $JAK3_{inh}$, attenuates the effect of the inact-H5N1 on IL-8 but not IL-6 mRNA expression (Fig. 3.19). This finding does not only put JAK3 as one of the important signaling molecules that mediate the infection-independent effect of H5N1, but also confirms that H5N1 regulates IL-6 and IL-8 by multiple signaling pathways, some of which are independent.

CHAPTER 5

CONCLUSION

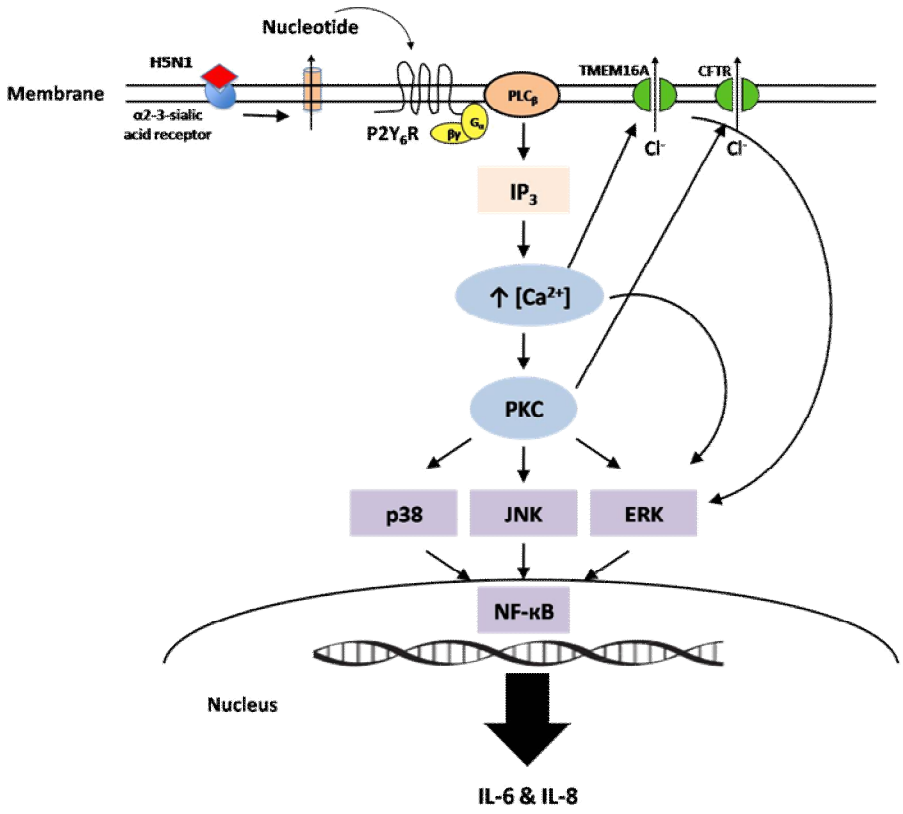

Fig. 5.1: A working model for the mechanism by which inact-H5N1 avian influenza virus increases IL-6 and IL-8 mRNA expression.

In summary, data from the present study suggest that H5N1 can increase mRNA expressions of IL-6 and IL-8 in the respiratory epithelium in an infection-independent manner and that this effect of the virus requires an interaction between the viral hemagglutinin and the α-2,3 sialic acid receptors at the cell membrane of the host cells. The mechanism for this induction of cytokine production involves (i) stimulation of nucleotide release from the host cells; (ii) activation of the $P2Y_6$ purinegic receptor at the host cell membrane; and (iii) propagation of the G protein-coupled receptor signaling via PLC, PKC and $[Ca^{2+}]_i$ signaling. This signaling cascade, in turn activates MAPK signaling including that of the ERK1/2 and p38 MAPK. Activation of the $P2Y_6R$ by H5N1 also increase Cl^- conductance of the

respiratory epithelium resulting in a Cl^- secretion. This change of the Cl^- conductance, and perhaps the change in the cytosolic Cl^- concentration during the purinergic receptor activation, is essential for the regulation of IL-6 and IL-8 mRNA expression by H5N1. A summary of intracellular signaling molecules involved is depicted in Fig. 5.1.

There are a few remaining issues that should be investigated to further our understanding of this infection-independent effect of H5N1 on the innate immunity. One of the most fundamental issues that require investigation is whether this effect of the virus causes an increase in the concentration of IL-6 and IL-8 in the alveolar fluid and the surrounding tissue. An analysis of the level of IL-6 and IL-8 in the cell culture medium that is used to grow 16HBE14o- cells treated with the inact-H5N1 should give a useful insight. Further study in an animal model to determine the effect of the inact-H5N1 on the alveolar fluid should be conducted. It is also interested to determine whether the infection-independent effect of H5N1 on IL-6 and IL-8 production plays an important role in triggering the innate immune response to H5N1 infection and, subsequently, in initiating the cytokine storm which is the cause of fatality in H5N1 infection. Data from the present study suggest that $P2Y_6$ receptor plays a critical role in the mediating the effect of the virus. It would be interesting to see if the effect of life H5N1 on cytokine production is attenuated in the commercially available $P2Y_6$ knock-out mice and that, whether the mortality rate of the $P2Y_6R^{-/-}$ infected mice is less than that of the wild-type mice. From the novel finding of the present study that the effect of the inact-H5N1 on IL-6 and IL-8 mRNA expression depends on activity of the TMEM16A and CFTR Cl^- channels, it can be hypothesized that if Cl^- secretion alone can trigger the IL-6 and IL-8 expression, an increase in the Cl^- driving force across the apical membrane, such as a decreasing in Cl^- concentration in the medium bating the apical membrane, should mimic the effect of the virus on IL-6 an IL-8 mRNA expression. Moreover, an inhibition of the basolateral Cl^- transport mechanism such as the Na/K/2Cl co-transporter should attenuate the effect of virus. To elucidate these issues, further examinations of the bioelectric property of the membrane of 16HBE14o- cells using Ussing chamber or patch-clamp techniques will be required.

REFERENCES

Abbracchio, M.P., G. Burnstock, J.M. Boeynaems, E.A. Barnard, J.L. Boyer, C. Kennedy, G.E. Knight, M. Fumagalli, C. Gachet, K.A. Jacobson, and G.A. Weisman. 2006. International Union of Pharmacology LVIII: update on the P2Y G protein-coupled nucleotide receptors: from molecular mechanisms and pathophysiology to therapy. Pharmacological reviews. 58:281-341.

Abdel-Ghafar, A.N., T. Chotpitayasunondh, Z. Gao, F.G. Hayden, D.H. Nguyen, M.D. de Jong, A. Naghdaliyev, J.S. Peiris, N. Shindo, S. Soeroso, and T.M. Uyeki. 2008. Update on avian influenza A (H5N1) virus infection in humans. N Engl J Med. 358:261-273.

Adams, S., and C. Sandrock. 2010. Avian influenza: update. Medical principles and practice : international journal of the Kuwait University, Health Science Centre. 19:421-432.

Akira, S. 1997. IL-6-regulated transcription factors. The international journal of biochemistry & cell biology. 29:1401-1418.

Almansa, R., R. Ortiz de Lejarazu, M.a.Á. Jiménez-Sousa, L. Rico, E. Largo, V. Iglesias, E. Golvano, and J.F. Bermejo-Martin. 2011. H5 influenza haemagglutinin and cytokine profiles in cultured PBMCs from adults and children. Inmunología. 30:79-84.

Aoki, F.Y., G. Boivin, and N. Roberts. 2007. Influenza virus susceptibility and resistance to oseltamivir. Antiviral therapy. 12:603-616.

Ashby, M.C., and A.V. Tepikin. 2002. Polarized calcium and calmodulin signaling in secretory epithelia. Physiological reviews. 82:701-734.

Baggiolini, M. 1993. Novel aspects of inflammation: interleukin-8 and related chemotactic cytokines. The Clinical investigator. 71:812-814.

Baggiolini, M., and I. Clark-Lewis. 1992. Interleukin-8, a chemotactic and inflammatory cytokine. FEBS letters. 307:97-101.

Beigel, J.H. 2008. Influenza. Critical care medicine. 36:2660-2666.

Bhattacharyya, S., U. Gutti, J. Mercado, C. Moore, H.B. Pollard, and R. Biswas. 2011. MAPK signaling pathways regulate IL-8 mRNA stability and IL-8 protein expression in cystic fibrosis lung epithelial cell lines. American journal of physiology. Lung cellular and molecular physiology. 300:L81-87.

Blackwell, T.S., and J.W. Christman. 1997. The role of nuclear factor-kappa B in cytokine gene regulation. American journal of respiratory cell and molecular biology. 17:3-9.

Boeynaems, J.M., D. Communi, N.S. Gonzalez, and B. Robaye. 2005. Overview of the P2 receptors. Seminars in thrombosis and hemostasis. 31:139-149.

Boots, A.W., M. Hristova, D.I. Kasahara, G.R. Haenen, A. Bast, and A. van der Vliet. 2009. ATP-mediated activation of the NADPH oxidase DUOX1 mediates airway epithelial responses to bacterial stimuli. The Journal of biological chemistry. 284:17858-17867.

Bouvier, N.M., and P. Palese. 2008. The biology of influenza viruses. Vaccine. 26 Suppl 4:D49-53.

Brown, H.A., E.R. Lazarowski, R.C. Boucher, and T.K. Harden. 1991. Evidence that UTP and ATP regulate phospholipase C through a common extracellular 5'-nucleotide receptor in human airway epithelial cells. Molecular Pharmacology. 40:648-655.

Brydon, E.W., S.J. Morris, and C. Sweet. 2005. Role of apoptosis and cytokines in influenza virus morbidity. FEMS microbiology reviews. 29:837-850.

Bucheimer, R.E., and J. Linden. 2004. Purinergic regulation of epithelial transport. The Journal of physiology. 555:311-321.

Buchholz, K.R., and R.S. Stephens. 2007. The extracellular signal-regulated kinase/mitogen-activated protein kinase pathway induces the inflammatory factor interleukin-8 following Chlamydia trachomatis infection. Infection and immunity. 75:5924-5929.

Burnstock, G. 2007. Purine and pyrimidine receptors. Cellular and molecular life sciences : CMLS. 64:1471-1483.

Burnstock, G., and G.E. Knight. 2004. Cellular distribution and functions of P2 receptor subtypes in different systems. International review of cytology. 240:31-304.

Burnstock, G., and M. Williams. 2000. P2 purinergic receptors: modulation of cell function and therapeutic potential. The Journal of pharmacology and experimental therapeutics. 295:862-869.

Button, B., M. Picher, and R.C. Boucher. 2007. Differential effects of cyclic and constant stress on ATP release and mucociliary transport by human airway epithelia. The Journal of physiology. 580:577-592.

Chakraborti, S. 2003. Phospholipase A(2) isoforms: a perspective. Cellular signalling. 15:637-665.

Chan, M.C., C.Y. Cheung, W.H. Chui, S.W. Tsao, J.M. Nicholls, Y.O. Chan, R.W. Chan, H.T. Long, L.L. Poon, Y. Guan, and J.S. Peiris. 2005. Proinflammatory cytokine responses induced by influenza A (H5N1) viruses in primary human alveolar and bronchial epithelial cells. Respiratory research. 6:135.

Chan, R.W., K.M. Yuen, W.C. Yu, C.C. Ho, J.M. Nicholls, J.S. Peiris, and M.C. Chan. 2010. Influenza H5N1 and H1N1 virus replication and innate immune responses in bronchial epithelial cells are influenced by the state of differentiation. PloS one. 5:e8713.

Chang, W.C. 2006. Store-operated calcium channels and pro-inflammatory signals. Acta pharmacologica Sinica. 27:813-820.

Chen, J., and Y.-M. Deng. 2009. Influenza virus antigenic variation, host antibody production and new approach to control epidemics. Virology journal. 6:30.

Chen, W., P.A. Calvo, D. Malide, J. Gibbs, U. Schubert, I. Bacik, S. Basta, R. O'Neill, J. Schickli, P. Palese, P. Henklein, J.R. Bennink, and J.W. Yewdell. 2001. A novel influenza A virus mitochondrial protein that induces cell death. Nat Med. 7:1306-1312.

Chen, W., M.M. Monick, A.B. Carter, and G.W. Hunninghake. 2000. Activation of ERK2 by respiratory syncytial virus in A549 cells is linked to the production of interleukin 8. Experimental lung research. 26:13-26.

Chen, X.-J., S. Seth, G. Yue, P. Kamat, R.W. Compans, D. Guidot, L.A. Brown, D.C. Eaton, and L. Jain. 2004. Influenza virus inhibits ENaC and lung fluid clearance. L366-L373 pp.

Cheng, X., Q. Xu, E. Song, C.F. Yang, G. Kemble, and H. Jin. 2010. The hemagglutinin protein of influenza A/Vietnam/1203/2004 (H5N1) contributes to hyperinduction of proinflammatory cytokines in human epithelial cells. Virology. 406:28-36.

Claas, E.C., J.C. de Jong, R. van Beek, G.F. Rimmelzwaan, and A.D. Osterhaus. 1998. Human influenza virus A/HongKong/156/97 (H5N1) infection. Vaccine. 16:977-978.

Clapham, D.E. 2007. Calcium signaling. Cell. 131:1047-1058.

Cox, M.A., B. Gomes, K. Palmer, K. Du, M. Wiekowski, B. Wilburn, M. Petro, C.C. Chou, C. Desquitado, M. Schwarz, C. Lunn, D. Lundell, S.K. Narula, P.J. Zavodny, and C.H. Jenh. 2005. The pyrimidinergic P2Y6 receptor mediates a novel release of proinflammatory cytokines and chemokines in monocytic cells stimulated with UDP. Biochemical and biophysical research communications. 330:467-473.

Cressman, V.L., E. Lazarowski, L. Homolya, R.C. Boucher, B.H. Koller, and B.R. Grubb. 1999. Effect of loss of P2Y(2) receptor gene expression on nucleotide regulation of murine epithelial Cl(-) transport. The Journal of biological chemistry. 274:26461-26468.

Damjanovic, D., C.L. Small, M. Jeyanathan, S. McCormick, and Z. Xing. 2012. Immunopathology in influenza virus infection: uncoupling the friend from foe. Clinical immunology. 144:57-69.

Davis, I.C., W.M. Sullender, J.M. Hickman-Davis, J.R. Lindsey, and S. Matalon. 2004. Nucleotide-mediated inhibition of alveolar fluid clearance in BALB/c mice after respiratory syncytial virus infection. L112-L120 pp.

de Jong, M.D., and T.T. Hien. 2006. Avian influenza A (H5N1). Journal of clinical virology : the official publication of the Pan American Society for Clinical Virology. 35:2-13.

de Jong, M.D., C.P. Simmons, T.T. Thanh, V.M. Hien, G.J. Smith, T.N. Chau, D.M. Hoang, N.V. Chau, T.H. Khanh, V.C. Dong, P.T. Qui, B.V. Cam, Q. Ha do, Y. Guan, J.S. Peiris, N.T. Chinh, T.T. Hien, and J. Farrar. 2006. Fatal outcome of human influenza A (H5N1) is associated with high viral load and hypercytokinemia. Nature medicine. 12:1203-1207.

Douillet, C.D., W.P. Robinson, 3rd, P.M. Milano, R.C. Boucher, and P.B. Rich. 2006. Nucleotides induce IL-6 release from human airway epithelia via P2Y2 and p38 MAPK-dependent pathways. American journal of physiology. Lung cellular and molecular physiology. 291:L734-746.

Droebner, K., S.J. Reiling, and O. Planz. 2008. Role of hypercytokinemia in NF-kappaB p50-deficient mice after H5N1 influenza A virus infection. Journal of virology. 82:11461-11466.

Ebisawa, I.T., O. Kitamoto, Y. Takeuchi, and M. Makino. 1969. Immunocytologic study of nasal epithelial cells in influenza. The American review of respiratory disease. 99:507-515.

Edelmann, K.H., S. Richardson-Burns, L. Alexopoulou, K.L. Tyler, R.A. Flavell, and M.B. Oldstone. 2004. Does Toll-like receptor 3 play a biological role in virus infections? Virology. 322:231-238.

Eder, W., M.J. Ege, and E. von Mutius. 2006. The Asthma Epidemic. New England Journal of Medicine. 355:2226-2235.

Erb, L., Z. Liao, C.I. Seye, and G.A. Weisman. 2006. P2 receptors: intracellular signaling. Pflugers Archiv : European journal of physiology. 452:552-562.

Feghali, C.A., and T.M. Wright. 1997. Cytokines in acute and chronic inflammation. Frontiers in bioscience : a journal and virtual library. 2:d12-26.

Flory, E., M. Kunz, C. Scheller, C. Jassoy, R. Stauber, U.R. Rapp, and S. Ludwig. 2000. Influenza Virus-induced NF-κB-dependent Gene Expression Is Mediated by Overexpression of Viral Proteins and Involves Oxidative Radicals and Activation of IκB Kinase. Journal of Biological Chemistry. 275:8307-8314.

Fritz, R.S., F.G. Hayden, D.P. Calfee, L.M. Cass, A.W. Peng, W.G. Alvord, W. Strober, and S.E. Straus. 1999. Nasal cytokine and chemokine responses in experimental influenza A virus infection: results of a placebo-controlled trial of intravenous zanamivir treatment. The Journal of infectious diseases. 180:586-593.

Fujita, T., H. Tozaki-Saitoh, and K. Inoue. 2009. P2Y1 receptor signaling enhances neuroprotection by astrocytes against oxidative stress via IL-6 release in hippocampal cultures. Glia. 57:244-257.

Gabel, C.A. 2007. P2 purinergic receptor modulation of cytokine production. Purinergic signalling. 3:27-38.

Geiler, J., M. Michaelis, P. Sithisarn, and J. Cinatl, Jr. 2011. Comparison of pro-inflammatory cytokine expression and cellular signal transduction in human macrophages infected with different influenza A viruses. Medical microbiology and immunology. 200:53-60.

Gewirtz, A.T., A.S. Rao, P.O. Simon, Jr., D. Merlin, D. Carnes, J.L. Madara, and A.S. Neish. 2000. Salmonella typhimurium induces epithelial IL-8 expression via Ca(2+)-mediated activation of the NF-kappaB pathway. The Journal of clinical investigation. 105:79-92.

Grygorczyk, R., and J.W. Hanrahan. 1997. CFTR-independent ATP release from epithelial cells triggered by mechanical stimuli. The American journal of physiology. 272:C1058-1066.

Guo, Y., E. Rumschlag-Booms, J. Wang, H. Xiao, J. Yu, J. Wang, L. Guo, G.F. Gao, Y. Cao, M. Caffrey, and L. Rong. 2009. Analysis of hemagglutinin-mediated entry tropism of H5N1 avian influenza. Virology journal. 6:39.

Hayashi, R., N. Yamashita, S. Matsui, T. Fujita, J. Araya, K. Sassa, N. Arai, Y. Yoshida, T. Kashii, M. Maruyama, E. Sugiyama, and M. Kobayashi. 2000. Bradykinin stimulates IL-6 and IL-8 production by human lung fibroblasts through ERK- and p38 MAPK-dependent mechanisms. European Respiratory Journal. 16:452-458.

Hayden, F.G., R. Fritz, M.C. Lobo, W. Alvord, W. Strober, and S.E. Straus. 1998. Local and systemic cytokine responses during experimental human influenza A virus infection. Relation to symptom formation and host defense. The Journal of clinical investigation. 101:643-649.

Hebert, C.A., and J.B. Baker. 1993. Interleukin-8: a review. Cancer investigation. 11:743-750.

Hedges, J.C., C.A. Singer, and W.T. Gerthoffer. 2000. Mitogen-activated protein kinases regulate cytokine gene expression in human airway myocytes. American journal of respiratory cell and molecular biology. 23:86-94.

Hoffmann, E., O. Dittrich-Breiholz, H. Holtmann, and M. Kracht. 2002. Multiple control of interleukin-8 gene expression. Journal of leukocyte biology. 72:847-855.

Holmes, W.E., J. Lee, W.J. Kuang, G.C. Rice, and W.I. Wood. 1991. Structure and functional expression of a human interleukin-8 receptor. Science (New York, N.Y.). 253:1278-1280.

Homolya, L., T.H. Steinberg, and R.C. Boucher. 2000. Cell to cell communication in response to mechanical stress via bilateral release of ATP and UTP in polarized epithelia. The Journal of cell biology. 150:1349-1360.

Homolya, L., W.C. Watt, E.R. Lazarowski, B.H. Koller, and R.C. Boucher. 1999. Nucleotide-regulated Calcium Signaling in Lung Fibroblasts and Epithelial Cells from Normal and P2Y2 Receptor (−/−) Mice. Journal of Biological Chemistry. 274:26454-26460.

Horimoto, T., and Y. Kawaoka. 2005. Influenza: lessons from past pandemics, warnings from current incidents. Nature reviews. Microbiology. 3:591-600.

Hsieh, Y.C., T.Z. Wu, D.P. Liu, P.L. Shao, L.Y. Chang, C.Y. Lu, C.Y. Lee, F.Y. Huang, and L.M. Huang. 2006. Influenza pandemics: past, present and future. Journal of the Formosan Medical Association = Taiwan yi zhi. 105:1-6.

Hui, K.P., S.M. Lee, C.Y. Cheung, I.H. Ng, L.L. Poon, Y. Guan, N.Y. Ip, A.S. Lau, and J.S. Peiris. 2009. Induction of proinflammatory cytokines in primary human macrophages by influenza A virus (H5N1) is selectively regulated by IFN regulatory factor 3 and p38 MAPK. Journal of immunology. 182:1088-1098.

Huipao, N. 2011. Effect of avian influenza virus H5N1 on ion transport in human respiratory epithelium. MSc. Thesis, Prince of Songkla University, Hat Yai, Songkhla.

Imai, Y., K. Kuba, G.G. Neely, R. Yaghubian-Malhami, T. Perkmann, G. van Loo, M. Ermolaeva, R. Veldhuizen, Y.H. Leung, H. Wang, H. Liu, Y. Sun, M. Pasparakis, M. Kopf, C. Mech, S. Bavari, J.S. Peiris, A.S. Slutsky, S. Akira, M. Hultqvist, R. Holmdahl, J. Nicholls, C. Jiang, C.J. Binder, and J.M. Penninger. 2008. Identification of oxidative stress and Toll-like receptor 4 signaling as a key pathway of acute lung injury. Cell. 133:235-249.

Jelinek, I., J.N. Leonard, G.E. Price, K.N. Brown, A. Meyer-Manlapat, P.K. Goldsmith, Y. Wang, D. Venzon, S.L. Epstein, and D.M. Segal. 2011. TLR3-specific double-stranded RNA oligonucleotide adjuvants induce dendritic cell cross-presentation, CTL responses, and antiviral protection. Journal of immunology (Baltimore, Md. : 1950). 186:2422-2429.

Jeter, C.R., W. Tang, E. Henaff, T. Butterfield, and S.J. Roux. 2004. Evidence of a novel cell signaling role for extracellular adenosine triphosphates and diphosphates in Arabidopsis. The Plant cell. 16:2652-2664.

Julkunen, I., K. Melen, M. Nyqvist, J. Pirhonen, T. Sareneva, and S. Matikainen. 2000. Inflammatory responses in influenza A virus infection. Vaccine. 19 Suppl 1:S32-37.

Julkunen, I., T. Sareneva, J. Pirhonen, T. Ronni, K. Melen, and S. Matikainen. 2001. Molecular pathogenesis of influenza A virus infection and virus-induced regulation of cytokine gene expression. Cytokine & growth factor reviews. 12:171-180.

Kobasa, D., A. Takada, K. Shinya, M. Hatta, P. Halfmann, S. Theriault, H. Suzuki, H. Nishimura, K. Mitamura, N. Sugaya, T. Usui, T. Murata, Y. Maeda, S. Watanabe, M. Suresh, T. Suzuki, Y. Suzuki, H. Feldmann, and Y. Kawaoka. 2004. Enhanced virulence of influenza A viruses with the haemagglutinin of the 1918 pandemic virus. Nature. 431:703-707.

Koch, A., M. Giembycz, R.G. Stirling, S. Lim, I. Adcock, K. Wassermann, E. Erdmann, and K.F. Chung. 2004. Effect of smoking on MAP kinase-induced modulation of IL-8 in human alveolar macrophages. The European respiratory journal. 23:805-812.

Korteweg, C., and J. Gu. 2008. Pathology, molecular biology, and pathogenesis of avian influenza A (H5N1) infection in humans. The American journal of pathology. 172:1155-1170.

Kujime, K., S. Hashimoto, Y. Gon, K. Shimizu, and T. Horie. 2000. p38 Mitogen-Activated Protein Kinase and c-Jun-NH2-Terminal Kinase Regulate RANTES Production by Influenza Virus-Infected Human Bronchial Epithelial Cells. The Journal of Immunology. 164:3222-3228.

Kunzelmann, K., A.H. Beesley, N.J. King, G. Karupiah, J.A. Young, and D.I. Cook. 2000. Influenza virus inhibits amiloride-sensitive Na+ channels in respiratory epithelia. Proceedings of the National Academy of Sciences of the United States of America. 97:10282-10287.

Kunzelmann, K., J. Konig, J. Sun, D. Markovich, N.J. King, G. Karupiah, J.A. Young, and D.I. Cook. 2004. Acute effects of parainfluenza virus on epithelial electrolyte transport. The Journal of biological chemistry. 279:48760-48766.

Kunzelmann, K., J. Sun, J. Meanger, N.J. King, and D.I. Cook. 2007. Inhibition of Airway Na+ Transport by Respiratory Syncytial Virus. Journal of virology. 81:3714-3720.

Lam, W.Y., A.C. Yeung, I.M. Chu, and P.K. Chan. 2010. Profiles of cytokine and chemokine gene expression in human pulmonary epithelial cells induced by human and avian influenza viruses. Virology journal. 7:344.

Lazarowski, E.R., and R.C. Boucher. 2009. Purinergic receptors in airway epithelia. Current opinion in pharmacology. 9:262-267.

Lee, D.C., C.Y. Cheung, A.H. Law, C.K. Mok, M. Peiris, and A.S. Lau. 2005. p38 mitogen-activated protein kinase-dependent hyperinduction of tumor necrosis factor alpha expression in response to avian influenza virus H5N1. Journal of virology. 79:10147-10154.

Leverkoehne, I., and A.D. Gruber. 2002. The murine mCLCA3 (alias gob-5) protein is located in the mucin granule membranes of intestinal, respiratory, and uterine goblet cells. The journal of histochemistry and cytochemistry : official journal of the Histochemistry Society. 50:829-838.

Lim, S.A., K.Y. Hwang, and S.H. Chung. 2013. Niflumic acid reduces histamine-induced interleukin-6 and -8 expression in human conjunctival epithelial cells. Ophthalmic research. 50:192-196.

Ludwig, S., C. Ehrhardt, E.R. Neumeier, M. Kracht, U.R. Rapp, and S. Pleschka. 2001. Influenza virus-induced AP-1-dependent gene expression requires activation of the JNK signaling pathway. The Journal of biological chemistry. 276:10990-10998.

Ludwig, S., S. Pleschka, O. Planz, and T. Wolff. 2006. Ringing the alarm bells: signalling and apoptosis in influenza virus infected cells. Cellular microbiology. 8:375-386.

Marshall-Clarke, S., L. Tasker, O. Buchatska, J. Downes, J. Pennock, S. Wharton, P. Borrow, and D.Z. Wiseman. 2006. Influenza H2 haemagglutinin activates B cells via a MyD88-dependent pathway. European journal of immunology. 36:95-106.

Matsushima, K., K. Morishita, T. Yoshimura, S. Lavu, Y. Kobayashi, W. Lew, E. Appella, H.F. Kung, E.J. Leonard, and J.J. Oppenheim. 1988. Molecular cloning of a human monocyte-derived neutrophil chemotactic factor (MDNCF) and the induction of MDNCF mRNA by interleukin 1 and tumor necrosis factor. J Exp Med. 167:1883-1893.

McGill, J., J.W. Heusel, and K.L. Legge. 2009. Innate immune control and regulation of influenza virus infections. Journal of leukocyte biology. 86:803-812.

Medina, R.A., and A. Garcia-Sastre. 2011. Influenza A viruses: new research developments. Nature reviews. Microbiology. 9:590-603.

Meusel, T.R., and F. Imani. 2003. Viral induction of inflammatory cytokines in human epithelial cells follows a p38 mitogen-activated protein kinase-dependent but NF-kappa B-independent pathway. Journal of immunology (Baltimore, Md. : 1950). 171:3768-3774.

Mihara, M., M. Hashizume, H. Yoshida, M. Suzuki, and M. Shiina. 2012. IL-6/IL-6 receptor system and its role in physiological and pathological conditions. Clinical science (London, England : 1979). 122:143-159.

Mogensen, T.H., and S.R. Paludan. 2001. Virus-cell interactions: impact on cytokine production, immune evasion and tumor growth. European cytokine network. 12:382-390.

Moss, R.B., R.C. Bocian, Y.P. Hsu, Y.J. Dong, M. Kemna, T. Wei, and P. Gardner. 1996. Reduced IL-10 secretion by CD4+ T lymphocytes expressing mutant cystic fibrosis transmembrane conductance regulator (CFTR). Clinical and experimental immunology. 106:374-388.

Moss, R.B., Y.P. Hsu, and L. Olds. 2000. Cytokine dysregulation in activated cystic fibrosis (CF) peripheral lymphocytes. Clinical and experimental immunology. 120:518-525.

Mukaida, N. 2003. Pathophysiological roles of interleukin-8/CXCL8 in pulmonary diseases. American journal of physiology. Lung cellular and molecular physiology. 284:L566-577.

Muller, T., H. Bayer, D. Myrtek, D. Ferrari, S. Sorichter, M.W. Ziegenhagen, G. Zissel, J.C. Virchow, Jr., W. Luttmann, J. Norgauer, F. Di Virgilio, and M. Idzko. 2005. The P2Y14 receptor of airway epithelial cells: coupling to intracellular Ca2+ and IL-8 secretion. American journal of respiratory cell and molecular biology. 33:601-609.

Nain, M., F. Hinder, J.H. Gong, A. Schmidt, A. Bender, H. Sprenger, and D. Gemsa. 1990. Tumor necrosis factor-alpha production of influenza A virus-infected macrophages and potentiating effect of lipopolysaccharides. Journal of immunology (Baltimore, Md. : 1950). 145:1921-1928.

Nayak, D.P., R.A. Balogun, H. Yamada, Z.H. Zhou, and S. Barman. 2009. Influenza virus morphogenesis and budding. Virus research. 143:147-161.

Nichols, W.G., A.J. Peck Campbell, and M. Boeckh. 2008. Respiratory viruses other than influenza virus: impact and therapeutic advances. Clinical microbiology reviews. 21:274-290, table of contents.

Okada, S.F., R.A. Nicholas, S.M. Kreda, E.R. Lazarowski, and R.C. Boucher. 2006. Physiological regulation of ATP release at the apical surface of human airway epithelia. The Journal of biological chemistry. 281:22992-23002.

Osterholm, M.T. 2005. Preparing for the Next Pandemic. New England Journal of Medicine. 352:1839-1842.

Pahl, H.L., and P.A. Baeuerle. 1995. Expression of influenza virus hemagglutinin activates transcription factor NF-kappa B. Journal of virology. 69:1480-1484.

Peiris, J.S., C.Y. Cheung, C.Y. Leung, and J.M. Nicholls. 2009. Innate immune responses to influenza A H5N1: friend or foe? Trends in immunology. 30:574-584.

Peiris, J.S., W.C. Yu, C.W. Leung, C.Y. Cheung, W.F. Ng, J.M. Nicholls, T.K. Ng, K.H. Chan, S.T. Lai, W.L. Lim, K.Y. Yuen, and Y. Guan. 2004. Re-emergence of fatal human influenza A subtype H5N1 disease. Lancet. 363:617-619.

Pleschka, S., T. Wolff, C. Ehrhardt, G. Hobom, O. Planz, U.R. Rapp, and S. Ludwig. 2001. Influenza virus propagation is impaired by inhibition of the Raf/MEK/ERK signalling cascade. Nature cell biology. 3:301-305.

Portela, A., and P. Digard. 2002. The influenza virus nucleoprotein: a multifunctional RNA-binding protein pivotal to virus replication. The Journal of general virology. 83:723-734.

Presti, R.M., G. Zhao, W.L. Beatty, K.A. Mihindukulasuriya, A.P. da Rosa, V.L. Popov, R.B. Tesh, H.W. Virgin, and D. Wang. 2009. Quaranfil, Johnston Atoll, and Lake Chad viruses are novel members of the family Orthomyxoviridae. Journal of virology. 83:11599-11606.

Rane, S.G., and E.P. Reddy. 2000. Janus kinases: components of multiple signaling pathways. Oncogene. 19:5662-5679.

Rincon, M. 2012. Interleukin-6: from an inflammatory marker to a target for inflammatory diseases. Trends in immunology. 33:571-577.

Saatian, B., Y. Zhao, D. He, S.N. Georas, T. Watkins, E.W. Spannhake, and V. Natarajan. 2006. Transcriptional regulation of lysophosphatidic acid-induced interleukin-8 expression and secretion by p38 MAPK and JNK in human bronchial epithelial cells. The Biochemical journal. 393:657-668.

Sakabe, S., K. Iwatsuki-Horimoto, R. Takano, C.A. Nidom, M. Le, T. Nagamura-Inoue, T. Horimoto, N. Yamashita, and Y. Kawaoka. 2011. Cytokine production by primary human macrophages infected with highly pathogenic H5N1 or pandemic H1N1 2009 influenza viruses. The Journal of general virology. 92:1428-1434.

Schmolke, M., and A. Garcia-Sastre. 2010. Evasion of innate and adaptive immune responses by influenza A virus. Cellular microbiology. 12:873-880.

Seo, K.Y., S. Jeon, S.H. Choi, and S.H. Chung. 2011. Niflumic Acid Reduces Histamine-Induced MUC5AC Expression in Human Conjunctival Epithelial Cells. Ophthalmic research. 46:181-186.

Servant, G., O.D. Weiner, P. Herzmark, T. Balla, J.W. Sedat, and H.R. Bourne. 2000. Polarization of chemoattractant receptor signaling during neutrophil chemotaxis. Science (New York, N.Y.). 287:1037-1040.

Shi, L., D.M. Manthei, A.G. Guadarrama, L.Y. Lenertz, and L.C. Denlinger. 2012. Rhinovirus-induced IL-1beta release from bronchial epithelial cells is independent of functional P2X7. American journal of respiratory cell and molecular biology. 47:363-371.

Shinya, K., M. Ebina, S. Yamada, M. Ono, N. Kasai, and Y. Kawaoka. 2006. Avian flu: influenza virus receptors in the human airway. Nature. 440:435-436.

Simpson, R.J., A. Hammacher, D.K. Smith, J.M. Matthews, and L.D. Ward. 1997. Interleukin-6: structure-function relationships. Protein science : a publication of the Protein Society. 6:929-955.

Skoner, D.P., D.A. Gentile, A. Patel, and W.J. Doyle. 1999. Evidence for cytokine mediation of disease expression in adults experimentally infected with influenza A virus. The Journal of infectious diseases. 180:10-14.

Song, B.M., Y.M. Kang, H.S. Kim, and S.H. Seo. 2011. Induction of inflammatory cytokines and toll-like receptors in human normal respiratory epithelial cells infected with seasonal H1N1, 2009 pandemic H1N1, seasonal H3N2, and highly pathogenic H5N1 influenza virus. Viral immunology. 24:179-187.

Tamerius, J., M.I. Nelson, S.Z. Zhou, C. Viboud, M.A. Miller, and W.J. Alonso. 2011. Global influenza seasonality: reconciling patterns across temperate and tropical regions. Environmental health perspectives. 119:439-445.

Tang, J.W., N. Shetty, T.T. Lam, and K.L. Hon. 2010. Emerging, novel, and known influenza virus infections in humans. Infectious disease clinics of North America. 24:603-617.

Tarran, R., L. Trout, S.H. Donaldson, and R.C. Boucher. 2006. Soluble mediators, not cilia, determine airway surface liquid volume in normal and cystic fibrosis superficial airway epithelia. The Journal of general physiology. 127:591-604.

Taubenberger, J.K., and D.M. Morens. 2008. The pathology of influenza virus infections. Annual review of pathology. 3:499-522.

Thomas, J.K., and J. Noppenberger. 2007. Avian influenza: a review. American journal of health-system pharmacy : AJHP : official journal of the American Society of Health-System Pharmacists. 64:149-165.

To, K.F., P.K. Chan, K.F. Chan, W.K. Lee, W.Y. Lam, K.F. Wong, N.L. Tang, D.N. Tsang, R.Y. Sung, T.A. Buckley, J.S. Tam, and A.F. Cheng. 2001. Pathology of fatal human infection associated with avian influenza A H5N1 virus. Journal of medical virology. 63:242-246.

Tosh, C., H.V. Murugkar, S. Nagarajan, S. Tripathi, M. Katare, R. Jain, R. Khandia, Z. Syed, P. Behera, S. Patil, D.D. Kulkarni, and S.C. Dubey. 2011. Emergence of amantadine-resistant avian influenza H5N1 virus in India. Virus genes. 42:10-15.

Tseng, J., J. Do, J.H. Widdicombe, and T.E. Machen. 2006. Innate immune responses of human tracheal epithelium to Pseudomonas aeruginosa flagellin, TNF-alpha, and IL-1beta. American journal of physiology. Cell physiology. 290:C678-690.

Tumpey, T.M., A. Garcia-Sastre, J.K. Taubenberger, P. Palese, D.E. Swayne, M.J. Pantin-Jackwood, S. Schultz-Cherry, A. Solorzano, N. Van Rooijen, J.M. Katz, and C.F. Basler. 2005. Pathogenicity of influenza viruses with genes from the 1918 pandemic virus: functional roles of alveolar macrophages and neutrophils in limiting virus replication and mortality in mice. Journal of virology. 79:14933-14944.

Us, D. 2008. [Cytokine storm in avian influenza]. Mikrobiyoloji bulteni. 42:365-380.

Vareille, M., E. Kieninger, M.R. Edwards, and N. Regamey. 2011. The airway epithelium: soldier in the fight against respiratory viruses. Clinical microbiology reviews. 24:210-229.

Vogel, A.J., S. Harris, N. Marsteller, S.A. Condon, and D.M. Brown. 2014. Early cytokine dysregulation and viral replication are associated with mortality during lethal influenza infection. Viral immunology. 27:214-224.

Wang, H., and C. Jiang. 2009. Avian influenza H5N1: an update on molecular pathogenesis. Sci. China Ser. C-Life Sci. 52:459-463.

Warny, M., S. Aboudola, S.C. Robson, J. Sevigny, D. Communi, S.P. Soltoff, and C.P. Kelly. 2001. P2Y(6) nucleotide receptor mediates monocyte interleukin-8 production in response to UDP or lipopolysaccharide. The Journal of biological chemistry. 276:26051-26056.

Wolk, K.E., E.R. Lazarowski, Z.P. Traylor, E.N. Yu, N.A. Jewell, R.K. Durbin, J.E. Durbin, and I.C. Davis. 2008. Influenza A virus inhibits alveolar fluid clearance in BALB/c mice. American journal of respiratory and critical care medicine. 178:969-976.

World Health Organization. Cumulative number of confirmed human cases of avian influenza A/(H5N1) reported to WHO. 2014. http://www.who.int/influenza/human_animal_interface/H5N1_cumulative_table_archives/en/; (accessed 15/03/14), part of World Health Organization. http://www.who.int/en/ (accessed 15/03/14).

Wu, X., D. Kim, A.T. Young, and C.L. Haynes. 2014. Exploring inflammatory disease drug effects on neutrophil function. The Analyst. 139:4056-4063.

Xing, Z., C.J. Cardona, J. Anunciacion, S. Adams, and N. Dao. 2010. Roles of the ERK MAPK in the regulation of proinflammatory and apoptotic responses in chicken macrophages infected with H9N2 avian influenza virus. The Journal of general virology. 91:343-351.

Xu, W., M. Chen, N. Ge, and J. Xu. 2012. Hemagglutinin from the H5N1 virus activates Janus kinase 3 to dysregulate innate immunity. PloS one. 7:e31721.

Zeitlin, G.A., and M.J. Maslow. 2005. Avian Influenza. Current infectious disease reports. 7:193-199.

Zimmermann, H. 2000. Extracellular metabolism of ATP and other nucleotides. Naunyn-Schmiedeberg's archives of pharmacology. 362:299-309.

APPENDICES

APPENDIX A

CHEMICAL PREPARATION

1. 1 L of 10x PBS stock solution

- Weigh NaCl = 80 g, KCL = 2 g, $Na_2HPO_4.7H_2O$ = 26.8 g and KH_2PO_4 = 2.4 g.
- Dissolve all components with distilled water 3B in beaker size 1 L and mix with magnetic bar on magnetic stirrer until precipitate disappeared.
- Transfer to 1 L of volumetric flask and then adjust volume to 1 L by adding distilled water 3B until the final volume equal to 1 L, autoclave at 121ºC, pressure 15 Pa (30 min) and keep at room temperature (RT).
- To make 1x PBS working solution, dilute solution 1 in 10 by mixing 100 ml of 10x PBS with 900 ml distilled water 3B, autoclave, filtrate using bottle-top filter (0.2 μm) and keep at RT.

2. 1 L of Minimum Essential Medium (MEM) (basal medium)

- Add powdered medium to beaker size 1 L, rinse the inside of package to remove all traces of powder with sterile distilled water 3B.
- Weigh $NaHCO_3$ = 2.2 g, and add into beaker.
- Dissolve all components with sterile distilled water 3B and mix with magnetic bar on magnetic stirrer until precipitate disappeared.
- Transfer to 1 L of volumetric flask and then adjust volume to 1 L by adding sterile distilled water 3B until the final volume equal to 1 L.
- Filtrate using bottle-top filter (0.2 μm), keep at 4ºC.
- To make 200 ml of MEM culture medium, aliquot basal medium = 176 ml, FBS = 20 ml, L-glutamine =2 ml, and pen/strep = 2 ml.

- Mix all solutions and filtrate using sterile syringe and sterile syringe filter (0.2μm), keep at 4°C.

3. 1 L of 1x HEPES buffer

- Weigh NaCl = 7.592 g, KCl = 0.2982 g, H-HEPES = 1.1515 g, Na-HEPES = 1.3015 g and glucose = 0.9158 g.
- Dissolve all components with distilled water 3B in beaker size 1 L and mix with magnetic bar on magnetic stirrer until precipitate disappeared.
- Add 1 M $MgCl_2$ = 1 ml and 1 M $CaCl_2$ = 1 ml and mix.
- Transfer to 1 L of volumetric flask and then adjust volume to 1 L by adding distilled water 3B until the final volume equal to 1 L.
- Adjust the pH of solution to 7.4, keep at 4ºC.

4. Primer preparation

- Equalibrate -20ºC lyophilized primer at RT and spin down with microcentrifuge.
- Dilute lyophilized primer (both forward and reverse) with PCR water (the volume added is following instruction volume to get 100 μM stock), mixed with vortex, keep at -20ºC.
- To make 10 μM working solution, dilute solution 1 in 10 by mixing 20 μl of 100 μM (stock solution) primer with 180 μl PCR water, keep at -20ºC.

5. DEPC

- Prepare 1 L of distilled water 2A in Duran® bottle.
- Add 1 ml of DEPC solution into Duran® bottle and shaking.
- Autoclave and keep at RT.

6. 100 ml of lower Tris (4x) buffer, pH 8.8

- Weigh Tris-base = 18.15 g and SDS = 0.4 g.
- Dissolve all components with distilled water 2A in beaker size 150 ml and mix with magnetic bar on magnetic stirrer until precipitate disappeared.
- Adjust the pH of solution to 8.8.
- Transfer to 100 ml of cylinder and then adjust volume to 100 ml by adding distilled water 2A until the final volume equal to 100 ml, keep at RT.

7. 100 ml of upper Tris (4x) buffer, pH 6.8

- Weigh Tris-base = 6.052 g and SDS = 2 g.
- Dissolve all components with distilled water 2A in beaker size 150 ml and mix with magnetic bar on magnetic stirrer until precipitate disappeared.
- Adjust the pH of solution to 6.8.
- Transfer to 100 ml of cylinder and then adjust volume to 100 ml by adding distilled water 2A until the final volume equal to 100 ml, keep at RT.

8. 100 ml of 30% acrylaminde-bis

- Weigh acrylamine = 30 g and bis-acrylaminde = 4 g.
- Dissolve all components with distilled water 2A in beaker size 150 ml and mix with magnetic bar on magnetic stirrer until precipitate disappeared.
- Transfer to 100 ml of cylinder and then adjust volume to 100 ml by adding distilled water 2A until the final volume equal to 100 ml, keep at 4ºC.

9. 1 L of 10x Tris-glycine buffer

- Weigh Tris-base = 30.3 g and glycine = 144 g.
- Dissolve all components with distilled water 2A in beaker size 1 L and mix with magnetic bar on magnetic stirrer until precipitate disappeared.
- Transfer to 1 L of cylinder and then adjust volume to 1 L by adding distilled water 2A until the final volume equal to 1 L, keep at RT.

10. 1 L of 10x Tris buffer saline (TBS)

- Weigh NaCl = 80 g.
- Dissolve component with distilled water 2A in beaker size 1 L and mix with magnetic bar on magnetic stirrer until precipitate disappeared.
- Add 1M Tris-HCl pH 7.6 = 200 ml.
- Transfer to 1 L of cylinder and then adjust volume to 1 L by adding distilled water 2A until the final volume equal to 1 L, keep at RT.

11. 50 ml of 2x sample buffer

- Weigh SDS = 1 g and bromophenol blue = 0.02 g.
- Dissolve all components with distilled water 2A in beaker size 100 ml and mix with magnetic bar on magnetic stirrer until precipitate disappeared.
- Add glycerol = 5 ml and upper Tris (4x) buffer = 6.25 ml.
- Transfer to 50 ml of cylinder and then adjust volume to 50 ml by adding distilled water 2A until the final volume equal to 50 ml, keep at RT.
- Before use, add β-mercapto ethanol at a concentration = 50 µl/ml.

12. 10% ammonium persulfate (APS), fresh daily

- Weigh APS = 0.1 g.
- Dissolve with 1 ml 2A water.

13. 1 L of 1x running buffer

- Aliquot 10x Tris-glycine buffer = 100 ml and 20% SDS = 5 ml.
- Mix all solutions with distilled water 2A in beaker size 1 L with magnetic bar on magnetic stirrer.
- Transfer to 1 L of cylinder and then adjust volume to 1 L by adding distilled water 2A until the final volume equal to 1 L, keep at RT.

14. 1 L of 1x transfer buffer

- Aliquot 10x Tris-glycine buffer = 100 ml and methanol = 200 ml.
- Mix all solutions with distilled water 2A in beaker size 1 L with magnetic bar on magnetic stirrer.
- Transfer to 1 L of cylinder and then adjust volume to 1 L by adding distilled water 2A until the final volume equal to 1 L, keep at RT.

15. 1 L of 1x Tris buffer saline-Tween 20 (TBST)

- Aliquot 10x TBS = 100 ml and tween 20 = 1 ml.
- Mix all solutions with distilled water 2A in beaker size 1 L with magnetic bar on magnetic stirrer.
- Transfer to 1 L of cylinder and then adjust volume to 1 L by adding distilled water 2A until the final volume equal to 1 L, keep at RT.

APPENDIX B

PASSAGING AND SEEDING 16HBE14o- cells

Protocol for trypsinizing 16HBE14o- cells from a T-25 flask:

1. Aspirate all media.
2. Rinse cells with 5 ml of PBS and swirl for 5 seconds. Aspirate PBS. This removes all remaining traces of serum.
3. Add 1 ml of 0.25% trypsin-EDTA, swirl to completely cover the cell monolayer
4. Incubate for 10 min and check for cell attachment.
5. Gently hit the sides of the flask to help dislodge cells.
6. Add 4 ml of culture medium to neutralise trypsin and gently rinse the sides of the flask using the medium and pipette. Avoid producing bubbles.
7. Transfer ~5 ml of cell suspension (media + trypsin + cells) into a 15-ml sterile centrifuge tube.
8. Centrifuge the cell suspension at approximately.l 500 × g for 5 minutes.
9. Gently resuspend the cells in culture medium, and count cells via hemocytometer.
10. Perform a cell count (25 µl of cell suspension + 100 µl of trypan blue for hemocytometer). T-25 flasks at about 70-80% confluency should give a count between 50 and 100 (~8 x 10^5 cells/ml).

Seeding cell on a culture plate:

1. For cytokine mRNA expression experiments, cells were seed on 24 well culture plate.

2. Take 500 µl of the cell suspension to seed wells at $2x10^5$ cells for each well using a 1000-ml mechanical pipette with 1000-ml pipette tip.
3. During adding cells, gently dispense the cell suspension with a single trust while the pipette is perpendicular and at the center of the well.
4. Gently swirl and incubate the plate at 37°C, 5% CO_2 for 24 hr.
5. Gently wash the cells using PBS while the plate is raised at one side to remove dead cells and cell debris.
6. After washing, add 500 µl of serum free medium for 18-24 hr before the experiment.

Seeding Snapwell inserts:

1. For Ussing chamber experiments, Costar Snapwell culture membranes (12 mm in diameter) should be pre-incubated for 24 hr prior to seeding with 1.5 ml of culture medium in the lower compartment and around 300 µl of the culture medium in the insert well.
2. Take 300 µl of the cell suspension to seed wells at $3x10^5$ cells for each membrane using a 1000-ml mechanical pipette with 1000-ml pipette tip.
3. During adding cells, gently dispense the cell suspension with a single trust while the pipette is perpendicular and at the center of the insert. This will produce an even distribution of the cells without any manipulation to disperse.
4. Incubate a Snapwell plate at 37°C, 5% CO_2 for 24 hr.
5. Gently wash the inserts using the medium over the cell monolayer while the plate is raised at one side to remove dead cells and cell debris.
6. After washing, add 100 µl of culture medium. Change media for both sides of the compartment in every 2 days.

APPENDIX C

RNA extraction and reat-time PCR analysis

RNA extraction:

1. Add cold Trizol 500 µl in each well, leave for a few minute and homogenize cells with pipette ~ 30 times, then collect sample in 1.5 ml microcentrifuge tube**.**
2. Adjust Trizol volume to 1 ml and vortex 15 sec, then incubate at RT for 5 min.
3. Add cold chloroform 200 µl and vortex 15 sec, then incubate at RT for 5 min.
4. Centrifuge at 12,000 g (4°C, 15 min), transfer the supernatant (colorless aqueous phase) to new 1.5 ml microcentrifuge tube.
5. Add cold isopropanol 500 µl, invert tube mildly, then incubate at RT for 10 min.
6. Centrifuge at 12,000 g (4°C, 10 min), discard supernatant (should see RNA gel-like pellet as gel).
7. Resuspension with cold 70% ethanol 1 ml and vortex 15 sec, then centrifuge at 7500 g (4°C, 5 min) and discard supernatant (be careful losing pellet).
8. Open tubes and leave in cabinet hold for air-dry until nearly complete dry, then resuspend RNA with cold DEPC water 15 µl.
9. Measure RNA concentration by Nano Drop.

Note : Genomic DNA contamination of the extracted RNA can be eliminated by DNase I (DNase treatment, Thermo Scientific, #EN0521) follow manufacturer' s instructions protocol before convertion RNA to cDNA.

cDNA synthesis:

1. Thaw all components except iScript reverse transcriptase. Mix thoroughly and briefly centrifuge to collect contents to the bottom of the tube before using.

2. Add the following components to a 0.2 ml PCR tube/1 reaction (on ice)

Components	**Volume**
Nuclease-free water	13 – RNA Sample (1 µg)
RNA Sample	Variable (1 µg)
Oligo(dT)20 Primer	2 µl
5x iScript Select Reaction Mix	4 µl
iScript Reverse Transcriptase	1 µl
Total	**20 µl**

Note : For multiple reactions, prepare a master mix with the above components, except nuclease-free water and RNA sample, and dispense 7 µl to each reaction.

3. Mix gently (total reaction volume = 20 µl) and incubate for 60 min at 42°C. Then, incubate at 85°C for 5 min to heat-inactivate the reverse transcriptase

4. Store cDNA at -20°C.

Real-time PCR analysis:

1. Prepare the PCR reaction for single reaction according to the volumes in the following table

Component	Volume
SYBR® Select Master Mix (2×)	7.5 µl
10 µM Forward Primer	0.5 µl
10 µM Reverse Primer	0.5 µl
cDNA template	Variable (10 ng)
Nuclease-free water	6.5 – cDNA template (10 ng)
Total	**15 µl**

2. Add the above components to a 0.2 ml 1×8 PCR tube strips. Then, close the strips with optically clear flat cap strips, and centrifuge briefly to spin down the contents and eliminate any air bubbles.

3. Place the reaction strips in the instrument.

4. Set the thermal cycling conditions using the default PCR thermal-cycling conditions specified in the following table

Step	Temperature	Duration	Cycles
UDG Activation	50°C	2 min	Hold
AmpliTaq®DNA Polymerase, UP Activation	95°C	2 min	Hold
Denature	95°C	15 sec	40
Anneal/Extend	60°C	1 min	

5. Set the instrument to perform a default dissociation step.

6. Start the run.

APPENDIX D

Transfection of siRNA

siRNA transfection:

1. For each transfection sample, prepare siRNA-lipofectamine^{TM} 2000 complexes as follows:
    a. Dilute 100 pmol of siRNA (5 µl of 20 µM siRNA) in 50 µl of Opti-MEM® I reduced serum medium. Mix gently.
    b. Mix lipofectamine^{TM} 2000 gently before use, then dilute 1 µl in 50 µl of Opti-MEM® I reduced serum medium. Mix gently and incubate for 15 min at RT.
    c. After the 15 min incubation, combine the diluted siRNA and the diluted lipofectamine^{TM} 2000 (total volume = 106 µl). Mix gently and incubate for 15 min at RT to allow complexes to form.
2. Trypsinizing 16HBE14o- cells from a T-flask, then take 400 µl of the cell suspension (in culture medium without antibiotics) at a density of $2.5x10^5$ cells add into siRNA-lipofectamine^{TM} 2000 complexes. Mix gently and seed on a 24 well culture plate.
3. Gently swirl and incubate the plate at 37°C, 5% CO_2 for 24 hr.
4. Gently wash the cells using PBS while the plate is raised at one side to remove dead cells and cell debris.
5. After washing, add 500 µl of serum free medium for 18-24 hr before the experiment.

APPENDIX E

Protein extraction and Western blot analysis

Protein extraction:

1. Place plate on ice and remove culture media, then wash cells twice with 1 ml of cold PBS. Aspirate PBS.
2. Add cold RIPA (lysis buffer) solution containing protease inhibitor and phosphatase inhibitor 200 µl in each well. Shake plate with shaker for 20 min.

10. Transfer lysis buffer to to new 1.5 ml microcentrifuge tube.
11. Centrifuge at 12,000 g (4°C, 15 min), transfer the supernatant (avoid pellet) to new 1.5 ml microcentrifuge tube.
12. Store protein at -70°C until measure protein concentration.

Protein concentration measurement: Bradford assay

1. Make 1 mg/ml of BSA to use as a standard protein concentration.
2. Standard curve:

BSA (µl)	Water (µl)	Bio-Rad reagent 1:5 Dilute in water (µl)
0	25	975
5	20	975
10	15	975
15	10	975
20	5	975
25	0	975

Note: wait for 5 min before measure by spectrometer at wavelength 595 nm.

3. Measure sample protein concentration by add 5 µl of cell lysates into 995 µl 1:5 diluted Bio-Rad reagent and incubate at RT for 5 min and read absorbance at 595 nm.

Western blot analysis:

1. Prepare 12% of separating gel: for 2 gels

30% acrylamide-bis	4	ml
4x lower buffer	2.5	ml
2A water	3.3	ml
10% APS	100	µl
TMED	6	µl

2. Add 12% separating gel into a glass plate (bottom portion, 0.5 cm distance from comb 1.0 mm thickness).

3. Add 2A water to prevent air that can inhibits polymerization and wait about 15 min, then remove 2A water using tissue paper.

4. Prepare 4% of stacking gel: for 2 gels

30% acrylamide-bis	0.85	ml
4x upper buffer	1.25	ml
2A water	3	ml
10% APS	50	µl
TMED	5	µl

5. Add 4% stacking gel until cover glass plate (upper portion).

6. Attach comb on the top and avoid bubble and wait about 15 min.

7. Remove comb from the gel and set gel into electrophoresis box, add 1 L of running buffer.

8. Load Precision plus protein standards (Kaleidoscope) in the first and the last lane (15 µl) and follow by 20 µl (30 µg protein concentration) of each sample by using loading tip.

9. Start run the gel at 100 V for 5 min and then change to 120 V for 20 min to stack the protein.

10. Change voltage to 150 V for 60 min (observe the loading dye run out of the gel).

11. When finish separating protein, cut the PVDF membrane size 6 x 8.5 cm and soak PVDF membrane in methanol for 30 sec and put into transfer buffer.

12. Move out thick and thin glass plates with spacer, then remove stacking gel, and place separating gel into transfer buffer.

13. Place a wet sponge → wet filter membrane → wet separating gel → wet PVDF → wet filter membrane → wet sponge.

Note: before place upper sponge, remove bubble on the membrane by using small tube, then lock and place into a transfer set.

14. Add 800 ml of transfer buffer and place into ice box, then set the voltage at 100 V for 1.5 hr (protein will be transferred from negative to positive side).

15. When finish transferring, rinse PVDF membrane with distilled water and block non-specific protein with 5% milk+TBST for 1 hr on shaking with slow shaking at RT.

16. Add 1º antibody in 1 ml of 5% milk+TBST and mix with vortex as follow:

Host species	**1ºantibody**	**Dilution**	**Volume (µl)**
Rabbit	Phosphor-ERK1/2	1:2000	0.5
Rabbit	Total-ERK1/2	1:2000	0.5
Rabbit	Phospho-p38	1:1000	1
Rabbit	Total-p38	1:2000	0.5

17. Discard 5% milk+TBST, then incubate membrane with 1º antibody overnight at 4ºC.

18. Wash 1º antibody with TBST (5 min x 4) on shaker with high speed at RT.

19. Prepare 2º antibody by diluting 1 µl into 5 ml of 5% milk+TBST (1:5000).

20. Incubate 2º antibody for 1 hr on shaker with slow shaking at RT.

21. Wash 2º antibody with TBST (5 min x 4) on shaker with high speed at RT.

22. Take the membrane to the dark room, place, membrane into x-ray cassette, remove excess fluid by using tissue paper. Turn off the light.

23. Add substrate distribute throughout the membrane and wait for 5 min.

24. Place the Kodak x-ray film on top of the membrane. Expose the film for 5 min (for ERK1/2) or 10 min (for p38), then develop.

25. Analyze developed film using ImageJ software.